Optimisation d'une formulation EOR chimique pour des réservoirs pétroliers conventionnels et Tight.

Seif El Islam Lebouachera

N° d'ordre :

REPUBLIQUE ALGERIENNE DEMOCRATIQUE ET POPULAIRE
MINISTERE DE L'ENSEIGNEMENT SUPERIEUR ET DE LA RECHERCHE SCIENTIFIQUE

COTUTELLE INTERNATIONALE DE THESE

Préparée entre

L'UNIVERSITÉ DES SCIENCES ET DE LA TECHNOLOGIE HOUARI BOUMEDIENE
Pour l'obtention du diplôme de **DOCTORAT**
En : Génie des Procédés
Spécialité : Génie des Procédés Industriels

et

L'UNIVERSITÉ DE PAU ET DES PAYS DE L'ADOUR
Opérée au sein de
L'Ecole Doctorale Sciences Exactes et Leurs Applications (ED 211)
Pour l'obtention du diplôme de **DOCTORAT**
En : Physique
Spécialité : Physico-chimie des Matériaux

Présentée par Seif El Islam LEBOUACHERA

Optimisation d'une formulation EOR Chimique pour des réservoirs pétroliers conventionnels et Tight

Soutenue publiquement, le-- /--/---- devant le jury composé de :

Mohamed BELMEDANI	Professeur à l'USTHB	Président
Rachida CHEMINI	Professeur à l'USTHB	Directrice de thèse
Bruno GRASSL	Professeur à l'UPPA	Directeur de thèse
Salah CHIKH	Professeur à l'USTHB	Examinateur
Amane JADA	HDR /Chargé de Recherche CNRS	Rapporteur
Julien GIGAULT	HDR/ Chargé de Recherche CNRS	Rapporteur
Nadjib DROUICHE	Directeur de Recherche/ CRTSE	Invité
Mohamed KHODJA	Directeur de Recherche/ SONATRACH	Invité

PhD THESIS INFORMATIONS

I completed my PhD thesis at three different organizations **(USTHB (Algeria) / SONATRACH (Algeria) / UPPA (France)).** During my first two years in Algeria **(January 2016- December 2017)**, I worked in the project of Chemical Enhanced Oil Recovery under the supervision of **Prof. Rachida CHEMINI (USTHB)** & **Dr. Mohamed KHODJA (Head of Research-SONATRACH)** on the aspect of the adsorption phenomena of the surfactant-based formulations and the interaction with the reservoir rock of Hassi Messaoud.

From 1 January 2018, I worked under the supervision of **Pr. Bruno GRASSL (IPREM-UPPA/France)** & **Dr. Stephanie REYNAUD (CNRS/France)** on the different formulations based on Hydrolyzed Polyacylamide-Polystyrene microspheres blends as well as the formulations based on Hydrolyzed Polyacrylamide- Polyethylenimine blends for Chemical Enhanced Oil Recovery and Conformance Control applications respectively.

This project was supported by an internship of **PROFAS B+ 2017** based on **Campus France** which allowed the mobility of the PhD student during his internship in **France.**

ARTICLES PUBLISHED

1) **Rheological behaviour and adsorption phenomenon of a polymer–particle composite based on hydrolysed polyacrylamide/functionalized poly(styrene acrylic acid) microspheres**

Authors: **Seif El Islam Lebouachera**; Laurence Pessoni ; Mohammed Abdelfetah Ghriga; Nathalie Andreu ; Rachida Chemini ; Bruno Grassl; Stéphanie Reynaud

2) **Experimental investigations of SDS adsorption on the Algerian rock reservoir: Chemical Enhanced Oil Recovery case**

Authors: **Seif El Islam Lebouachera**, Rachida Chemini, Mohamed Khodja, Bruno Grassl, Djilali Tassalit ,Nadjib Drouiche

3) **Experimental design methodology as a tool to optimize the adsorption of new surfactant on the Algerian rock reservoir: cEOR applications**

Authors: **Seif El Islam Lebouachera**, Rachida Chemini, Mohamed Khodja, Bruno Grassl Mohammed Abdelfetah Ghriga , Djilali Tassalit,Nadjib Drouiche

4) **Review of recent advances in polyethylenimine crosslinked polymer gels used for conformance control applications**

Authors: Mohammed Abdelfetah Ghriga, Bruno Grassl ,Mourad Gareche, Mohamed Khodja, **Seif El Islam Lebouachera**,Nathalie Andreu, Nadjib Drouiche

5) **Structure–property relationships of the thermal gelation of partially hydrolyzed polyacrylamide/polyethylenimine mixtures in a semidilute regime**

Authors: Mohammed Abdelfetah Ghriga, Mourad Gareche, Mohamed Khodja, Nathalie Andreu, **Seif El Islam Lebouachera**, Abdelouahed Khoukh, Nadjib Drouiche, Bruno Grassl

6) **Thermal gelation of Partially Hydrolysed Polyacrylamide/Polyethyleneimine mixtures: Statistical and experimental analysis using design of experiments**

Authors: Mohammed Abdelfetah Ghriga, Mahdi Hasanzadeh, Mourad Gareche,

Seif El Islam Lebouachera, Nadjib Drouiche, Bruno Grassl

SUMMARY

SUMMARY

Introduction Générale

INTRODUCTION GENERALE

L'injection de polymères est le procédé de récupération chimique assistée de pétrole (*Chemical Enhanced Oil Recovery - cEOR*) le plus largement utilisé dans le secteur pétrolier. Il a été appliqué pour la première fois au début des années 1960. Il y a eu une poussée d'applications des processus d'injection de polymère (polymer flooding) entre 1980 et 1986, mais elle a été limitée parce que ces applications étaient dominées par des considérations économiques : " L'injection chimique pour la récupération assistée du pétrole ne sera jamais viable parce que le prix des polymères (et autres produits chimiques) est lié au prix du pétrole", était l'argument majeur des compagnies pétrolières. Cependant, depuis l'injection massive de polymère à Daqing en Chine en 1996, les injections de polymère en cEOR ont connu une innovation et une croissance impressionnantes dans les applications sur champs.

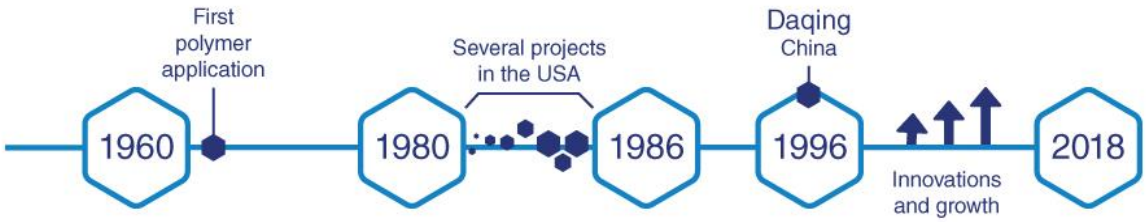

Randy Seright dans la préface du livre d'Antoine Thomas sur les techniques d'injection de polymère [1] propose plusieurs défis clés dont la solution contribuerait grandement à la viabilité de l'injection de polymère. Tout d'abord, la capacité à distribuer l'énergie (gradient de pression induite) pour amener le polymère en profondeur dans le réservoir (où se trouve la grande majorité du pétrole) doit être amélioré. Jusqu'à présent, cette question a été en grande partie réglée par le forage intercalaire, c'est-à-dire par le rapprochement des puits d'injection et de production. L'utilisation de puits horizontaux parallèles a également été utile à cet égard. Malgré tout, avec les injections de solution de polymère existantes, des fractures dans les puits d'injection doivent être provoqué afin d'atteindre des taux d'injection rentable pour ces solutions visqueuses. Le cEOR pourrait bénéficier de l'amélioration de la caractérisation, du placement et de l'exploitation des fractures (naturelles et induites) dans les réservoirs. C'est particulièrement vrai dans les réservoirs moins perméables.

Un deuxième grand domaine à améliorer est la réduction de la rétention (parfois appelée adsorption) des polymères par la roche réservoir. Le polymère doit pénétrer profondément

dans la roche poreuse du réservoir pour entrer en contact avec l'huile et la déplacer. Si une trop grande quantité de polymère est retenue par la roche, il se peut que le polymère ne pénètre jamais suffisamment dans le réservoir. La rétention des polymères représente le plus grand obstacle économique lors d'une injection de polymères. Dans le passé, les études en laboratoire ont souvent été trop optimistes quant à la rétention - surtout dans les roches moins perméables et pour les polymères associatifs.

Un troisième défi important est le déploiement de l'injection de polymères vers des réservoirs plus chauds. De grands progrès ont été réalisés dans l'identification de monomères/polymères suffisamment stables pour être utilisés dans ces réservoirs. Cependant, le coût et la viscosité associés à ces polymères sont souvent économiquement prohibitifs. L'amélioration des méthodes de fabrication peut s'avérer très utile à cet égard.

Le traitement des solutions de polymères dans les eaux de production est un quatrième domaine critique à améliorer. La nature visqueuse des solutions de polymères produit souvent des émulsions huile/eau qui sont difficiles à séparer. La capacité de recycler les polymères produits est aussi un point à considérer. Il est également nécessaire d'améliorer l'échantillonnage des fluides produits pour en savoir plus sur la propagation, le transfert et le devenir des polymères injectés.

Depuis quelques années, des efforts importants sont réalisés pour répondre à ces défis et, parmi les solutions envisagées, l'utilisation de nanomatériaux associés aux polymères usuellement utilisé en injection pour applications pétrolières est apparue dans des travaux à l'échelle du laboratoire. La récente revue de Afeez O. Gbadamosi et al.[2] et les travaux de Chaos Zheng et al.[3], Lady Galardo et al.[4] montrent l'intérêt de combiner des nanomatériaux au polyacrylamide pour améliorer les taux de récupération, la tenue en température et leurs rôles comme agent viscosifiant. L'attrait de ces systèmes est lié au comportement rhéologique particulier de ces mélanges dénommés composites polymère-particule qui peuvent développer une recrudescence d'effets viscosifiants. Ces effets sont principalement dûs aux différentes caractéristiques présentes dans le système, telles que le diamètre des particules (d), le rayon de giration des chaînes de polymères (Rg), les interactions entre les particules et le polymère, la plage de concentration du polymère et des particules. Cependant, peu de travaux se sont attachés à évaluer le rôle de ces caractéristiques et les mécanismes pouvant gouverner les effets viscosifiants observés.

INTRODUCTION GENERALE

L'objectif principal et fondamentale de ces travaux de thèse est de répondre à cette problématique afin de préciser le rôle de quelques caractéristiques physico-chimiques sur des composites polymère-particule à base de polyacrylamide hydrolysé (HPAM) et de particule bien définie en termes de taille, dispersité, et fonctionnalité. Afin d'associer cet objectif aux réponses des défis d'application cité ci-dessus, le choix du HPAM s'est orienté sur un polyacrylamide commercial (SNF Floerger), le choix des particules vers des latex, i.e. des émulsions aqueuses industrialisable de microsphères de polystyrène fonctionnalisées en surface par des acide carboxylique (PSL).

Ce manuscrit de thèse est composé de quatre chapitres dont la lecture se veut à la fois indépendante et complémentaire.

Le chapitre 1 décrit le contexte de la récupération assistée (cEOR) et l'état de l'art sur l'utilisation et les performances de systèmes composites polymère-particule.

Le chapitre 2 est consacré à l'étude des formulations basée sur une approche plan d'expériences permettant d'optimiser les paramètres à l'origine des effets d'épaississement observés dans ces systèmes composites.

Dans le chapitre 3, nous aborderons les comportements épaississants et les mécanismes gouvernant l'interaction entre les HPAM et les microsphères de polystyrène fonctionnalisées en surface par des acides carboxyliques (PSL), et nous proposerons une nouvelle approche pour la quantification des polymères adsorbés à l'aide de mesures simples en viscosité capillaire.

Le dernier chapitre de la thèse est consacré à la caractérisation du comportement de ses systèmes sur la base des effets rhéologiques montrés dans les chapitres précédents, sous l'influence des paramètres opérationnels tel que la température et le cisaillement dans une restriction capillaire.

Ces travaux réalisés à l'UPPA s'inscrivent dans un projet de cotutelle internationale de thèse entre L'USTHB et l'UPPA, soutenue par Campus France (bourse PROFAS-B+) en partenariat avec la compagnie pétrolière algérienne SONATRACH. Tous les échantillons de polymères ont été fournis par la société SNF. Ce projet a fait l'objet de publications acceptées et soumises dont une partie répond à la problématique de thèse et fait l'objet des chapitres 2 et 3 du manuscrit.

References

1. Thomas, A., *Essentials of Polymer Flooding Technique*2019: Wiley.
2. Gbadamosi, A.O., et al., *Hybrid suspension of polymer and nanoparticles for enhanced oil recovery.* Polymer Bulletin, 2019: p. 1-38.
3. Zheng, C., et al., *Suspension of surface-modified nano-SiO2 in partially hydrolyzed aqueous solution of polyacrylamide for enhanced oil recovery.* Colloids and Surfaces A: Physicochemical and Engineering Aspects, 2017. **524**: p. 169-177.
4. Giraldo, L.J., et al., *The effects of SiO2 nanoparticles on the thermal stability and rheological behavior of hydrolyzed polyacrylamide based polymeric solutions.* Journal of Petroleum Science and Engineering, 2017. **159**: p. 841-852.

CHAPTER I: State Of Art

I. Enhanced Oil Recovery

I.1. General context

The production of an oil field generally takes place in three stages, the first two stages of which recover one third (33%) of the hydrocarbons in place. The first stage of production (primary recovery), begins with the first drilling of the well where a pressure gradient is created between the reservoir (high pressure) and the surface of the well which is close to the atmospheric pressure, this difference in pressure constitutes the driving force allowing the rise of oil or gas to producing wells. Generally, the recovery of hydrocarbons in the primary phase is often assisted by surface pumps. After a certain time of production, the pressure difference weakens to reach a limit that can no longer ensure the production of hydrocarbons by natural drainage. Generally, the production rate decreases when the reservoir pressure falls below a certain critical value. The recovery rate in the primary phase depends on the initial pressures as well as the viscosity and compressibility of the fluids. It is generally between 5 and 20% of the total volume of the oil present in the reservoir [5].

In order to guarantee continuous hydrocarbon production efficiency, it is needful to maintain the pressure gradient by gas or water injection, in which case the reservoir enters a secondary recovery phase. Beyond the maintenance of the pressure, the injection of gas or water also contribute to sweep the most possible surface of the reservoir rock, the recovery mechanism is relative to an immiscible bi-phasic displacement and the sweep is dependent the permeability of the rock. In general, the injection of the substances (gas or water) is cyclic; the second phase of production reaches its technical and economic limits when the fluid / injected oil / product ratio becomes too great. The secondary phase targets an additional average oil recovery of 10 to 15%, i.e. a production yield of 35% of the total volume of oil present [6].

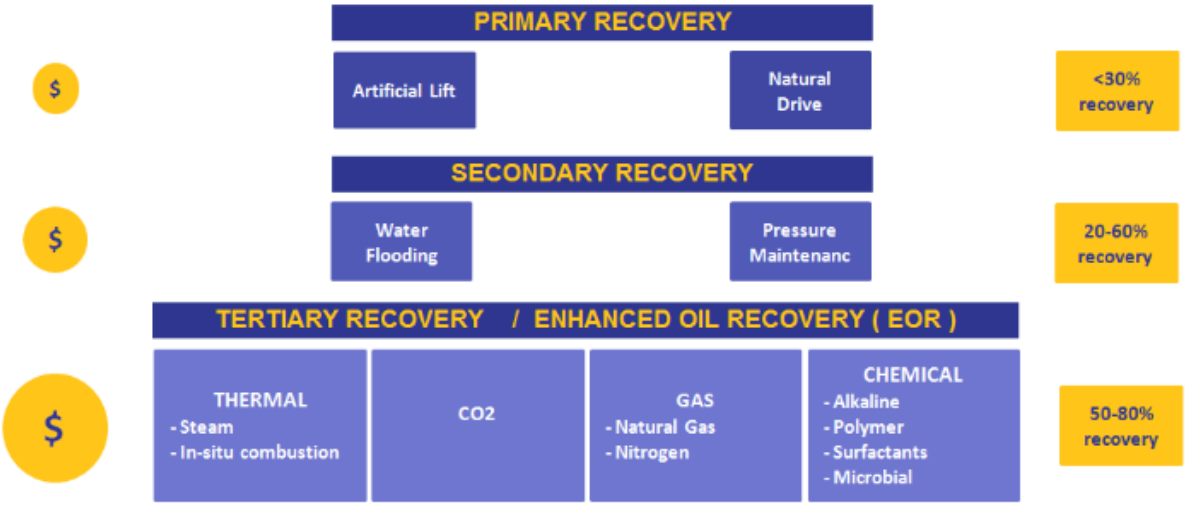

Figure I.1.: Oil extraction process based on three main stages primary, secondary and tertiary recovery

The relatively low production efficiency by the secondary recovery technique generally results from the intrinsic characteristics of the reservoir, such as the heterogeneous properties of the reservoir which disturb the flow of the fluids (fractured rock, sedimentary layers having a high permeability contrast or impermeable), unfavorable condition of the rock wettability and finally presence of capillary forces [7]. Tertiary recovery or assisted recovery targets two-thirds of residual oil that is inaccessible or unavailable by conventional techniques and therefore increases recoverable hydrocarbon reserves while maintaining economically viable production. The process of oil extraction includes three steps: primary, secondary, and tertiary oil recovery methods were illustrated in the figure I.1.

I.2.Historical aspect

Between October and December 1973 broke out the first "oil shock" in history. Until the 1970s, the big oil companies imposed low oil prices on oil-producing countries, where a barrel of oil is worth less than $ 2. In the early 1970s the high demand for oil from industrialized countries and the discovery of new deposits in Alaska and the North Sea (whose high operating costs require higher prices to be profitable), create favorable circumstances for the countries oil prices to raise prices. A second factor is the Arab-Israeli conflict. Following this event, the price of oil is multiplied by more than four and goes from $ 2.59 / barrel in October 1973 to $ 11.65 / barrel in December 1973, with reference to light

Arab crude [8].

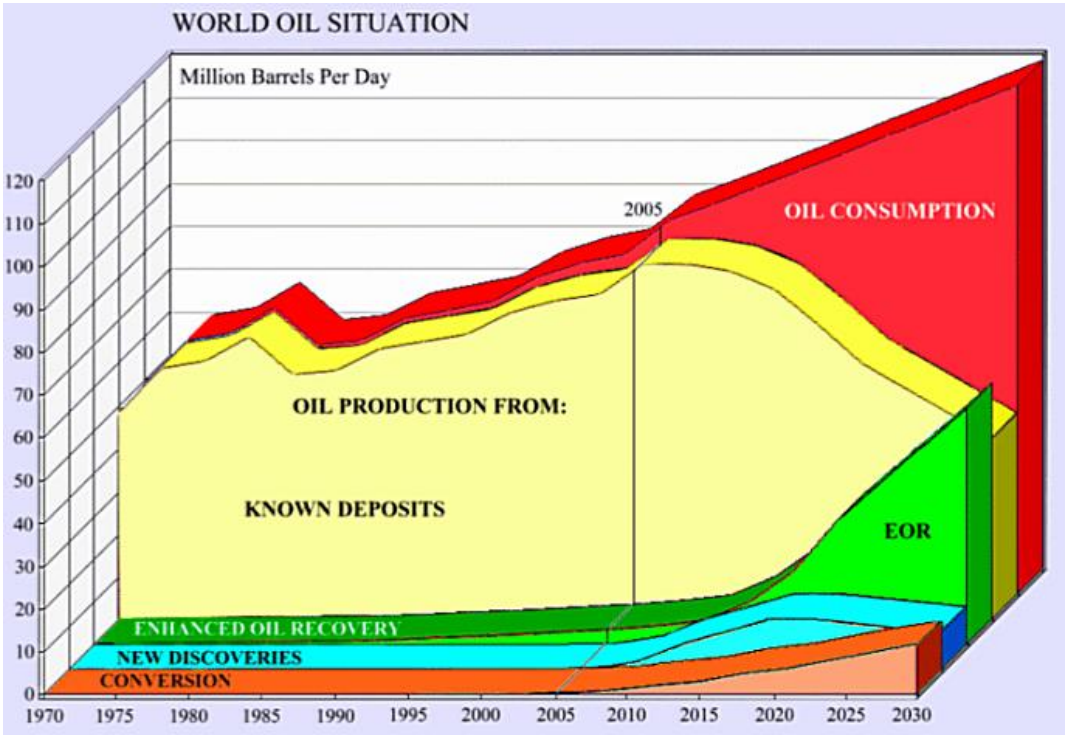

Figure I.2: Oil consumption until 2030 and estimated proportions of production sources. **EOR** represents a significant fraction of the oil produced in these estimates [9].

At that time, it was operated primarily using primary recovery techniques, but from the time when prices increased (between $ 40 and $ 65 per barrel between 1974 and 1981) [8], companies sought to develop assisted recovery techniques to increase the recovery coefficient. Subsequently, the fall in oil prices in the 1980s made it economically unprofitable to use these enhanced recovery techniques. With an average oil price around $ 65 / barrel for 2009, the EOR now becomes an economically reasonable option. The 1% increase in the recovery rate corresponds to 2 years of consumption at the current rate. These factors explain why oil economists' estimates for the coming years (**Figure I.2**), predict the EOR a future full of opportunities for expansion.

I.3.Technical aspect

Normally, oil that cannot be extracted by primary recovery or secondary recovery remains fixed in the rock by the action of capillary forces (case of light oil tanks) or because of the

very high viscosities (case of heavy crudes or oil sands). That is, there remains in the well an important amount of oil which is measured by a quantity called "oil saturation". The tertiary recovery then aims to push the crude more efficiently towards the producing wells. In general, the tertiary recovery methods are divided into thermal methods (very used and effective in the recovery of heavy crudes) and non-thermal methods (for the recovery of light crudes) themselves classified as miscible, immiscible and chemical [10].

The chemical methods, although relatively little used on a vaste scale to date, consist in injecting into the well chemical formulations whose main objective is to improve the mobility of the oil on a macroscopic scale and / or to remobilize the residual oil stuck in the tank by decreasing the interfacial tension between the oil in place and aqueous phase. These techniques are considered adequate strategies for many light oil deposits, but their cost is high.

I.4.Methods of Enhanced Oil Recovery

There are three main mechanisms for crude recovery that are based on the reduction the viscosity of the crude, the extraction of the crude by a gas and the alteration of the capillary forces between the crude, the injected fluid and the rock. EOR methods are classified as follows[11]:

*Thermal methods (heat injection);

*Gas injection methods;

*Chemical methods (surfactant injections, polymers and chemical formulations).

I.4.1.Thermal methods

These methods involve injecting a thermal source (heat) at the reservoir; the support of this heat source can be in the form of a gas stream or water at high temperature or by in-situ combustion. The main mechanism of thermal recovery is mainly related to the reduction of the viscosity of the oil by increasing the temperature to facilitate its flow through the porous system of the rock. This method is aimed primarily at maximizing the production yield of highly viscous and heavy oils [12]. It becomes all the more energy-consuming for light hydrocarbons because the extent of the reduction in the viscosity of light oils compared to heavy is significantly lower and therefore this technique is less effective for light oil.

I.4.2.Gaz Injection

This process consists in injecting miscible gas with the oil. The most commonly used gas is carbon dioxide (CO_2) because it is miscible with oil at relatively low pressures and temperatures, but it can also be nitrogen depending on the availability of the source. The mechanism for recovering the residual oil by injecting miscible gas is mainly related to the reduction of the interfacial tension between the oil and the pusher fluid (the miscible gas), in other words a microscopic displacement. The problems most often encountered in this technique are related to the viscous digitation resulting from the weak sweep of the reservoir due to the large difference in viscosity and density of the fluids (oil and gas). On the other hand, the gas injection operation such as CO_2 can cause corrosion problems in the pipes and production wells, therefore special prevention provisions must be taken into account [13-16].

I.4.3. Chemical methods

This technique involves the injection at the reservoir of the water containing chemical additives. Depending on the nature of the latter, the chemical assisted recovery reduces the interfacial tension (usually surfactants and alkaline agents) and the mobility ratio (addition of polymer) between the oil residual and injected water, so the mechanism of displacement is microscopic and / or macroscopic. The chemical method has been considerably developed as a means of enhanced recovery from the 1960s [17].The first research projects focused on the injection of polymer solutions to reduce the mobility ratio and increase reservoir sweeping and were quickly followed by the addition of surfactants [18] to reduce the interfacial tension between oil and water. A little later, the addition of alkaline agents was considered in order to reduce the adsorption of surfactants on the reservoir rock and also a substantial production of in situ surfactants with acid oils [19]. The alkaline agent also controls the salinity to ensure minimal interfacial tension. The simultaneous injection Alkaline-Surfactant-Polymer (ASP) allows to combine the advantages of the three agents and consequently to increase the efficiency of production in an effective way [20-22] with an estimated production cost per barrel of 2.42 USD. The key to the success of chemical-assisted recovery is the selection, formulation and performance evaluation at the laboratory scale.

I.5.Control of mobility

Mobility control is a key element in the crude recovery process. It can be reached by the injection of chemical species that will change the viscosity of the fluid displacing or reducing the relative permeability of the crude in the tank.

The mobility λ is defined as the ratio of the permeability K (m^2) on the dynamic viscosity μ (Pa.s) of a phase following the equation (I.1):

$$\lambda = \frac{K}{\mu} \qquad (I.1)$$

The permeability K depends only on the geometry of the porous medium and characterizes the ability of a fluid to flow through the porous medium

In the case of a two-phase flow in porous media, the term mobility ratio is also used which is defined as the ratio between the mobility of the displacing fluid and the mobility of the mobile fluid following the equation (I.2):

$$M = \frac{\lambda_d}{\lambda_o} \qquad (I.2)$$

A mobility ratio equal to or less than 1 (M≤1) is favourable (Craig, 1971) because in this case we will obtain an optimal displacement of the "plug" type. In the crude recovery process, we are in the case where a mobile fluid (the crude) is displaced by another fluid (water). The mobility of the fluid moving upstream (λ_d) must be equal to or less than the fluid displaced downstream (λ_o) following the equation:

$$\lambda_d < \lambda_o \qquad (I.3)$$

In the case where the viscous fluid is displaced by a less viscous fluid in the tank (M> 1), the interface between the two liquids becomes unstable and the less viscous fluid, water, moves faster and enters the tank. More viscous fluid, the interface then forms "fingers". This instability phenomenon is known as viscous fingering or Saffman-Taylor instability for two immiscible fluids. This phenomenon renders tank sweeping inefficient and therefore results in very low oil recovery. Polymer flooding is considered the most mature and most commonly used chemical method. The injection of long chains of water-soluble polymers makes it possible to increase the viscosity of the water injected into the reservoir, which will reduce the mobility of the aqueous phase. The two main types of synthetic polymers used are hydrolyzed polyacrylamide (HPAM) and biopolymers such as xanthan gum. The

understanding of phenomena related to the behavior of polymers in porous media for the EOR has progressed a lot over the last 20 years and the process is now economically viable[23, 24].

I.6.Reduction of capillary forces

The capillary forces limit the microscopic displacements of the fluids in the porous medium. This phenomenon was identified very early and gave the idea to add chemical species to reduce these forces by acting on the gross / water interfacial properties. The pressure difference ΔP (in Pa) on either side of the oil-water interface in the tank is given by the Laplace equation (I.4)

$$\Delta P = \gamma * \left(\frac{1}{R} + \frac{1}{R'}\right) \qquad \text{(I.4)}$$

Where γ is the interfacial tension (N/m) and R and R ' (m) are the main radius of curvature. Due to the geometric complexity of the porous network, the Laplace equation cannot be solved exactly in all cases. However, we can illustrate the phenomena involved between capillary and viscous forces by considering the case of an oil ganglion trapped in a branch of the porous network (**Figure I. 3**).

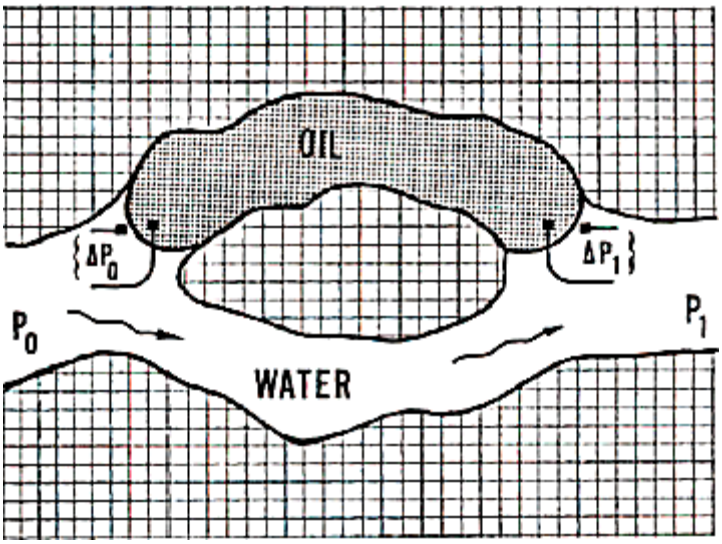

Figure I.3: Ganglion of oil trapped in a branch of a porous network [25]

The flow water in the lower branch imposes an external pressure difference P_0-P_1 which corresponds to the viscosity forces necessary to mobilize the oil trapped. However, the curvature at the interfaces and the interfacial tension cause different pressures (ΔP_0 and

ΔP_1) for each of the water and oil phases. Capillary pressure is the pressure difference ΔP between the two phases. As one cannot play on the curvature of the interface which depends on the contact angle and the pore size, only a reduction of the interfacial tension makes it possible to reduce the capillary forces.

In the case of chemical Enhanced Oil Recovery (EOR) applications which is based on several parameters. The displacement from a microscopic point of view is governed by the capillary pressure which itself depends on the interfacial tension and the wettability. On the other hand, the macroscopic displacement is mostly controlled by the average velocity of fluid displacement and the mobility ratio. Considering each phenomenon independently is a complex task. The capillary number (Nca) (equation I.5) is a dimensionless dimension which unifies the different descriptions of the water-oil-rock system, which represents the ratio between the capillary forces and the viscous forces:

$$N_{Ca} = \frac{\upsilon * \mu}{\gamma} \qquad (I.5)$$

Where υ is the flow fluid velocity (m / s), μ is the viscosity (Pa.s) of the moving phase (water) and γ the interfacial tension (N / m). Its numerical value is directly related to the efficiency of the current recovery [26-29].

The relationship between the capillary number and the desaturation of the residual oil is shown in **figure I.4** in which it is noted that for a capillary number of 10^{-6}-10^{-5}, the saturation of the residual oil is almost constant and that, starting from a certain value of N_{ca}, the residual oil saturation begins to decrease, moreover indicating a recovery of the oil.

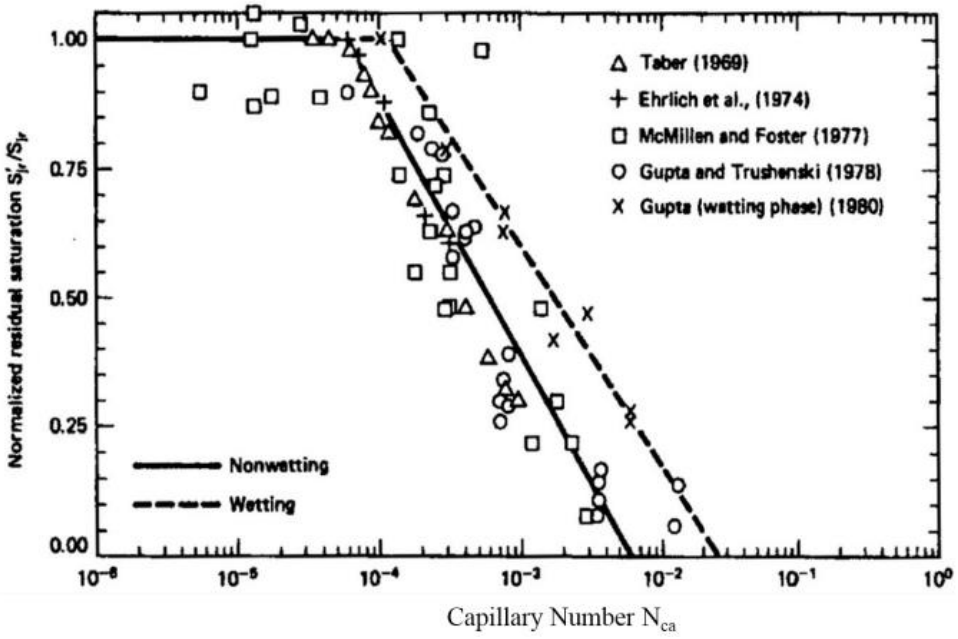

Figure I.4: Relationship between the Capillary Number N_{ca} capillary number and the residual saturation [30]

Many authors [31] have experimentally measured the amount of residual oil in the tank as a function of the N_{Ca} number. For a good oil recovery yield, the capillary number must be greater than 10^{-3} in order to reach a residual saturation close to zero.

To increase N_{ca} it is possible to increase the flow velocity and **the viscosity of the displacing fluid or to reduce the interfacial tension between the crude and the water**. However, the flow velocity of the fluid cannot be significantly increased for reasons of injection pressure limitation. Similarly, the viscosity of the aqueous phase cannot be considerably increased because an increase in viscosity will also lead to an increase in the injection pressure near the wells**. Additives to increase the viscosity such as polymers can save a single order of magnitude for the capillary number.**

I.7.Surfactants for Enhanced Oil Recovery

Surfactants are amphiphilic molecules that tend to position themselves at the interface of two immiscible fluids while reducing the interfacial tension. For enhanced oil recovery, they are used to act at the pore scale by reducing the interfacial tension between oil and water. As a result, they make it possible to greatly increase the capillary number and thus to

improve the displacement of the oil in the rock. The use of the surfactants makes it possible in particular to move the residual oil not displaced by imbibition and to reach an oil saturation close to zero, provided that interfacial tensions of the order of 10^{-3} mN / m are attained. For this purpose it is necessary to use micro-emulsion systems. In assisted recovery, the surfactant solutions are injected over a relatively short period of time, so as to have a plug which is followed by drainage with a polymer solution. This drainage makes it possible to ensure a mobility control by viscosity so that the residual oil remobilized by the plug of surfactants is displaced uniformly and efficiently towards the production well. Good mobility control ensures the integrity of the surfactant plug and avoids the effects of viscous digitations.

Interactions between the fluid and the rock may have effects on the effectiveness of the injection of surfactants. These are adsorption, capillary phenomena, cation exchange and precipitation-dissolution phenomenon. These phenomena can directly or indirectly affect the retention of surfactant molecules and reduce the efficiency of this method [32].

I.8.Alkaline for Enhanced Oil Recovery

The use of alkaline solution makes it possible to act at the microscopic scale by the in situ creation of surfactant compounds. These compounds result from a reaction between crude oils and bases. The creation of these compounds reduces the interfacial water-oil tension. For example, Jennings showed that out of 160 crude oils tested, 80% have marked surface activity when placed in the presence of bases [23]. The compounds that react are molecules of high molecular weight such as asphaltenes and resins. However, reducing interfacial tension is not the main mechanism for improving oil production. As we have seen previously, it is necessary to obtain very low interfacial tensions before obtaining an effect on oil recovery. In the majority of cases described in the literature, the interfacial tensions measured are greater than 0.01 mN / m [20], which is not sufficient to have an effect on the capillary number. Nevertheless, such values of interfacial tensions favor the formation of oil / water emulsions inside the rock. If the size of the oil drops is smaller than the pore size, oil drops are easily carried by the fluid moving to the production well. When the size of the drops is greater than the pores, the drops are trapped in the medium, and the improvement in production is the result of a reduction in the mobility of the aqueous phase on a macroscopic scale. In addition to the effect on interfacial tension, alkaline solutions can also

have an effect on the wettability of the rock [24] and thus facilitate the production of oil. However, depending on the bases used, the effectiveness of this method can be altered by interactions with the rock, inducing the formation of precipitates and thus a reduction in permeability. In general, the alkaline solutions are coupled to solutions of polymers and / or surfactants, giving rise to the ASP (Alkaline-Surfactant-Polymer) method. This method has been laboratory and field tested and has been shown to be effective in moving residual saturation to oil [25, 26, 27]. Thus, the use of this method in the Daqing Reservoir in China has resulted in an increase in production of 20% of the oil in place compared to the imbibition [28]. The combination of these three chemical agents not only makes it possible to combine their advantages. There is also a synergy between them that is to say that taken together, their action is better than the sum of their individual effects. Thus, the presence of polymer makes it possible for example to reduce the adsorption of the surfactants, which makes it possible to obtain a lower interfacial tension than if the surfactant were used alone. Similarly, the surfactants formed in situ by the reaction between the base and the oil combine with the surfactants injected and improve their effect. This is added to the viscosity or wettability effects induced respectively by the presence of polymer or base. This method therefore makes it possible to recover the maximum of the oil in place, provided that the good proportions of the various constituents and the injection strategy are found. Indeed, it is difficult to find the right proportions because the excess of one or other of the constituents may be counterproductive. For example, a base that is too strong may react with certain ions in the rock and cause precipitates. Or, too high a base concentration may cause a reduction in the viscosity of the polymer. Thus, the ASP is a method whose effectiveness has been proven but it can be very expensive and difficult to develop, hence the usefulness of developing other methods of recovery.

I.9.Polymer injection for Enhanced Oil Recovery

Polymers are used primarily to reduce the mobility ratio, by increasing not only the viscosity of the water by adding a few hundred ppm, but also by decreasing the permeability of the rock to water. The objective here is not the residual oil trapped by the capillary forces at the microscopic scale, but rather the one that would not have been swept at the end of the secondary recovery (waterflooding or gaz injection) It is therefore a macroscopic action that reduces the sweeping time by generating a faster recovery of the oil. Indeed, according to

Sorbie [33], the oil recovered by injection of polymers theoretically would have ended up being so with the imbibition if it had lasted longer. Thus, the residual oil saturation is not changed. That is why, to benefit from this method, it is important to choose the right moment to inject the polymers.

When they circulate in a porous medium, the polymer molecules are retained, which has the advantage of reducing the permeability of the rock to water but the disadvantage of reducing the effectiveness of the injection. Mechanisms leading to polymer retention are adsorption, hydrodynamic retention and mechanical entrapment (see figure I.5).

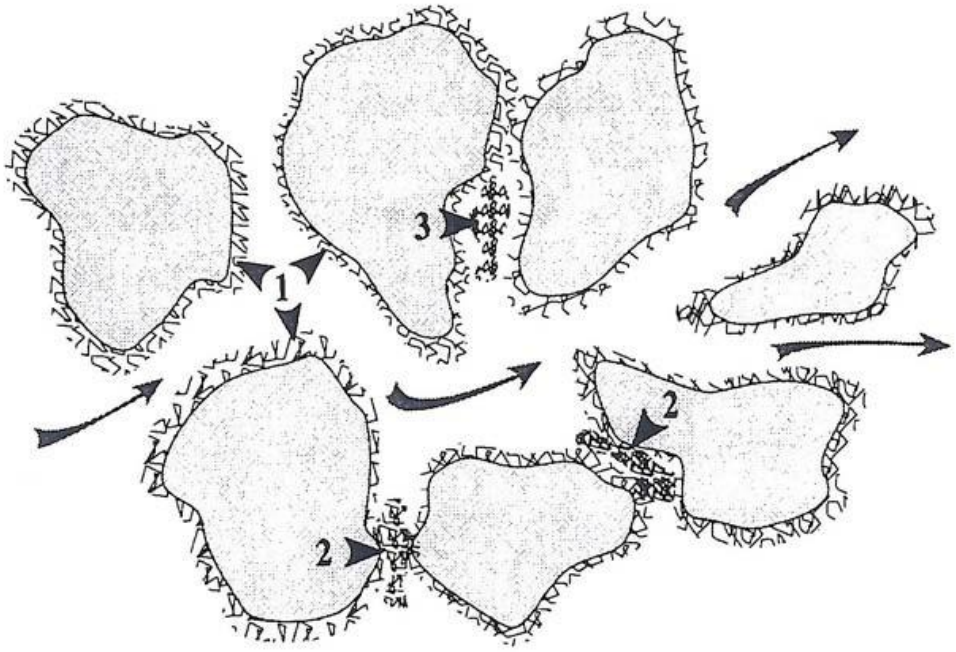

Figure I.5: Different types of trapping [34]

The failures most often encountered in the polymer flooding operations are the loss of the polymer (by adsorption in the rock) and the degradation of the formulation depending on the high shear stresses during the injection.

a) **Adsorption**: results from an interaction between the polymer molecules and the solid surface. This interaction is characterized by a binding of molecules to the surface of the rock due mainly to physical bonds (Van der Waals, hydrogen bonds) rather than to chemical bonds. This interaction causes the molecules to attach to the wall, which ends up lining the accessible solid surface. This could be the main polymer retention mechanism.

b) **Mechanical entrapment:** retention takes place when large polymer molecules

become lodged in small pore sizes. It leads to an obstruction of certain pores and therefore to a permeability reduction that can be irreversible.

c) Hydrodynamic retention: It corresponds to the entrapment of certain macromolecules in pores where stagnant points appear. This retention is reversible and varies with the injection rate.

Ideal for the use of polymer flooding are high permeability and low clay content deposits with an oil viscosity not exceeding 0.1 mPa.s in situ [35]. Moreover, in cases where the permeability of the deposit is variable, this type of formulation erases the contrast effects of permeability, avoiding the appearance of preferential paths. It should be remembered that the shear conditions in a well can go above 100 s^{-1} during drainage, being 10 s^{-1} a typical average value [36, 37] , and even beyond 1000 s^{-1} at the injection [38].

I.10. Properties of polymers in solution

I.10.1. Choice of polymer

Enhanced oil recovery begins with the selection of the polymer. The choice of a polymer is based on its viscosity, its cost and its ability to withstand different physicochemical conditions and the attack of different external chemical agents

The polymers used primarily to increase the viscosity of the aqueous phase are synthetic polymers such as polyacrylamides and natural such as polysaccharides. Among the polymers used in EOR applications, Xanthan and polyacrylamide can be used.

Xanthan is a biopolymer obtained by microbial fermentation of xanthomascampestris, it is a polysaccharide of molar mass around $1*10^6$ g / mol and is considered a rigid polyelectrolyte[39] This limits its ability to adopt certain configurations. This rigidity gives it resistance to mechanical degradation and the maintain of viscosity in the deposits even if the salinity is high[40] .On the other hand, Xanthan has disadvantages which limit its effectiveness: clogging of porous media, thermal and microbial degradation.

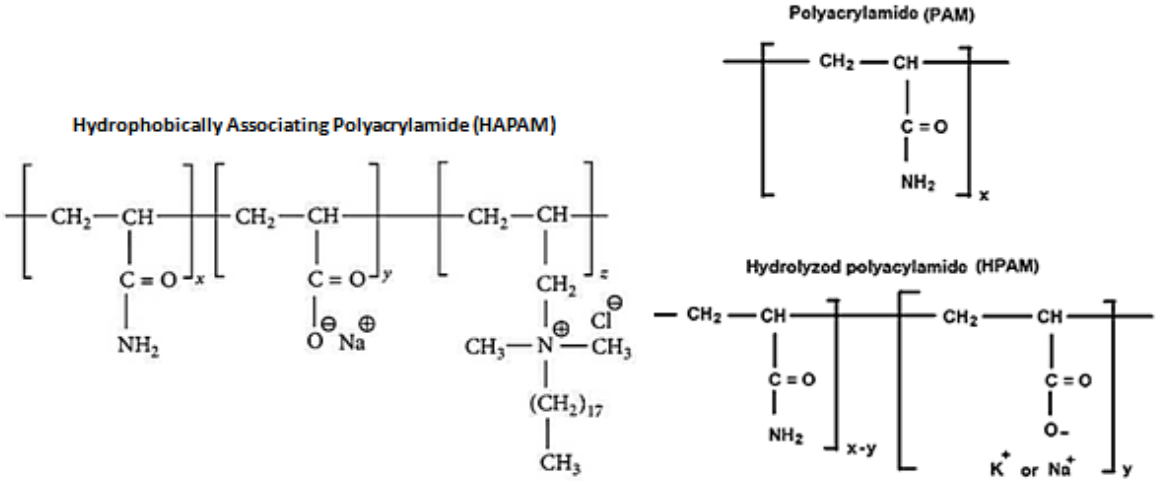

Figure I.6: Structure of polyacrylamide (**PAM**)/ partially hydrolysed polyacrylamide (**HPAM**) and Hydrophobically Associating Polyacrylamude (**HAPAM**)

The polyacrylamides illustrated in the **figure I.6** are synthetic polymers soluble in the aqueous phase, which can be linear or crosslinked, with molecular weights generally ranging between a few thousand and 10^7 g/mol [41]. At the polyacrylamide level, in aqueous solution, a fraction of the acrylamide can be hydrolyzed to produce acrylic acid; this results in an increase in its viscosity in water without electrolytes, but its viscosity decreases abruptly in salt water [36]. Indeed, polyacrylamides are likely to have their rheological characteristics modified if the salt concentrations are high (more than 1% of salt, as is the case in brines) but also by mechanical degradation due to significant shear (change to through a valve or through the pores of the rock). Moreover, on the same concentration, polyacrylamides of high molar mass give more viscous solutions and more resistant to the loss of viscosity by the effect of salt, pH and temperature; however, they are more prone to degradation mechanical.

The polyacrylamide (PAM) concentrations conventionally used are between **200 ppm** and **2000 ppm** (30% hydrolysed PAM) for high molar mass FLOOPAM for example SNF product (3630S) [9].

I.10.2.Rheology of polymer solutions out-side the porous medium

Over a wide range of shear rates, polyacrylamide exhibits non-Newtonian behavior. For low shear rates the solutions show a Newtonian plateau where the viscosity is constant, followed by a decrease in viscosity for higher shear rates. This dependence of the viscosity of the shear rate is included in Newton's law (I.6) [42]

$$\tau_{xy}=-\eta\frac{\delta vx}{\delta y}=\eta(\dot{\gamma})\,\dot{\gamma} \qquad (I.6)$$

Where η is the apparent dynamic viscosity which is a function of shear rate $(\dot{\gamma})$.

For sufficiently large concentrations, all polymer solutions exhibit non-Newtonian behavior. The apparent viscosity curves η=f $(\dot{\gamma})$ are generally presented in terms of relative viscosity η_r= f$(\dot{\gamma})$ where η_r is the ratio between the viscosity of the polymer solution and the viscosity of the solvent (η_s).

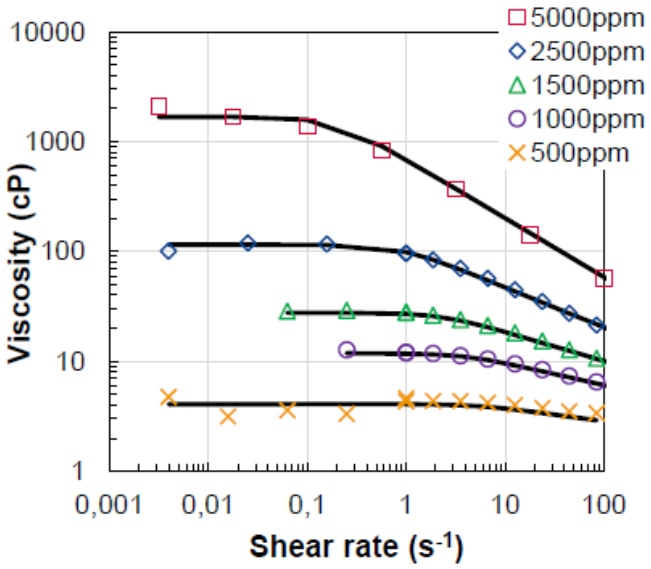

Figure I.7: Evolution of the HPAM (3530) viscosity at different concentrations versus shear (T=25°C, 0.2M Na_2SO_4) [43]

In the figure I.7 above we observe two well-differentiated regimes, a Newtonian regime and a non-Newtonian pseudo-plastic regime, separated by a transition zone characterized by a critical shear rate. The most used relationship, is the power law to describe the pseudo-plastic region following the equation (I.7) [42]

$$\eta = m\,(\dot{\gamma})^{\,n-1} \qquad (I.7)$$

Where m and n are the constants characteristic of each polymer at a given concentration. For Newtonian fluids the value of the exponent n is equal to 1 for the pseudo-plastic behavior n<1 (typically n=0, 4 -0,7 and for n> 1 the solution has a dilating or rheo-thickening behavior.

The power law remains insufficient for low and very high shear rates. The Carreau model is more apt to describe both the Newtonian and the shear thinning behaviours (eq. 1) [44]. In this model the apparent viscosity is given by equation (I.8) this model describes.

$$\eta = \eta_{inf} + (\eta_0 - \eta_{inf})(1 + (\lambda\dot{\gamma})^2)^{(n-1)/2} \qquad \text{(I.8)}$$

Where η_0 and η_{inf} the viscosity are at zero and infinite shear rate (Pa.s), λ is the relaxation time (s) and *n* is a power index.

The characteristic time λ will be expressed from the viscosity of the solvent η_s, the molecular weight of the polymer M_w, the concentration C, the temperature T, the perfect gas constant R (8.314 J / mol K) and the intrinsic viscosity [η], it is written for a linear polymer using the equation (I.9)

$$\lambda = \eta_s CM[\eta]/RT \qquad \text{(I.9)}$$

The intrinsic viscosity [η] represents the hydrodynamic volume occupied for macromolecule, giving an idea of the size and the extension of the polymer molecule in the solution, it appears as the limit of the reduced specific viscosity $\eta_R=\frac{\eta-\eta s}{C*\eta s}$ when the concentration C tends to zero [33]:

To describe the viscosity of the solutions of the polymers, the relative viscosity η_r which is the ratio between the viscosity of the polymer solution [η] and the viscosity of the solvent η_s is defined using the equation (I.10):

$$\eta_r = \frac{\eta}{\eta_s} \qquad \text{(I.10)}$$

The intrinsic viscosity makes it possible to determine the average molar mass according to the Mark-Houwink law. The equation that defines the relationship between these two parameters is:

$$[\eta]=k*M^{a} \qquad (I.11)$$

Where M, is the molar mass of the polymer chain; a and k are the Mark-Houwink constants and depend on the solvent-polymer pair. There are specific values of these constants for each of the combinations, solvent – polymer. Intrinsic viscosity measurements [η] were performed only in the dilute regime ($c_p < c^*$).In this work, we used the classical method by carrying out several dilutions and several measurements of reduced viscosities. When the dilution is sufficient, the reduced viscosity η_{red} is characterized by the Huggins equation: $\eta_{red} = [\eta] + k_h[\eta]^2$; k_h : Huggins coefficient .Moreover, the inherent viscosity could be used as follow:

$\eta_{inh} = \frac{\mathrm{Ln}\,\eta_r}{c} = k'' [\eta]^2 c + [\eta]$ (3) k'' is the Kraemer coefficient with k'- k'' should be equal to 0.5. After that, we obtain two lines whose ordinate at the origin is $[\eta]$.

A good solvent is considered when the polymer / solvent interactions are favoured (the polymer chains are swollen by the solvent), a bad solvent when the polymer / polymer interactions are favored and the polymer chains collapse on themselves and are considered a solvent θ when it is indifferent between the interactions polymer / solvent and polymer / polymer.

If a polymeric material dissolves in a solvent, it is because the attractive interactions (usually of van der Waals type) between the monomers and the molecules of solvent are stronger than the attractive interactions between monomers that provided the cohesion of the massive material. In a good solvent, the contacts between monomers are therefore energetically unfavorable. This effect generates an effective interaction called excluded volume between monomers: two monomers cannot be in the same neighborhood at the same time.

In the case of a good solvent, where the chains only come into contact with the solvent, two spherical macromolecules of identical volumes cannot occupy exactly the same position and a repulsive interaction will appear, and the characteristic distance of the repulsion defines the excluded volume which depends on the relative values of the solvent / segment segment and solvent / solvent interactions (figure I.8).

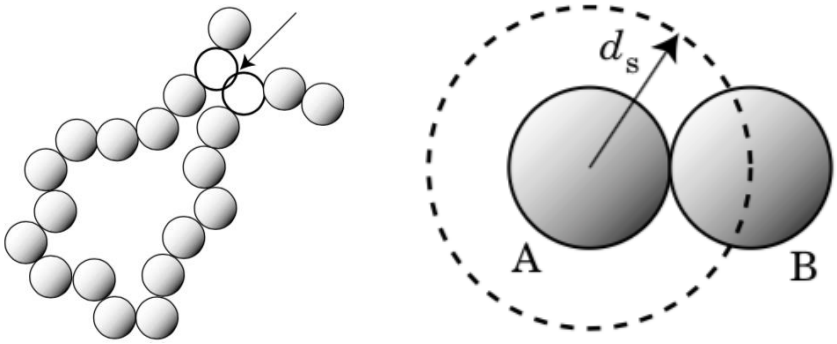

Figure I.8: Representation of the excluded volume between two in the case of two volume identical spheres [45]

Flory (1953) [46] treats the expansion of a macromolecular ball as a field of forces where two components of opposite natures exist, one of repulsion therefore of expansion, and the other of retraction, of entropic origin. The chain adopts a conformation that is characterized by the square root of the mean squared distance between the equilibrium chain ends, without the excluded volume effects R_0 and the Rg the radius of gyration. This is described by the expansion factor ε which is then defined in the equation (I.12) as:

$$<R_0^2>= \varepsilon < R_g^2> \qquad (I.12)$$

The radius of gyration can be estimated through Flory's correlation by the equation (I.13):

$$[\eta]M_w=\phi' R_g^3 \qquad (I.13)$$

In which ϕ' is a dimensionless universal constant of value $3.66*10^{24}$ mol^{-1}. Physically, R_g (Radius of gyration) represents the radial distance at which the entire mass of the chain could be located in such a way that the moment of inertia is the same as that of the actual mass distribution.

I.11.Limitations of polymer injection in chemical Enhanced Oil Recovery

The polymers that have been tested for use in the injection of oil wells are classified into two important categories such as natural and synthetic polymers in order to be effective for the improvement of the mobility ratio as well as the reduction of the permeability in the porous medium. However, the use of polymers like Xanthan gum was limited because of higher bacterial degradation. In this case, synthetic polymers such as polyacrylamides have been widely used for the various applications of polymer injection in the oil fields [47-49]. We

have resumed the different works in the literature

Table I.1: Application of different polyacrylamide around the word

Country	Field targeted	Polymer used	Oil recovery (%OOIP)	References
Oman	Marmul	HPAM	12-35	[50]
Canada	Pelican Lake	HAPAM	12–24	[51]
China	Daqing	HPAM	19.4–28	[52]
India	Viraj	HPAM	--	[53]
Argentina	El Corcobo	HPAM	--	[54]
USA	Cambridge Minnelusa	PAM	--	[21]
USA	Tanner	PAM	--	[55]
Canada	Mooney	HAPAM	12-24.5	[56]
Canada	Seal	HPAM	5-6	[57]

*HAPAM hydrophobically associating poly- acrylamide ; *HPAM : Hydrolyzed Polyacrylamide ; *PAM: Polyacylamide; *OOIP: Original Oil In Place

These reasons have led researchers to develop or take a close interest in applications of nanotechnology to improve the robustness of the polymer that can be targeted at EOR applications. One of these reasons could because during the injection of the polymers, the polyacrylamides have undergone partial hydrolysis which causes a conversion of some of the amide groups ($CONH_2$) to carboxyl groups (COO^-). The explication is that the degree of hydrolysis (DH) defined many physical and rheological properties of the polymer solution, such as adsorption, viscosity and solubility in water because the molecule has a flexible chain structure known as a random coil and since it is a polyelectrolyte, it interacts with ions in solution. In the literature, the typical DH of polyaclymade is in the range of 15–35% based on the acrylamide (AM) monomers [58]. Several factors can affect the stability and properties of HPAM type polymers for example salinity of water, temperature and salinity. An others factors such as pH, shear rate, oxygen and iron (contaminants) [47, 59].

a) Effect of temperature

Temperature is one of the most parameters which affect any transformation or chemical reaction. For polymer systems in oilfields, it is important to quantify the effect of temperature on the stability of HPAM polymer types. When the temperature is lower, the polymer is thermally stable [60], but when the elevation of temperature is important, the pendant amide group present in the polymer backbone reach to hydrolyse [61].

It is preferable to avoid the use of a polymer with a high degree of hydrolysis (DH) because precipitation of the polymer occurs in the presence of divalent ions [62]. High temperature causes higher (DH), resulting in significant changes in solution properties, stability and rheology of the polymer system, resulting in phase separation. In cases where there is no formation of precipitates, strong cation interactions with the carboxylate group of the polymer result contribute to the reduction of HPAM viscosity and efficiency [47, 63-65]. For example, the work of Davison and Mentzer [66], who studied the viscosity measurements of several polymers at 90 ° C for possible application in the oil fields of the North Sea. Their results indicate that the viscosity of polyacrylamide was observed to be particularly poor at high temperature and precipitation of the polymer was observed.

In another work, Zhongliang Hu et al [67] studied the mechanism of the precipitation of the polyacrylamide solution and was proposed via Raman spectroscopic analysis of the solution at elevated temperature which shows the hydrolysis of the amide group on the backbone of the polymer to carboxylate group. The hydrolysis of amide side groups on the backbone of partially hydrolysed polymer at higher temperatures was corroborated by Seright et al. [37] Besides, they confirmed that the precipitation of HPAM noticed in previous researches was due to the presence of divalent cations. Moreover, in the absence of divalent cations and dissolved oxygen, their experiences indicate that the polymer backbone could remain stable for prolonged periods.

b) Effect of salinity

The viscosity property of polymers such as HPAM are polyelectrolytes with multiple charges distributed along their chain, is sensitive to solution salinity and hardness commonly encountered in reservoir formation brines [65, 68]. These types of polymer tend to conform when in solution and the average conformation of a typical flexible HPAM is random coil. However, it can change conformation, and from which overall size, quite easily [69]. In order to understand the effect of salt concentration on HPAM viscosity, it should be necessary to consider the interaction between the mobile ions in solution and the fixed charges at the interface of the polymer chain.

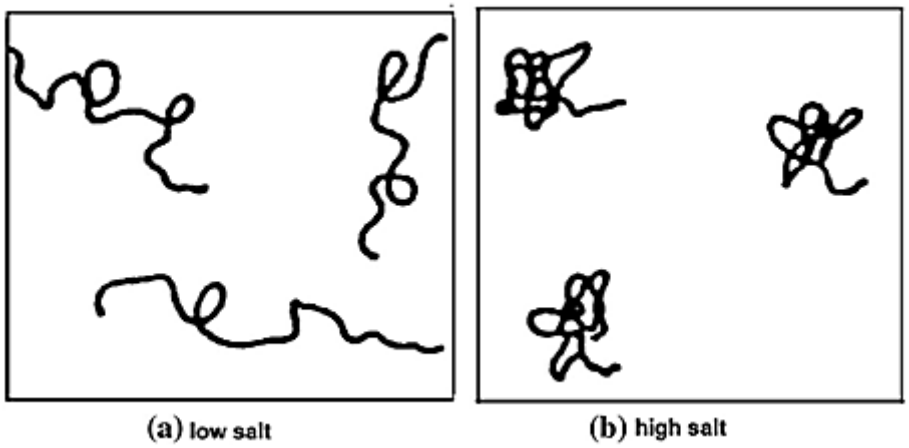

Figure I.10: Conformation for (a) low salt; (b) high salt [47]

In the case of lower salt concentration of solution, repulsion between the similar charged bodies will be greater, and the polyelectrolyte will enlarge because of the mutual repulsion of the charges along the chain however, in the case of higher concentration of salts (eg NaCl), the carboxylate group ($–COO^-$) on the backbone of the polymer is surrounded by the Na^+ cations, which coat the charge. Then again, $–COO^-$ group is lower, the thickness of the electric double layer decreases also, the hydrodynamic volume of the polymer be little, and the viscosity decreases **(See figure I.10)** [70].

Increase electric charge is very important because the presence of divalent ions for example Ca^{2+} and Mg^{2+} attach strictly to the $–COO^-$ on the backbone of HPAM. They reduce the viscosity of the polymer solution again and could result in precipitation of the polymer from solution [59, 71].

c) Other factors affecting the stability of polymers

In most cases, high shear conditions are sometimes encountered when: (1) transporting the polymer solution into pumps prior to injection, primers and valves (2) preparation and mixing the polymer solution in tanks, and (3) injection of polymer solutions, breaking down polymer chains at a loss of viscosity and hence the effectiveness of polymer flooding operations, the polymer is sensitive to the shear rates [72-74]. The behaviour of polymer solutions during their use in flooding operations can be affected by the pH changes. Low value of pH causes the protonation of carboxyl group present in the backbone of HPAM

polymer solution [75]. Hence, the polymer associates the hydrogen ion (H^+) to form an electrostatic repulsion of the inter molecular polymer. Thereafter, the effective screening of the polymer $–COO^–$ groups by the H^+ reduces the electrostatic repulsion within the polymer chain and the intermolecular action becomes weak. Thus, a tightly coil conformation of the HPAM molecules take place resulting in a decrease in the polymer viscosity [58].

Moreover, the presence of different contaminants affects negatively the viscosity and rheological behaviour of polymer. Iron (specifically Fe^{3+}) and oxygen often lead to oxidative degradation of HPAM polymer. Treiber, Yang and Shupe have studied in their research, the chemical stability of Hydrolyzed Polyacrylamide formulations and confirm that the mechanism of polymer degradation was governed by the presence of oxygen content in the solution, although they remarked that limited level of oxygen produced only limited degradation. The contaminants reduce their viscosity and chemical stability when it attacks the polymer [76-78].

II. Nanotechnology used for Enhanced Oil Recovery applications

II.1. Generality

The applications of synthesised nanoparticle in oil and gas industry is very important, many researchers have focused on this way to understand different mechanism which can improve academic and industrial interpretations. For this reason, the efficiency of different nanoparticles such as silicon oxide, alumina oxide, nickel oxide and titanium oxide for enhanced oil recovery from Berea sandstone were investigated by Alomair et al [79]**.** Mixed nanofluids injection exposed interesting results for better incremental oil recovery than other nanofluids, blends of silica and aluminum oxides at 0.05% concentration exposed an interesting incremental oil recovery among the others. Again ,The use of metal oxide nanoparticles for enhancing oil recovery has been done by Torseater and Hendraningrat (2014) [80] which compared the study with alumina (Al_2O3) and titanium (TiO_2) against silica (SiO_2) in case of Berea sandstone. In their conclusions, in was found that the nanofluids is more stable by varying the pH and surface conductivity use when the povidone is used as dispersant. They also stated that metal nanoparticles have higher recovery factor than silica nanoparticles. In other study, the performances of different nanoparticles and Nanofluids with different base solutions were studied by Ogolo et al [81-84]. They used different

nanospheres such as Silicon, Zirconium, Nickel, Zinc, Magnesium, Alumina, Tin and Iron in oil experiments with base fluids such as ethanol, distilled water, brine, and diesel. Among these nanoparticles alumina and iron nanoparticles were the best and gave best results. New synthesized monodispersed Al-suphonated polycarboxylic acid (Al-SPCA) nanospheres were elaborated by Later Yan et al [85-87] which are able to pass rapidly through the porous media. The size of these nanomaterials synthesized was controlled by applying hydrothermal synthetic method at about 80 nm with urea as slow neutralization agent. In the same trend, Alaskar et al. [88] have studied experimentally silica by synthesis root to prepare zinc-phosphonate blends the flow of nanospheres and microspheres through porous and fractured media. Their indicate that surface charge, particle size distribution, shape are the main influential parameters which can affect the transportation of nanospheres through porous media.

Several methods have been proposed in the past to improve the behaviour of polyacrylamide, their efficiency in high temperature and high salinity reservoirs and prevent the shear degradation of their molecules. Kamal et al. [47] published an interesting review of newly developed polymers for EOR while some were unsuccessful for EOR applications, others were found to be uneconomical. New trends in polymer EOR involves the incorporation of nanoparticles to polymers used during flooding operations to modify the viscosity of polymers used in EOR process.Recently, the advantages of nanoparticle application in EOR operations is the improvement of the overall oil recovery factor due to their unique properties such as small sizes and greater surface area per unit volume for different scales such as thermal properties (heat transfer), and properties of mechanical strength like ultra-high strength of material[89]

Several laboratories have been focussed on the application of nanoparticle. Using nanotechnology approach, many scientific demonstrate that addition of nanoparticles into polymers in solutions can lead to high-performance polymer characteristics, such as improved thermal, chemical resistance, enhanced viscosity and rheological behaviour and on the other side what traditional polymeric materials reveal. The mixture of nanoparticles and polymer system separately interact through several forces depending on the solution conditions which gouvern properties of the complex solution formed and at the same time

order the phase behaviour of their complex system. Maghzi et al. [90, 91] studied the effect of nanoparticle on the enhancement of polymer viscosity and states that the concentration of 0.1% nanoparticle added developed a higher viscosity than polymer solution alone even at same shear rate.

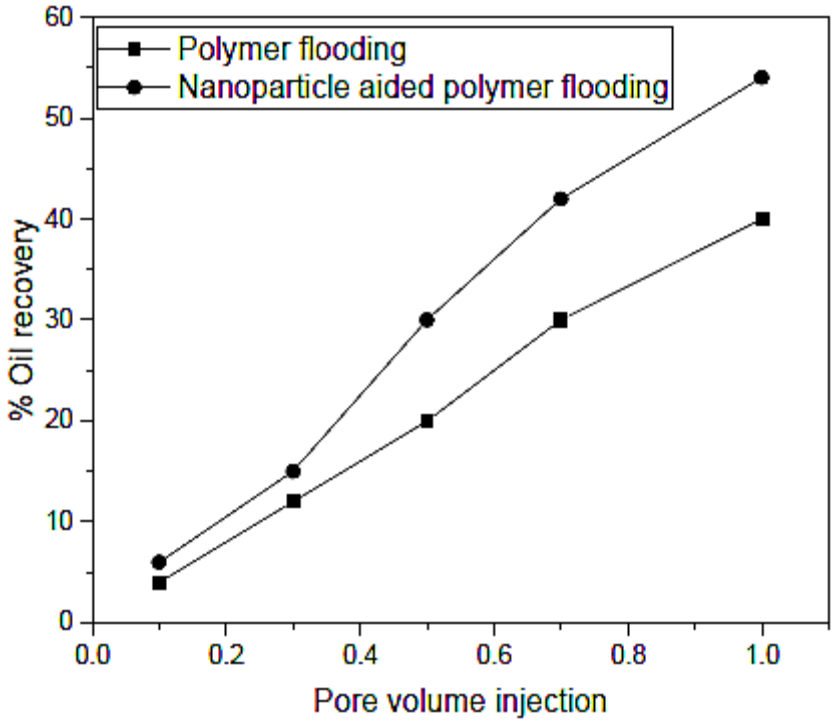

Figure I.11: Oil recovery (% OOIP) versus Pore volume injection of Polymer flooding/ nanoparicle compared to polymer flooding [92]

Addition of nanoparticles to polymer solution creates a network with polymer chain and as a result the viscosity of the solution increases and so an increase of oil recovered rate as seen in the **figure I.11.**

II.2.Previous work

Several developments related to the use and application of nanotechnology and hybrid polymers to oil recovery have focused on silica (SiO_2) because they are highly stable, have a high specific surface area, widely available in different sizes and can work effectively in the presence of other molecules. In this perspective, SiO_2-type is widely regarded as the reference nanospheres to be applied in the oil and gas industry. Recently, various nanomaterials have been contemplated and have been proposed as additives to improve the efficiency of polymers for EOR applications. This includes non-metallic oxide such as

nanoclay, carbon nonmaterial's (Graphene and carbon nanotubes) and metal oxides such as alumina (Al_2O_3), iron oxide (Fe_2O_3) and titanium oxide (TiO_2). Copper (II) oxide, CuO , nickel oxide (Ni_2O_3), magnesium oxide (MgO) , tin oxide (SnO_2), oxide of zinc **(**ZnO**)**, zirconium oxide (ZrO_2) [91, 93-98]. Based on the various studies conducted on the hybrid suspension of nanoparticles and polymers for recovery, the incorporation of the these substances leads to an improvement of the wettability, rheological behavior and viscosity, shear stability, as well as lower adsorption, resulting in the polymer injection process [92, 99-102]. Besides, higher incremental oil recovery for a composite system based on polymer /nano system studied by Barati et al [103] which could be explained by two important reasons. At first, they proposed that since nanoparticles are small enough to facilitate the penetration through little pores. These nanospheres could cause the augmented polymer solution to have less retention in porous media compared to conventional polymeric solution. The second suggestion was to refer the incremental oil recovery to improved rheological behaviour of polymer solutions in the presence of nanoparticles. To summarize this part, the blends of nanoparticles /polymers beyond a doubt improves the proprieties of polymeric systems such as viscosity and viscoelasticity of polymeric systems. Table 1 illustrated the different works by several authors.

TableI.1: Tabulated form of some works in the literature on laboratory experiments of composite system based on HPAM polymer

Authors	Objectives of work	Nano used/C_{nano}/ Size	Polymer/ Mw/ Cp	T (°C)	Salinity
Sharma et al. [104]	SiO_2 effect of an oilfield polymer on the interfacial tension	SiO_2 (**15 nm**) 5000–20000ppm	HPAM (ND) 1000ppm	30-60-90	-/-

Zheng et al. [3]	Effect of dispersed silica nanoparticles on the viscosity of HPAM at high temperature and high salinity conditions	SiO_2 hexamethyl modified dispersed nanosilica DNS—HD hexadecyl modified dispersed nanosilica (5000–20000 ppm)	HPAM **($2*10^7$) g/mol)** 1500–5000 ppm	80	NaCl, $CaCl_2$, $MgCl_2.6H_2O$ Na_2SO_4 Na_2HCO_3 60,000 ppm
Hu et al[67].	Using silica Improve the rheological properties of partially hydrolysed polyacrylamide for enhanced oil recovery	SiO_2 (**12 nm**) (0–10000 ppm)	HPAM **($5-22*10^6$ g/mol)** 1000–10,000 ppm	25.8	NaCl 80,000 ppm
Abdullahi et al[105].	Influence of $Al2O_3$ and TiO_2 on rheological and core flooding properties of HPAM	Al_2O_3 **(20-30 nm)** TiO_2**(20 nm)** (0–10,000 ppm)	HPAM **($13*10^6$Da)** 2000 ppm	27-50-70	NaCl 30,000 ppm
Cheraghian et al. [106]	Examine the roles of TiO_2 on polymer viscosity and improve heavy oil recovery	TiO_2 **(< 100nm)** (0-25,000 ppm)	HPAM **($12*10^6$)** 1200 - 4200 ppm	20-50	NaCl, Na_2SO_3, $CaCl_2$, $MgCl_2.6H2O$ Na_2HCO_3 20,000 ppm

Lima et al. [107]	Investigate rheological degradation rates and residual viscosities under shear rates conditions typical of simulated oil well injections	Carbon Black (**12 nm**) (0-10 ppm)	HPAM 2000 ppm	70	NaCl, KCl, KBr,$CaCl_2$. $2H_2O$, $MgCl_2.6H_2O$, Na_2SO_4 160,000 ppm
Cheraghian [108]	Investigate the potential of polymer flooding for heavy oil recovery with focus on the roles of clay nanoparticles on polymer viscosity and improved oil recovery	Clay **(<50 nm)** 9000 ppm	HPAM **($13*10^6$Da)** 3300 ppm	-/-	NaCl, $CaCl_2$, $MgCl_2.6H_2O$, Na_2HCO_3 20,000 ppm
Rezaei et al. [109]	Effect of surface modified clay nanoparticles (SMCN) on rheological behaviour of HPAM solution versus temperature and salinity	Clay (100-2000 ppm)	HPAM **($6*10^6$)** 2000 ppm	30-60-90	NaCl, $CaCl_2$, $MgCl_2$ 2000-100,000 ppm
Yousefvand / Jafari[99]	Performance of nanosilica/HPAM in the presence of salt on the oil recovery factor	SiO_2 (**11-13 nm**) 5000 ppm	HPAM **($16*10^6$Da)** 800 ppm	-/-	NaCl 30,000 ppm
Khalilinezhad et al. [110]	Effects of silica nanoparticles on flow behaviour of polymer solution in porous media by employing experimental and simulation studies	SiO_2 **(<75 nm)** 4500ppm Clay 9000ppm	HPAM **($12*10^6$Da)** 3150 ppm	-/-	NaCl, $CaCl_2$, $MgCl_2.6H_2O$ 20,000 ppm

Zeyghami et al. [111]	nanosilica addition on the thickening and stability of polymer solutions	SiO_2 (1000-40000 ppm)	HPAM, Sulphonated **(8 MDa)** PAM 1000 ppm	-/-	NaCl 1000 – 32,000 ppm
Haruna et al. [112]	Effect of temperatures / different salinity and long-term stability of on the rheological properties of GO/HPAM .	Graphene Oxide (GO) (100 -1000 ppm)	HPAM **(10 MDa)** 600ppm	25-85	-/-
Ehsan Aliabadian et al. [113]	Rheological behaviour study of HPAM/ AEROSIL 300 under the effect of salt and temperature	10000 ppm AEROSIL 300 20000 ppm AEROSIL R816	HPAM **($20*10^6$ g/mol)** 4000 ppm	35-70	NaCl 10000ppm
Giraldo et al. [4]	Thermal stability /rheological behavior of hydrolyzed based on HPAM/SiO_2	SiO_2 (**7 nm**) (100-3000 ppm)	HPAM **(6-8 MDa)** 500 ppm	25-70	-/-

II.3.Viscosity / Rheology

A study of polymer flooding was conducted by Maghzi et al. which have performed a series of polymer flooding in micromodel saturated by crude oil in order to study the role of nanoparticle effect and salt concentration effect on the nanocomposite system based on HPAM polymer. Different solutions of blend HPAM/Silica with different salinities are used as injectant during the flooding experiments. Measurements of viscosity were used to analyse the results of polymer injection and oil recovery values at different salinities. They found that the viscosity of silica nanosuspension was higher with increasing nanosphere concentration compared to HPAM polymer alone at the same salinity [91].

In addition, when the salt concentration increases, oil recovery decreases during HPAM injection, whereas, in the case of flooding with silica suspension in polyacrylamide matrix, an important oil recovery factor was obtained [90].

An experimental study of the Surface Modified Clay nanoparticles effect on the rheological behaviour of HPAM solution was conducted by Rezaei et al.[109] This type (SMCN) could resist against the elevated temperature, salinity and its ability to improve polymer flooding. The results indicate that the location of the clay between the polymer chains was found to cause an increase in the viscosity of the solution and enhance the polymer solution resistance against salinity, temperature, shear stress and mechanical degradation.

The role of another type of nanoparticle, TiO_2 on the enhancement of polymer viscosity and the consequent oil displacement efficiency was studied by Cheraghian et al. under synthetic field brine of 20,000 ppm containing varying proportions of monovalent and divalent ions. The formulation composed of HPAM/TiO_2 exhibit outstanding flow behaviour at shear rates of 0.001-100 s^{-1}[106]. Moreover, Kumar et al. used the TiO_2 to reduce sedimentation rate and homo-aggregation and enhanced the viscosity of HPAM/ TiO_2. Results from ultraviolet visible spectroscopy (UV–vis), electrical conductivity and scanning electron microscopy (SEM) confirmed that the presence of TiO_2 enhanced the dispersion stability for more than 10 weeks and led to an improved rheological behaviour of the nanocomposite system [114].

The effect of carbon black (CB) nanoparticles on the rheological properties of HPAM under high temperature and high salinity conditions was examined by Lima et al. because of the excellent chemical and thermal stability of the additive. Carbon Black surfaces were sequentially modified with ethylenediamine because of its poor dispersibility in polar solvents. The nanopolymer formulated exhibited 50% higher viscosity than the conventional polymer itself at 70°c and 0.6 mol/L ionic strength [107]. However, the hybrid dispersion was more stable under static conditions, thereby could be a good alternative for EOR applications. In the same context, an excellent formulation based on HPAM polymer and using multi walled carbon nanotube was developed by Kadhum et al. which demonstrated a high stability under elevated temperature (80°C) and salinity [115]. Hu et al. studied the effects of different temperatures, salinities, and ageing times on the rheological behaviour of HPAM/SiO_2 for chemical enhanced oil recovery case. Their experimental results show that

the incorporation of Silica significantly increased the viscosity of Hydrolyzed Polyacrylamide. Also, they found that the formulation exposed an impressive stability compared to ordinary polymer solution [67].

Gbadamosi et al. appraised the impact of Al_2O_3-HPAM and TiO_2-HPAM formulations on the rheological behaviour proprieties in different electrolyte solutions of monovalent and divalent ions at different shear rates. It found that the presence of Alumine and Dioxyde of Titane shielded the dilute polymer solution and minimised their degradation in the presence of synthetic reservoir brines [2]. In another study, the effect of (GO) as additive for the improvement of EOR polymers viscosity under at different concentrations of GO and for two temperatures (25°C & 85°C) which was illustrated by Nguyen el al in the **figure I.12.**

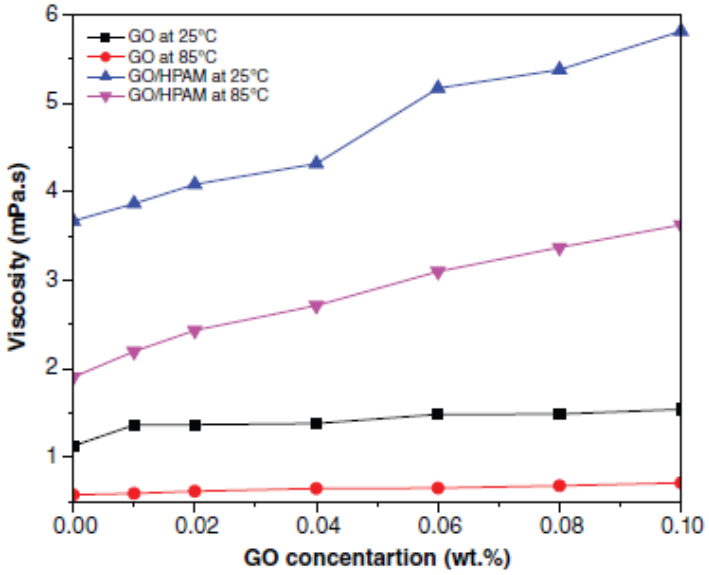

Figure I.12: Viscosity measurements of HPAM/GO formulations (C_{HPAM}=500 ppm; shear rates=1000 s^{-1})

The mechanism governed these interactions is good distribution of the GO's in the polymer network resulting from the integration of hydrophilic polymer chains and the functional group in the GO's surfaces [98].

II.4.Adsorption of polymers in chemical Enhanced Oil Recovery

The adsorption experiment of polymer on reservoir rock was conducted by Cheraghian et al. [116] which also investigated the presence of clay and SiO_2 on the adsorption of water-soluble polymers onto the solid surfaces of sandstone and carbonate rocks. It was shown in the **figure I.13** that the polymer mixed with nanoparticle have less retention obtained from static adsorption experiments based on weight per cent than polymer alone, and indicate that nanomaterials play an important role in the case of polymer adsorption on rock surface. The viscosity and rheological behaviour were not affected negatively which led to a higher oil recovery.

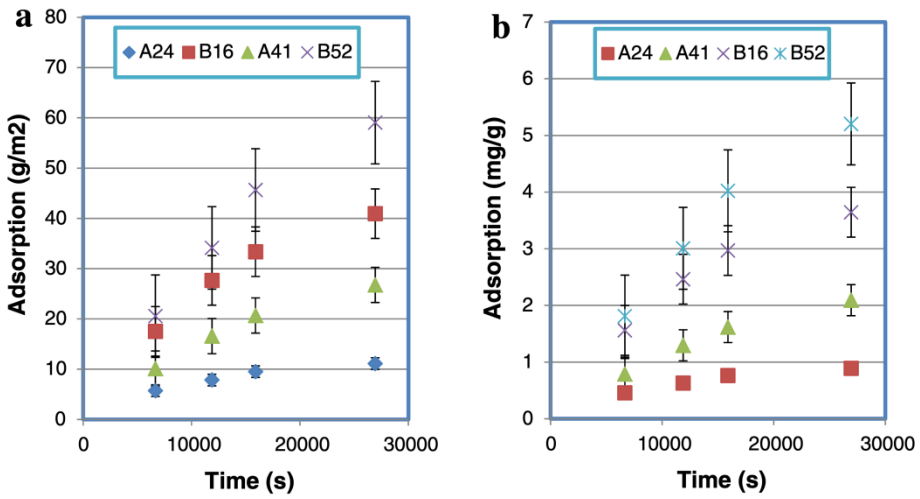

Figure I.13: Effect of nanoparticle on the adsorption of polymers (Cp=2000 ppm,TDS=20000ppm, T=20°C)

In the same context, the static adsorption of nano-SiO_2-polymer suspension on sandstone rock was evaluated by Khalilinezhad et al. [117] and AlamiNia et al. [118]. Based on their experiments, the results indicate ultra-low values of nano-polymer suspensions adsorption compared to conventional HPAM solution. Bagaria et al. [119] studied the stability and transportation behaviour of iron oxide nanoparticles in the presence of poly (2-acrylamido-2-methylpropane sulfonate-coacrylic acid) (AMPS–co–AA). Due to the steric stabilisation between the nanoparticle and polymer, the hybrid dispersion formed displayed colloidal stability in standard American Petroleum Institute (API) brine (8 wt% NaCl + 2 wt% $CaCl_2$) for 1 month at 90 °C and resist unacceptable retention on silica surfaces. Wisniewska et al. [120]

examined the adsorption interaction of Al_2O_3 and anionic polyacrylamide at different pH (in the range 3–9) ,temperature (15–35 °C) and carboxyl groups presents in the PAM (in the range 5–30%) based on turbidimetry method. The authors indicate also that polymer adsorption process causes the thermal stability changes of the hybrid systems. Moreover, the polyacrylamide adsorption decreases with variation of pH. At lower pH 3, adsorption proceeds due to hydrogen bond formation and slight electrostatic attraction for all examined temperatures. Meanwhile, stronger electrostatic interaction between the positively charged Al_2O_3 surface and negatively charged polymer surface accounts for the adsorption at pH 6. The smallest polymer adsorption is recorded at pH 9 as a result of repulsion between the polyacrylamide chains and Al_2O_3. Finally, they observed that large amounts of polyelectrolyte are adsorbed when the content of anionic carboxyl group and temperature are high [120, 121].

II.5.Shear stability and Degradation of composite systems in chemical Enhanced Oil Recovery

In order to overcome the major problems that may be related to the low shear stability of polymers commonly used for oil displacement, A copolymerization of nano- SiO_2 with acrylic acid (AA) and acrylamide (AM) polymer in order to obtain Hydrolysed Polyacrylamide nano-SiO_2 (HPMNS) suspension was carried out by Lai et al [72] **.** The result indicate a good shear resistance of the formulated HPMNS and a higher oil recovery compared to HPAM alone after shearing with Mixing Speed Governor and porous media shear model.

In the same context, another study was conducted by Zhu et al [122, 123] which developed nanopolymer hybrid suspension by incorporating silica nanoparticles into hydrophobically associating polyacrylamide (HAPAM) solution. A systematic effect of high salinity conditions (32868 ppm), high temperature (85 °C) and silica nanoparticles concentration on the shear resistance and rheological behavior was investigated. As illustrated in the **figure 1.14,** they concluded that HAHPAM/silica hybrid possesses a better long stability under high temperature observed and that the shear viscosity of corresponding HAHPAM solution was lower than hybrid nanopolymer suspension with the addition of silica nanoparticles and they exhibited a better shear resistance than the HPAM alone.

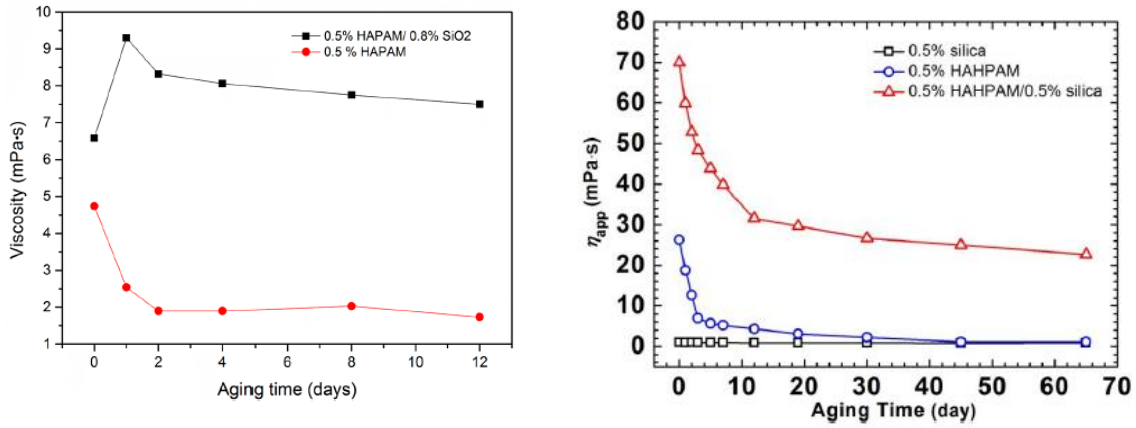

Figure 1.14: Long term stability of different formulations based on HAPAM polymer (T=85°C, TDS=32868 ppm (left), HPAM/Silica T=80°C; 8% NaCl)

This gap is mainly due to the physical interactions between HAPAM/silica and which can avoid the hydrolysis of amide in high-salinity and high-temperature oil reservoirs.

The shear degradation of nanopolymer suspension at typical reservoir shear rates was evaluated and the experimental data was validated with power law model by Rezaei et al [109] .Their results confirms the trend of previous work and state that by adding clay nanoparticles to polymer solution, the pseudoplasticity and shear-thinning behaviour of the polymer was improved in the case of low shear rates which can prevent the shear degradation of polymers in this region, the presence of the clay nanoparticle in the nanopolymer suspension enhances the mechanical degradation and resistivity of the polymer solution. Zhongliang Hu et al [67] studied the HPAM viscosity and shear degradation on the shear rate parameter (T= 85 °C; no electrolytes) in absence and presence of Silica. It exposes interesting shear stability when the HPAM concentration was lower than 0.1 wt %, the viscosities were independent of the shear rate, behaving like Newtonian fluids. However, shear-thinning effect was observed when the concentration was over 0.1 wt %, and the viscosities were gradually reduced with an increase of the shear rate. Recently, Mohammed Bashir Abdullahi et al**.** [105] have conducted a study to solve polymer chemical degradation challenges by investigating the influence of NPs types on HPAM solution viscosity under saline environment (30000 ppm) and at elevated temperature (up to 70 °C). The rheological properties of nano-HPAM hybrid dispersions were examined in the presence of mono- and divalent ions at different shear rates and NPs concentrations. The results revealed that increasing the salt dose decreases viscosity of the polymer solutions.

II.6. Mechanism of HPAM/nanoparticle systems for cEOR

Maghzi et al. [90] states that the reaction is not the same for the composite system of polyacrylamide/ nanospheres because when nanoparticles were incorporated under saline water which contains either monovalent or divalent ion or both, an ion–dipole interaction is created between the oxygen atom and the cation of the salts onto the surface of the nanoparticles. As a result, the diminution of polymer solution viscosity is not observed in the presence of the SiO_2 nanospheres used and the attack of cations on polymer molecules is decreased by the effect of these nanoparticle shielding.

Several authors reviewed the mechanism of different formulations based on the incorporation of different types of nanoparticles with Hydrolyzed Polyacrylamide. In the same context, the rheological properties of partially hydrolysed polyacrylamide seeded by SIO_2 nanoparticles was tested by Zhongliang Hu et al [67], and showed an excellent thermal stability after 12 days at T = 80 °C, and the viscosity was improved by ~5 times compared to HPAM solution at 0.8 wt % nanoparticles loading. The reason of viscosity incresase could be due to the formation of a hydrogen bond between the carbonyl groups in HPAM and the silanol functionalities on the surface of SiO_2 nanoparticles which were identified by FTIR measurements and illustrated in the **figure I.15**

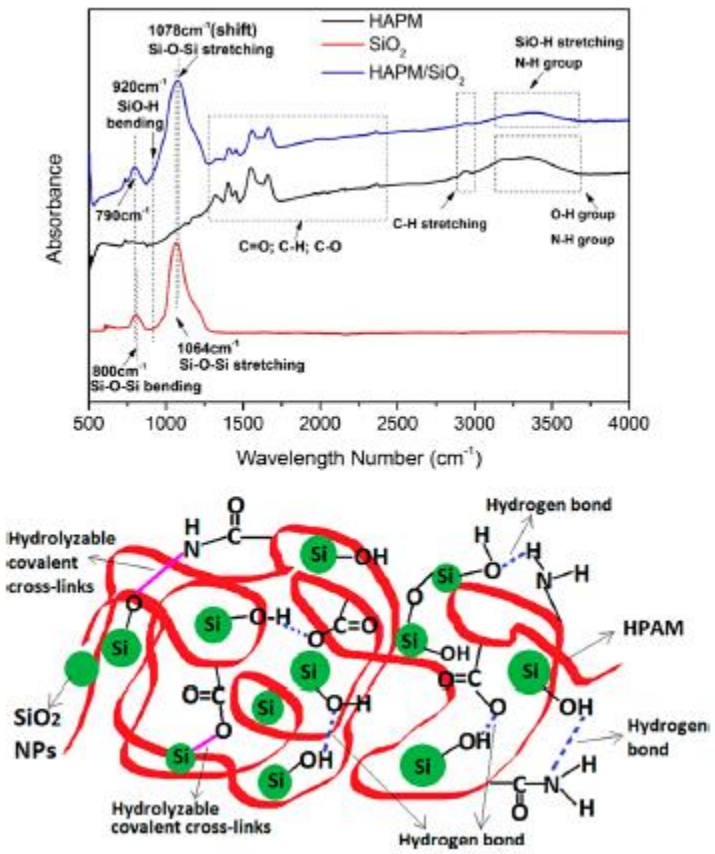

Figure I.15: FTIR spectres for (800 ppm SiO_2, (800ppm) SiO_2/ (500ppm) HPAM,(5 00ppm)HPAM) [67]

In another study, Maje Alhaji Haruna et al, improved the high-temperature stability and rheology of the formulation based on Hydrolyzed Polyacrylamide using Graphene Oxide nanoparticle[124].

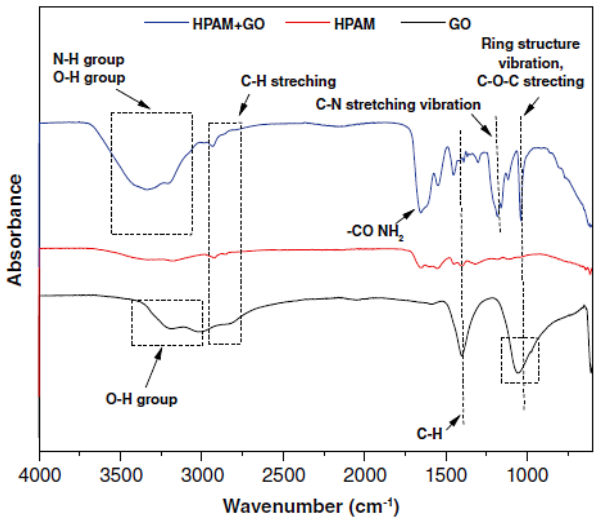

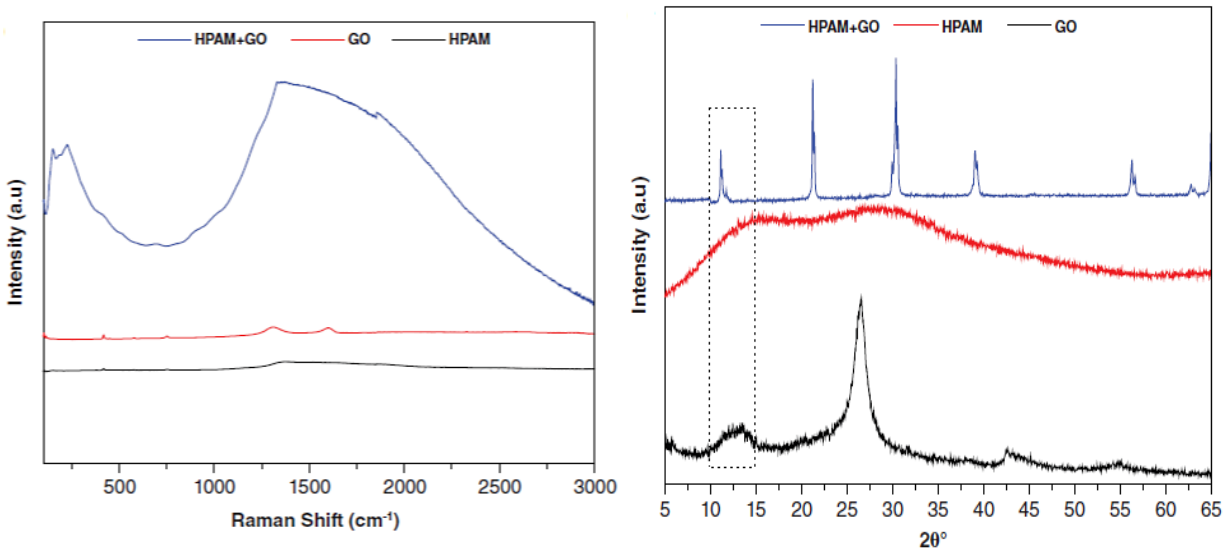

Figure I.16: Identification of HPAM/GO mechanism by (XRD, FTIR and Raman analysis) (C_{HPAM}=2000ppm, C_{NANO}= 0.1 wt%, T=25°C) [112]

As illustrated in the **figure I.16**, their results indicate the formation of electrostatic hydrogen bonding and covalent linkages between the functional groups of Graphene Oxide/ HPAM, leading to enhanced stability and viscosity of formulations. These mechanisms and trends have been confirmed by XRD, FTIR and Raman techniques measurements and other works made by Zhu et al [122, 123] ;

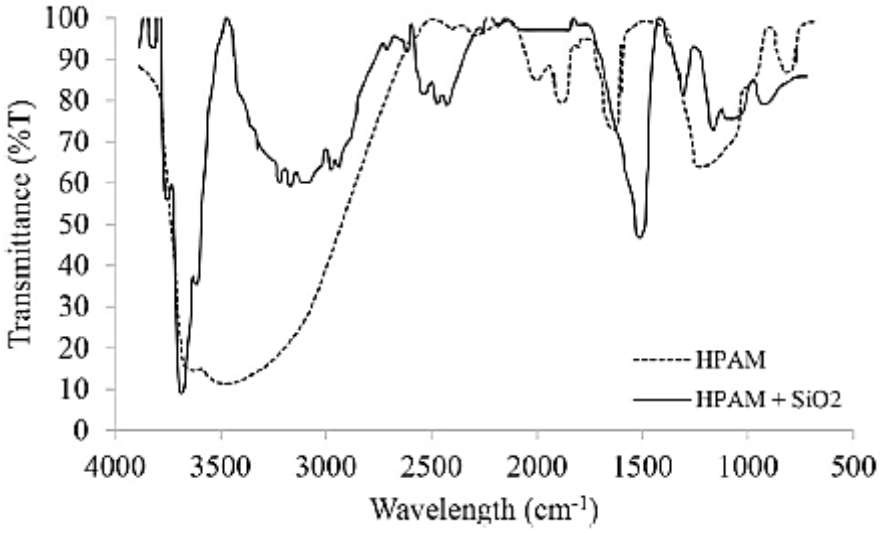

Figure I.17: HPAM – HPAM adsorbed onto SIO_2 spectra [4]

Maurya et al [125]**.** Lady J. Giraldo et al [4] observe the effects of SiO_2 nanoparticle on the thermal stability and rheological behaviour of Hydrolyzed Polyacrylamide based polymeric solutions by FTIR measurements and confirms that the mechanism governing the interaction is the adsorption of HPAM polymer onto SiO_2. **Figure I.17** illustrated the FTIR spectra for the HPAM and HPAM adsorbed onto SiO_2.

III. Formulation of the problem and methodology of the work

The detailed literature review exposed interesting results concerning the improvement of HPAM polymers for EOR and rate of oil recovery using this process. However, based on a large research, there is no work based on the formulation and interaction of Hydrolyzed Polyacrylamide/PSL microspheres. This led us to start a novelty study in order to develop a new formulation based on microspheres with the possibility of application in chemical Enhanced Oil Recovery (cEOR).

To do this, we first tested commercial microspheres to optimize the formulations and see the rheological behaviour of the new systems. The results were satisfactory from a rheological point of view but the cost forced us to synthesize new PSL microspheres in our laboratory (IPREM-Pau-France) by controlling the charge, size and morphology. A novel formulations was developed in the semi-dilute regime ($c_p > c^*$) of polymer and novel mechanism of interaction has been studied based on a new approach of capillary viscosity which enable quantifying the dose of the polymer chains adsorbed on microsphere in the dilute regime of polymer ($c_p < c^*$).

Subsequently, we have finished our work with applicative approach to study the behaviour of our optimized systems under operations parameters such as temperature and shear rates using capillary device.

CHAPTER II: Optimization of Hydrolyzed Polyacrylamide-polystyrene microspheres formulations using design of experiments approach

CHAPTER II: Optimization of Hydrolyzed Polyacrylamide-polystyrene microspheres formulations using design of experiments approach

Résumé

Dans ce chapitre, les effets de renforcement des microsphères de polystyrène dans une matrice de polyacrylamide hydrolysée (HPAM) a été étudiée afin d'améliorer le comportement rhéologique de ce dernier. Le plan d'expérience de Doehlert a été utilisé pour minimiser et optimiser les expériences tenant compte des effets de trois paramètres importants, à savoir la taille des microsphères, la concentration et la variation de la température sur la viscosité newtonienne (η_0) d'un polymère de type HPAM en utilisant la méthodologie de surface de réponse (RSM) et l'analyse ANOVA. Pour cela, différentes microsphères carboxylatées à base de polystyrene et commerciales, ont été utilisée. Les résultats montrent que la taille et la température ont été les facteurs les plus influents et que les paramètres optimaux du procédé sont les suivants: 20 ° C (température); 50 ppm (concentration en microspheres); 1000 nm (taille) pour une réponse prédite η_0 égale à 0,505 (Pa.s) avec une désirabilité du modèle de 0,997. La probabilité obtenue (p = 0,05) indique un bon accord entre les résultats prédits et ceux obtenus expérimentalement par les la méthode RSM.

I. Introduction

Composite systems based on nanoparticle/ polymer formulations are widely used indifferent fields such as drug delivery [126]; cementitious materials [127]; waste water treatment [128], hydogels [129] including contact lenses [130], biomedical, EOR [131, 132] and conformance control applications [133, 134]. The incorporation of these nanomaterials onto the organic matrix of polymer can be established in solid or aqueous phase which were employed to enhance barrier, thermal/ mechanical resistance and rheological properties. In terms of rheological behaviour in solution, the effects on the viscosity and their variation under the effect of shear rate particularly have attracted considerable research interest, especially in dilute or semi-dilute regimes of polymer concentrations [135]. For example, thickening and thinning effects have been obtained with colloidal formulations which depend on a variety of parameters such as the preparation methods, particles volume fraction (concentrations), particles shapes and sizes, temperature and polymer

concentration [136-139]. Many researchers studied the colloidal suspensions interactions to improve the rheological behaviour of HPAM. The introduction of nanosphere can modify the viscosity of polymer solution during polymer flooding to improve sweep efficiency. The conclusions made by Maghzi et al. indicate that strong interaction between silanol functional group of SiO_2 NPs and the polymer chain by forming hydrogen bonding was the mechanism governing the interaction which can increase the viscosity of HPAM polymer[105]. Consequently HPAM/SiO_2 nanoparticle was the most studied system in literature. Zhongliang Hu et al, Lady J. Giraldo et al. studied the novel formulations based on HPAM/SiO_2 nanoparticle to improve the rheological behaviour of polymer [67]. Zhongliang Hu et al. found that the viscosity increased ~5 times that of HPAM at 0.8 wt % NP loading. While Lady J. Giraldo et al. described the non-Newtonian behaviour using the Carreau and Herschel-Bulkley models [4]. In another study, Feng Yan et al studied the mixture of PEO/Silica to improve the rheological behaviour of polymer. The zero shear viscosity of the silica-PEO complexes increased by adding silica nanosphere with variation of particle/polymer number ratio [140].

In situations where relationships between several variables in a process can affect the end result, the design of experiments (DOE) is the appropriate choice based on the systematic variation of the variables by changing them all simultaneously, in a multivariable way, into performing a limited number of experiments, so material consumption is reduced, the cost of experimental work is decreased and experimental time is optimized [141]. Zulhelmi Amir et al. focused on the interaction of Polyacrylamide /Polyethylenimine using the Central composite design (CCD) to determine the optimized crosslinked polymer gel formulation. It was concluded that the viscosity could be controlled by adjusting both crosslinker and polymer and concentrations based on quadratic equation model[142]. Ghriga et al. tested the design of experiments approach to investigate the gelation time of HPAM/PEI mixtures based on Doehlert approach under different operational factors such as temperature, concentration of polymer and cross-linker and salinity. The most important parameters which affect the response were salinity, temperature and polymer concentration respectively [143]. Mahdi Hasanzadeh et al. studied the behaviour of colloidal concentrated suspensions on the zero shear viscosity using response surface methodology with central composite design. The individual and interaction effects of nanoparticle concentration and

temperature of suspensions showed a significant increase of zero shear viscosity [144]. Jasim Ahmed et al. illustrated the effects of temperature and concentration on the rheological characterization of combination guar and Xanthan gum polymer based on a central composite design and surface response methodology [145]. All factors and interactions considered that the concentration of gum were statistically significantly (p<0.05) and affected the rheological parameters and temperature was the least significant parameter on the viscosity of complex. Furthermore, the authors studied the effect of size and temperature on the rheological behaviour of particle suspensions using design of experiments. The mechanical rigidity of dispersion was influenced by the size of nanospheres while the temperature had the least effect on the rheology of dispersed suspensions [146]. Kennedy et al. demonstrated the previous hypothesis for formulations based on Xanthan Gum and biopolymer namely locust bean gum (LBG) and their combined gel using design of experiments approach. They showed that the addition of nanoparticles could alter the solution properties by favouring the increase in viscosity and elasticity [147].

In this chapter, we have chosen to study the statistical optimization of the rheological effects of a new formulation based on the Polyacrylamide/polystyrene functionalized microspheres (PSL) by carboxylic acid groups in aqueous phase. The main objective is to develop a model able to predict the best formulation with maximum viscosity at zero shear rates using these microspheres under the effects of the volume fraction in PSL (concentration), and their size on a semi-dilute polymer solution (2000 ppm) for a given temperature. The concentration range targeted in PSL is very low (< 1000ppm) compared to the concentrations usually described in the literature taking into account the economic aspect and the geometrical aspect of the formulations used which will be discussed in the following chapter III. Analysis of Variance (ANOVA) was also used to statistically assess the influence of each parameter on the response. The main effect and interaction graphs were extracted from the JMP8 software for analysis and interpretation of the experimental results. These methodologies fills the gap to divulge and explain in a schematic and summarized way the practical use of Doehlert design when many variables are present in polymer engineering and science.

II. Materials- Methods-Equipment

II.1. Materials

Polystyrene microspheres with a functionalized surface carboxylate were provided by Polyscience (France) and were used as supplied. Briefly Polysytene microspheres at different concentrations (100, 200, 300, 400, 600, 800 and 1000 ppm) were dispersed in milli Q water (resistivity of 18.2 M Ω cm) to form a stable dispersion. High molar mass of Partially hydrolysed polyacrylamide (HPAM), used as reference polymer, was kindly provided by SNF Floerger, France. The Hydrolyzed degree (HD) was calculated using the ^{13} C-NMR measurements using a Bruker Avance 400 MHz spectrometer based on the methods described in the literature, which was solubilized in deuterated water (D_2O) at a concentration of ~ 25 mg/ml, and analyses were performed at 25 °C. HD was determined as the ratio of the integrated areas under the peaks at 180 and 182 ppm, which corresponds to carbon in the carbonyl groups in the acrylamide and acrylate units (**figure II.1**), respectively [148, 149]. Sodium chloride (NaCl) (Sigma Aldrich) was used to make the water salinity.

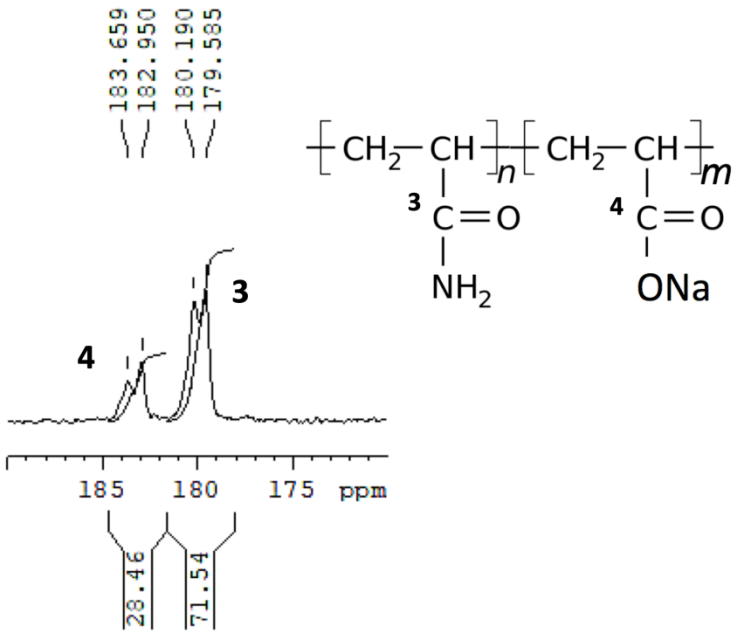

Figure II.1: RMN spectra of HPAM polymer

Rodriguez et al (**figure II.2**) [150] have developed in the laboratory IPREM a new capillary Rheometer, which was employed to measure and calculate the viscosities and in particularly

the intrinsic viscosity of dilute solutions of HPAM (c_p < c*) prepared in 6 g/l NaCl water salinity

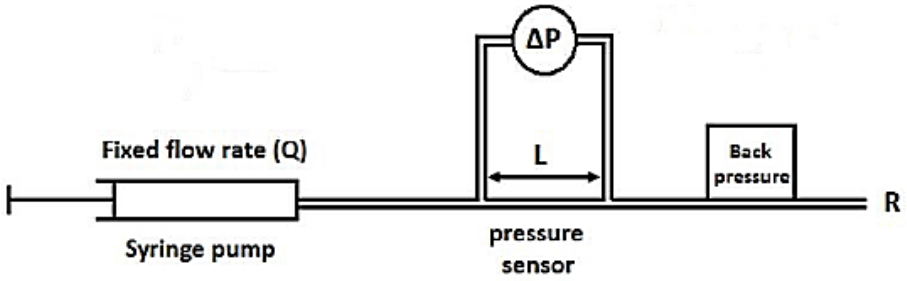

Figure II.2 : Capillary viscosimeter used in this study [150]

In the experimental device, A volume of 12 mL of different dilute solutions of HPAM were passed inside 1.3-m-long (PEEK) using a syringe pump (neMESYS mid pressure syringe pump) in oven at 20°C with an internal radius of 254 µm for different flow rates ranging from 3 to 0.25 µl/s to obtain shear rates as shown in figure II.2. The plot of the pressure drop (∆P) measured versus flow rate (Q) allows to calculate the viscosity using Poiseuille's law.

In the semi dilute regime of formulations (c_p > c*), the steady rheological studies were performed using a Bohlin Gemini Rheometer (Malvern Instruments, England) with coaxial cylinder geometry (DG 26.7) ,bob-cup system (inner radius 25.0 mm, height 37.5. mm and outer radius 27.5 mm) which acquired a sample volume of approximately 12 mL.

The characteristics of the Polyacrylamide/PSL microspheres solutions with concentrations of PSL ranging from 0 to 1000 ppm prepared in 6 g/l NaCl water were tested under steady shear rates between 0.001–100 s^{-1}. The tested temperatures were 20, 50 and 80 °C. The rheological behavior of polymer solutions in the absence or presence of PSL microspheres was modelled by the Carreau equation, and this model describes both the Newtonian and the shear thinning behaviours (eqn (II.1)).

$$\eta = \eta_{inf} + (\eta_0 - \eta_{inf})(1 + (\lambda\dot{\gamma})^2)^{(n-1)/2} \qquad \text{(II.1)}$$

Where η_0 and η_{inf} are the viscosity at zero and infinite shear rate (Pa s), l is the relaxation time (s) and n is a power index. Each sample was measured at least 3 times to check the reproducibility.

II.2. Determination of Intrinsic viscosity & molar mass of polymer

The intrinsic viscosity makes it possible to determine the average molar mass according to the Mark-Houwink law. The equation that defines the relationship between these two parameters is:

$[\eta]=k*M^a$ (2)

Where M, is the molar mass of the polymer chain; a and k are the Mark-Houwink constants and depend on the solvent-polymer pair. There are specific values of these constants for each of the combinations, solvent – polymer. Intrinsic viscosity measurements [η] were performed only in the dilute regime ($c_p < c^*$).In this work, we used the classical method by carrying out several dilutions and several measurements of reduced viscosities. When the dilution is sufficient, the reduced viscosity η_{red} is characterized by the Huggins equation (II.2):

$\eta_{red} = [\eta] + k_h[\eta]^2$ (II.2) ; k_h : Huggins coefficient .Moreover, the inherent viscosity could be used as follow:

$\eta_{inh} = \frac{\mathrm{Ln}\,\eta_r}{c} = k'' [\eta]^2 c + [\eta]$ (II.3); k'' is the Kraemer coefficient with k'- k'' should be equal to 0.5. After that, we obtain two lines whose ordinate at the origin is $[\eta]$.

II.3.Preparation of HPAM/ PSL microspheres formulations

In order to study the optimization of different formulations, concentrated stock polymer solutions were first prepared by the dissolution of the appropriate amount of polymer powders in PSL aqueous solution (Polystyrene microsphere+ milli Q water) under gentle magnetic stirring for 1 day at room temperature. NaCl powder was then poured into these solutions and the solution was stirred using a magnetic stirrer at 300 rpm and room temperature for another day. Before the measurements, these solutions were kept standing overnight to reach equilibrium.

II.4.PSL microspheres characterization (shape, size, zeta potential)

a) Microscopy

Scanning Electron Microscope (SH3000, Hirox, South Korea) was used to examine the shape of different carboxylate Polystyrene microspheres. Samples were placed on a copper-plate and coated with gold in a sputter coater (Denton Vacuum). SEM images were then collected using a field source emission of 20 kV accelerating voltage.

b) Zeta potential evaluation

Millipore water systems were used to obtain either deionized or ultrapure water (MilliQ®) in the IPREM laboratory of Pau. The surface charge of PSL microspheres was estimated by zeta-potential measurements using a Wallis zetameter Cordouan-Technologies, Pessac, France) at the temperature of 25 °C. Before the tests, the cell was rinsed carefully with ethanol and deionized water to ensure the accuracy of the measured data PSL samples at different sizes were diluted in milli-Q water to reach a final concentration of 100 ppm. For each sample five measurements were performed and the data were processed using the ZetaQ software.

c) Dynamic Light scattering (DLS)

The stability of PSL microspheres was characterized by Dynamic Light Scattering (DLS). This technique measures the light scattered of colloidal particles due to their Brownian motion, and associates its intensity with their size based on in *situ* DLS probe (Vasco flex, Cordouan Technologies) which was used to determine the hydrodynamic diameters at an angle of 170°.

The autocorrelation functions were fitted using the Cumulant algorithm to obtain the z-average diameters and polydispersity index (PID) (D_w/D_n), where D_w is the weight average diameter and D_n is the number average diameter. The samples of different samples were prepared and diluted in MilliQ water to ensure the targeted concentration of 100ppm for a good measurement

II.5.Experimental design and statistical analysis

The response surface methodology (RSM) is an empirical modelling technique, which mathematically corresponds to the experimental domain studied in the design, assessing the

relationship between the controlled experimental factors at more than three levels. RSM has many advantages, such as adequate distribution of information the experimental range (rotability). The fitted values are very close to the observed ones using minimal number of experimental combinations [151].

This method allows us to find an equation that relates the response with changes in the experimental chemical and environmental variables. The process consists of five main steps: (1) experimental model design selection, (2) regression coefficients estimation, (3) model analysis, (4) best experimental conditions location, and (5) predictive ability verification of the model [152, 153].

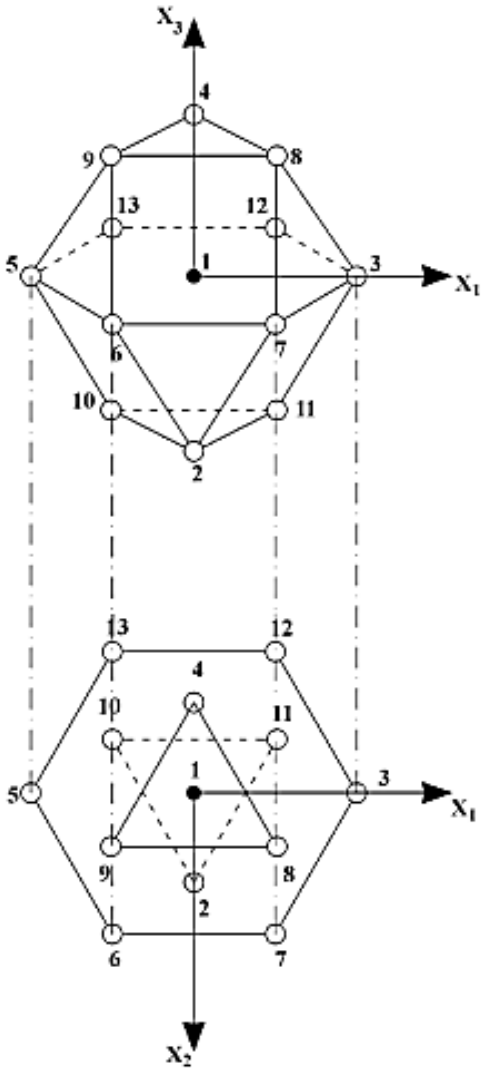

Figure II.3: Scheme of Doehlert design composed of 13 points uniformly distributed in the experimental domain and two additional points in the center of design. Experimental variables: Size (X_1), Concentration of PSL microspheres (X_2) and Temperature (X_3) [154].

Doehlert designs can be used in optimization processes, because they consist on a set of points uniformly distributed in a cubo-octahedron distribution of points over the whole experimental region ,as shown in **figure II.3** with a total number of experiments 13 with two replications of the center point [155-157]. They require the same number of experiments, N, related to the number of variables under study, k, as do Box–Behnken designs ($N = k^2 + k + 1$) [154, 158], but the latter has a structure that does not cover the whole experimental domain and a number less than that used in central composite designs ($N = 2^k + 2k + 1$).

Furthermore, in central composite and Box–Behnken designs, the number of levels, l, for each variable is always the same (for k = 3, l = 5 in a central composite design or l = 3 in a Box–Behnken design). In Doehlert design, the first variable is studied at five levels, the second at seven levels and the third at three levels. This makes it possible to select the order of the variables, to study the most critical at five and seven levels and considering only three levels for the least critical. Therefore, RSM has been selected to study the simultaneous effect of temperature and size of microspheres on the rheological behaviour of Polyacrylamide (HPAM) at a constant salinity of 6 g/L NaCl using the JMP software. Three levels of temperature (20, 50 and 80°C), five levels of PSL size of (50, 200, 520, 750 and 1000 nm) were selected. In our case, 13 experimental run followed by two replications of the central point to evaluate the experimental error. The coded values of our process variables were determined by eq. (II.4)

$$Xi=\frac{X_i - X_0}{\Delta X} \qquad \text{(II.4)}$$

Where Xi is the dimensionless code value of *i*th independent variable, X_0 is the value of Xi at the center point, Xi is the real value of independent variable, and ΔX is the step change value.

Table II.1: Doehlert three factors experimental design with experimental and predicted response by JMP software

Experimental number	X_1	X_2	X_3	Size (nm)	Concentration (ppm)	T (°C)	η_0 Experimental (Pa.s)	η_0 Predicted (Pa.s)
1	0	0	0	520	275	50	0.09	0.09
2	1	0	0	1000	275	50	0.13	0.14
3	0.5	0.866	0	750	500	50	0.04	0.04
4	-0.5	0.866	0	200	500	50	0.08	0.06
5	-1	0	0	50	275	50	0.16	0.15
6	-0.5	-0.866	0	200	50	50	0.11	0.11
7	0.5	-0.866	0	750	50	50	0.10	0.12
8	0.5	0.289	0.816	750	350	80	0.05	0.04
9	-0.5	0.289	0.816	200	350	80	0.07	0.09
10	0	-0.577	0.816	520	125	80	0.02	0.03
11	0.5	-0.289	-0.816	750	200	20	0.40	0.380
12	-0.5	-0.289	-0.816	200	200	20	0.35	0.34
13	0	0.577	-0.816	520	425	20	0.29	0.28
14	0	0	0	520	275	50	0.09	0.09
15	0	0	0	520	275	50	0.09	0.09

The coded and experimental values of the design as well as the experimental responses involved in the design of 2^3 were reported in table 1 is given in the table 1.

$$Y = a_0 + a_1X_1 + a_2X_2 + a_3X_3 + a_{12}X_1X_2 + a_{13}X_1X_3 + a_{23}X_2X_3 + a_{123}X_1X_2X_3 + a_{11}X_1^2 + a_{22}X_2^2 + a_{33}X_3^2 \quad (II.5)$$

Where Y is the viscosity at zero shear rate in (Pa.s). While, the a_0, a_i, a_{ij} represents the global mean. The regression coefficients assigned respectively to the principal factor effects and interactions.

III. Results and discussions

III.1.Characterization of Polymer

a) Intrinsic viscosity versus weight-average molar mass (M_w) and radius of gyration (R_g) of HPAM model in 6 g/L of NaCl

An intrinsic viscosity of $[\eta]$ = 4400 ml/g was determined using capillary viscosity using Huggin and Kramer methodology for experimental data processing To do so, the viscosity of dilute

polymer solutions prepared in 6 g/l NaCl water was recorded using the technique of capillary viscosity described in the materials et methods part.

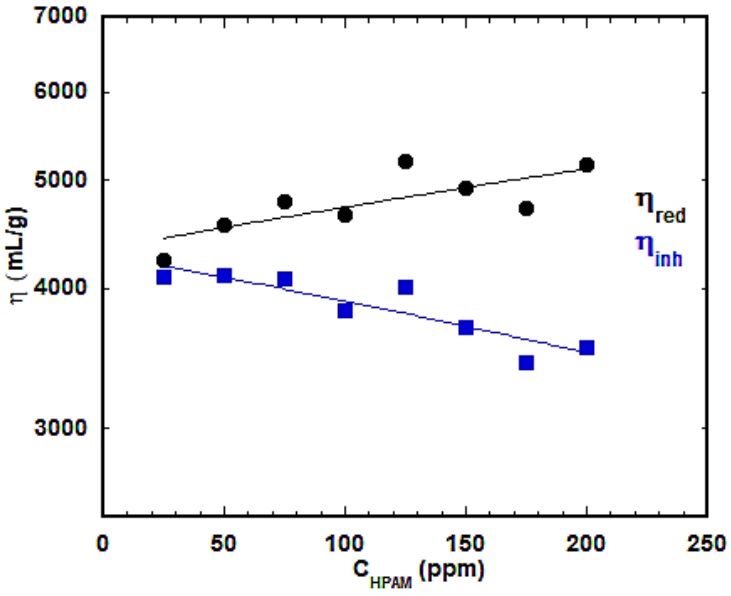

Figure II.4: Intrinsic viscosity [η] of Hydrolyzed Polyacrylamide (HPAM) used from reduced ●η_{red} and ■inherent η_{inh} viscosities

Figure II.4 shows the determination using the relation of Huggins and Kramer according to the equations x and y. The value of VI determined at zero concentration extrapolation is used to calculate the molar mass- mass average-molar mass and the radius of gyration were calculated. To do this, the scale law Rg = 0.022 $M_w^{0.59}$ and $[\eta]$=0.022 $M_w^{0.76}$ (Figure II.5) was established in the laboratory (IPREM) on the model HPAM obtained by controlled radical polymerization. Mw and Rg were determined by SEC-RI-MALS according to a method described in the literature [159]. The radius of gyration and molar mass of our HPAM are as follow : Mw = 10^7 g/mol and Rg = 300 nm.

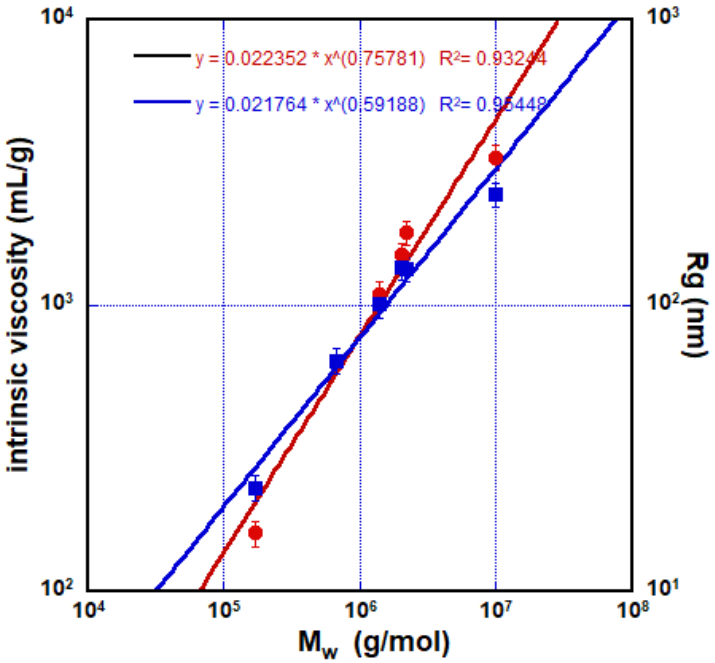

Figure II.5: Scaling laws of intrinsic viscosity versus weight-average molar mass (Mw) and radius of gyration (Rg) in 6g/L of NaCl(●Intrinsic viscosity ■R_g)

b) Characterization of PSL microspheres

The particle size of PLS passed through sieves were observed through Scanning Electron Microscopy. The average diameter size, smallest and largest microspheres and surface charge were determined using Dynamic Light Scattering and Zeta potential respectively, were reported in table II.2**.** The negative values of zeta-potential are higher than an electrostatic charge of -30 mV, which indicates along term stability of the aqueous dispersions [160]. It can be seen from figure II.6 that the microspheres exhibited a spherical, uniform and homogenous shape and found to be relatively consistent with manufacture reported values (Polyscience-France) and monodispersed which can be clearly observed from SEM and DLS (Figure II-7) measurements respectively and regrouped in table II.2

Table II.2: Characterization of the PSL microspheres used for the experiments

PSL	z-Average diameter (nm)	*PDI (D_w/D_n)	ξ potential (mV)
PSL 50	50	0.068	-35.4
PSL 200	198	0.016	-42.2
PSL 520	502	0.034	-43.7
PSL 750	725	0.11	-47.4
PSL 1000	922	0.018	-50.8

*PDI: Polydispersity Index

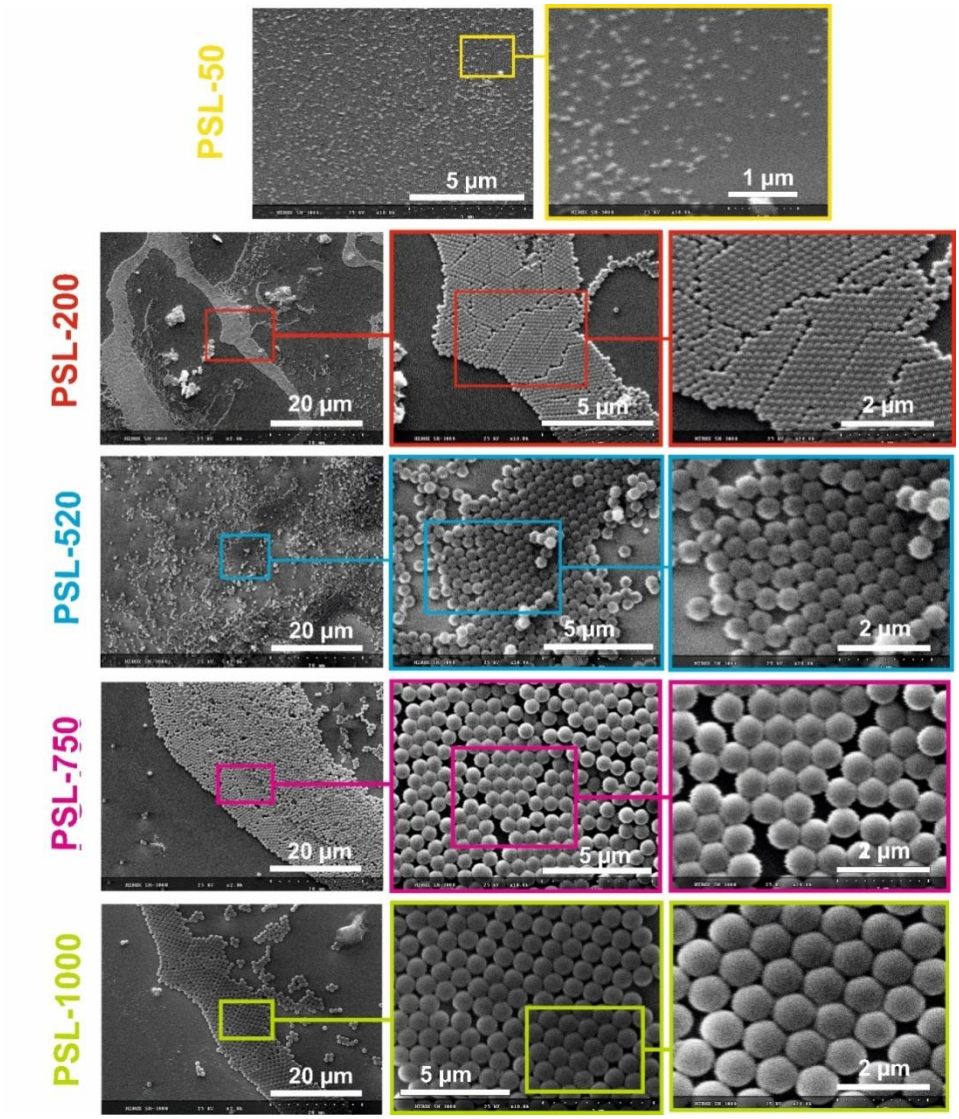

Figure II.6: SEM images of different polystyrene used

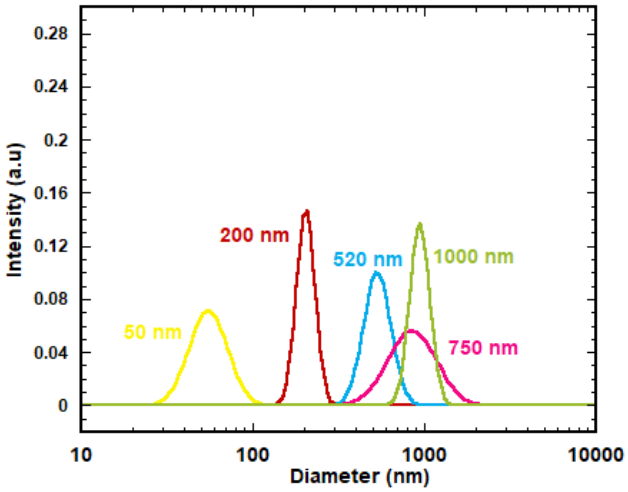

Figure II.7: Distribution using the cumulant algorithm in Dynamic Light Scattering of Polystyrene microspheres

c) Rheological behaviour

In this part, we have examined the rheological behaviour of HPAM in the presence and absence of PSL at the salinity of 6g/L NaCl. **Figure II.8** show the effect of HPAM & HPAM/PSL content on the shear rate dependency of the shear viscosity and zero shear viscosity of formulations at 2 g/L of HPAM. Both HPAM solution and the Polystyrene/HPAM suspensions displayed non-Newtonian behavior in almost the whole range of shear rate. The figure indicates that the shear viscosity continuously decreased with increasing shear rate; i.e., the shear thinning effect occurred for all the systems However with increasing of shear rate all flow curves converged; which indicates that the rheological properties of the Polystyrene/ HPAM suspensions depended on the viscoelastic character of the matrix polymer.

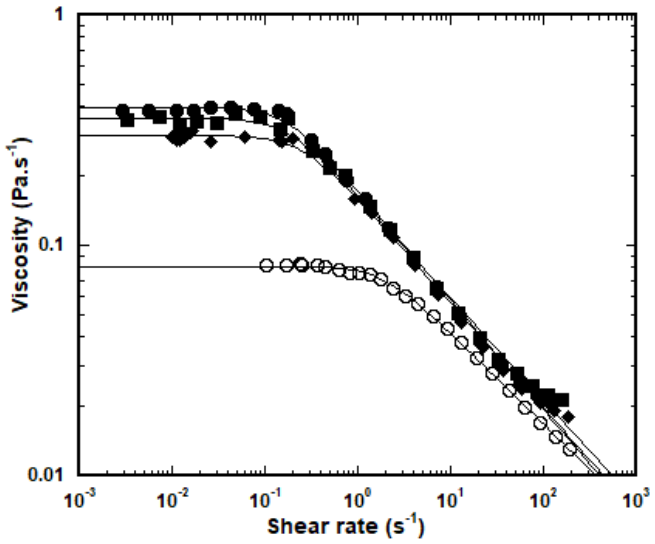

Figure II.8: Rheograms C_p=2 g/L C_{PSL} = 200ppm for (○ HPAM without PSL ● HPAM/ PSL (520 nm) ■ HPAM/PSL (200 nm) ◆ HPAM/PSL (750 nm) (6g/L in NaCl; T=20°C; pH=6.2) .The lines are fitted by eqn II.1 (carreau model)

It was shown that the viscosity at zero shear rates was improved in the case of formulations at 20°C compared to the value of pure HPAM prepared in 6 g/L NaCl. For example, the formulations 11, 12, 13 in the table II.1 based on the sizes 200; 520; 750 nm of polystyrene microspheres showed an important increase of the viscosity at zero shear rates). This shear thickening behaviour could be explained by the strong interaction of Hydrolyzed polyacrylamide chains at the surface of Polystyrene, which creates a larger effective particle size and therefore higher viscosity of the system via hydrogen bond. The same trend was confirmed by various works in the literature with other systems based on the interaction of polymer/ nanoparticle [161, 162]. Another interpretation could be the adsorption of HPAM molecules on the surface of NPs present in the liquid. The adsorption of HPAM molecules is caused by hydrogen bonding between HPAM molecules and the surface of the NPs which can be either electrostatic or hydrophobic adsorption[105, 111]. A more detailed discussion of the mechanism that governs interaction will be given in the next chapter (Chapter 3).

Based on these encouraging results obtained in this section, in terms of rheological behaviour for different Hydrolyzed Polyacrylamide/Carboxylate microspheres, we have conducted a systematic study of microspheres concentration, sizes and different temperatures using design of experiments approach to identify the best formulation for possible application in chemical Enhanced Oil Recovery.

III.2.Statistical Analysis

a) Model fitting

The evaluation of process effect variables on the viscosity at zero shear rate η_0, experiments were performed based on the Doehlert design matrix with two replicated points. The design points, experimental and predicted results of the zero shear viscosity η_0 are shown in the table II.1. To minimize the effects of uncontrolled factors, experiments were performed in a random sequence. The quadratic model proved to be adequate for predicting the zero shear viscosity η_0 as response given by the following equation (II.6):

$$\eta_{0experimental}\,(Pa.s) = 0.0948607-0.006008*X_1-0.036375*X_2-0.163266*X_3+0.011963*X_1X_2-0.051389*X_1X_3+0.1142459*X_2X_3+ 0.0548993*X_1^2-0.026932*X_2^2+0.1262683*X_3^2 \qquad (II.6)$$

In this model, all variables are indicated by the coded values, where X_1 is the size of PSL microspheres in (nm), X_2 is the microspheres concentration (ppm) and X_3 is the temperature (°C). As can be seen in Eq. (3), the interactions between variables had significant effects on the response; the results are therefore preferably presented and discussed in terms of interactions. The statistical significance of Eq. (3) is presented in Table 4.

The terms mean square, degree of freedom (D_F) and sum of squares are respectively, defined as the variance estimation of the model, the number of model and total of the sum of squares for model. The ANOVA (*F*-test) (Table II.3) shows that the second order model (quadratic polynomial) corresponds well to the experimental data.

The *p*-value is a quantitative measure to report the result of a test hypothesis. This is the probability that the test statistics are at least as extreme as those observed since the null hypothesis is true.

Table II.3: ANOVA analysis of zero shear viscosity $\eta_{0\,experimental}$ (Pa.s)

Source	Sum of squares	D_F	Mean square	*F*-ration	*p*-value
Model	0.15590056	9	0.017322	41,0902	0.0004*
Error	0.00210783	5	0.000422		
C.Total	0.15800839	14			

*$p<0.05$

The degree of freedom (D_F = 14) in table II.3 indicates the total number of model terms, including the intercept minus one. It is obvious that the model is highly significant, as suggested by the model *F*-value and a low probability value (*p*-value = 0.0004).

If the *p*-value is less than or equal to the chosen significance level alpha value of 0.05, the test suggests that the observed data are inconsistent with the null hypothesis. Therefore, the null hypothesis must be rejected and the factor effect is significant [163].

Table II.4: Estimated regression and coefficients of each factor using *t*-ratio and *p*-value in the nonlinear second order model

Parameter	Estimate	Standard Error	*t*-ratio	*p*-value
Intercept	0.0948607	0.011854	8	<.0005*
X_1 (Size)	-0.006008	0.010266	-0.59	0.5838
X_2 (C_{PSL})	-0.036375	0.010266	-3.54	0.0165*
X_3 (T°C)	-0.163266	0.010272	-15.89	0.0001*
X_1*X_2	-0.011963	0.023709	-0.5	0.6353
X_1*X_3	-0.051389	0.026526	-1.94	0.1104
X_2*X_3	0.1142459	0.026521	4.31	0.0077*
X_1* X_1	0.0548993	0.018743	2.93	0.0327*
X_2* X_2	-0.026932	0.018744	-1.44	0.2103
X_3* X_3	0.1262683	0.017803	7.09	0.0009*

*p<0.05

In our case, the table II.4 shows that the linear effects of PSL concentration and temperature are significant. The high coefficient value of -0.163266 and high *t*-ratio (-15.89) confirm the important effect of temperature on the zero shear viscosity η_0 of HPAM/PSL. The negative sign means that the factors and the response are inversely proportional. Size was the least significant parameter among the main linear parameters with (*t*-ratio=-0.59) and a low coefficient (0.094).

The interaction of (X_2*X_3) with a high (*t*-ratio=4.31) was the most significant compared to the other combinations (X_1*X_3) and (X_1* X_2). The latter was the least significant with *t*-ratio=-0.5 and high probability (0.6353).

The interaction (X_2*X_3) with a high *t*-ratio (4.31) was the significant parameter with the *p*–

value of 0.0077 ($p< 0.05$) compared to the other combinations (X_1*X_2) and (X_1*X_3) that were found no significant because the *p*-value was higher than 0.05. This confirms the trend with previous work in the rheological properties of colloidal suspensions by Jasim Ahmed et al [146].

The insignificant terms of X_1*X_2, X_1*X_3, X_2^2 in Eq. (II.6) are eliminated to improve the model. The quadratic equation reduced in terms of coded factors is proposed as follows:

$$\eta_0 \text{ (Pa.s)} = 0.0948607 - 0.006008*X_1 - 0.036375*X_2 - 0.163266*X_3 + 0.1142459*X_2X_3 + 0.0548993*X_1^2 + 0.1262683*X_3^2 \quad \text{(II.7)}$$

Figure II.9 presents the predicted values of the model with respect to the actual values of the experiment's results obtained with the zero shear viscosity η_0.

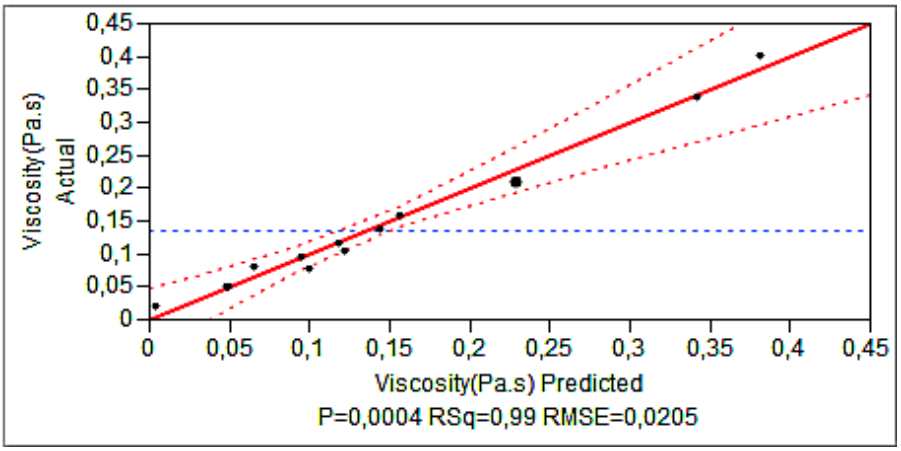

Figure II.9: Experimental data versus predicted values for zero shear viscosity with *p*< 0.05

To analyse the data, firstly, it is necessary to assume that the experimental values come from a normal distribution in order to define whether or not the data set is normally distributed. In the literature, the data set has a normal distribution if the points are close to the straight line[164]. In our case, it is evident from the figure II.9 that experimental values follow a straight line which suggests normal distribution of the data. The high value of R^2-square of the developed quadratic model was (0.986), which is close to the $R^2_{adjusted}$ (0.962) indicating that the model was successful in correlating zero shear viscosity η_0 to the studied parameters [165, 166].

On the other hand, the difference between the experimental and predicted values is illustrated on the residual plot of zero shear viscosity on the **figure II.10**.

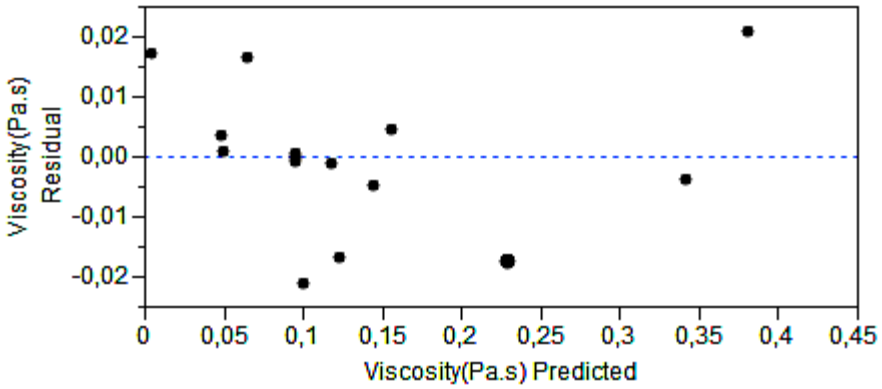

Figure II.10: Residual plot for zero shear viscosity in the model

There are points below and above the straight line, namely the point of zero line; the positive values observed on the residual plot indicate a low predictive result. On the other hand, negative values imply that the prediction was high; a value of zero means that the prediction is accurate since there is a total superposition between experimental and predicted values. The residual plot for η_0 following eq. 4 shows a random pattern. This indicates that the distribution of residuals for the response approximately follows the fitted normal distribution.

III.3. Interactions plots

Figure II.11 illustrates the possible positive and negative effects of two variables interactions, respectively among the three parameters on the zero shear viscosity of HPAM polymer.

(X_1*X_2) and (X_2*X_3) were not directly influential but were through interactions effects at the 95% confidence level as shown in **figure II-11**. The plots of interaction effects evidenced interaction existence between two factors, when the two curves of levels -1 and +1 are not parallel. The parallel (non superposable) curves indicate the absence of interaction between factors and that the concentration is the least significant or non-significant in the presence of other parameters simultaneously.

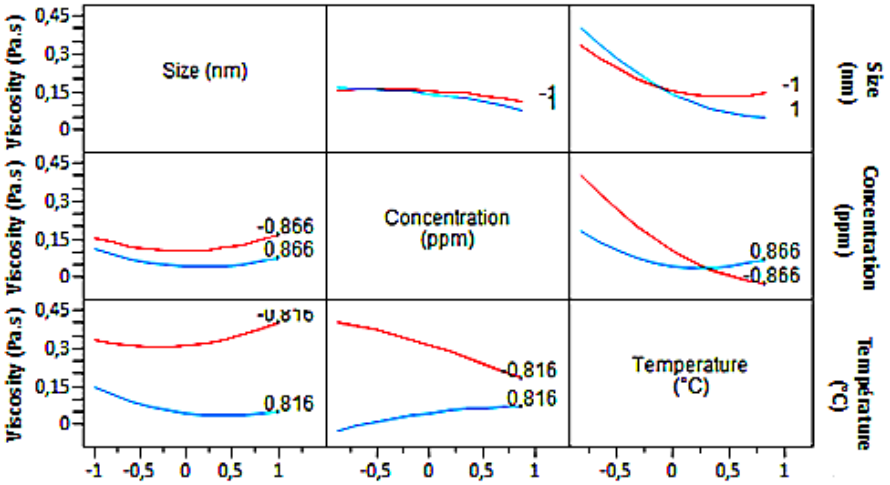

Figure II.11 : Interaction effect plots of the zero shear viscosity ($Pa.s^{-1}$) function of the studied parameters (Size; Concentration; Temperature)

The not-parallel curves indicate the presence of interaction that can be estimated between size and temperature. The negative sign of (X_1*X_3) interaction effect coefficient (-0.051389) means that zero shear viscosity of polymer decreases when temperature is higher. These results confirm the previous finding obtained from table 9, related to each parameter of influence on the polymer viscosity at zero shear rates

III. 4.Surface Response Methodology (RSM)

The response surfaces were drawn as three dimensional plots of two factors while the other factor was kept constant. The 3-dimentional response surface for viscosity at zero shear rates of HPAM/PSL solution is shown **figure II.12**.

In **the figure II.12.a** represents the viscosity at zero shear rates for different concentration and particle size for a constant temperature of 50°C. It is clear that the viscosity decreases when PSL concentration increase independently of the particle size while the zero shear viscosity increases when the particle size increases at the fixed concentration.

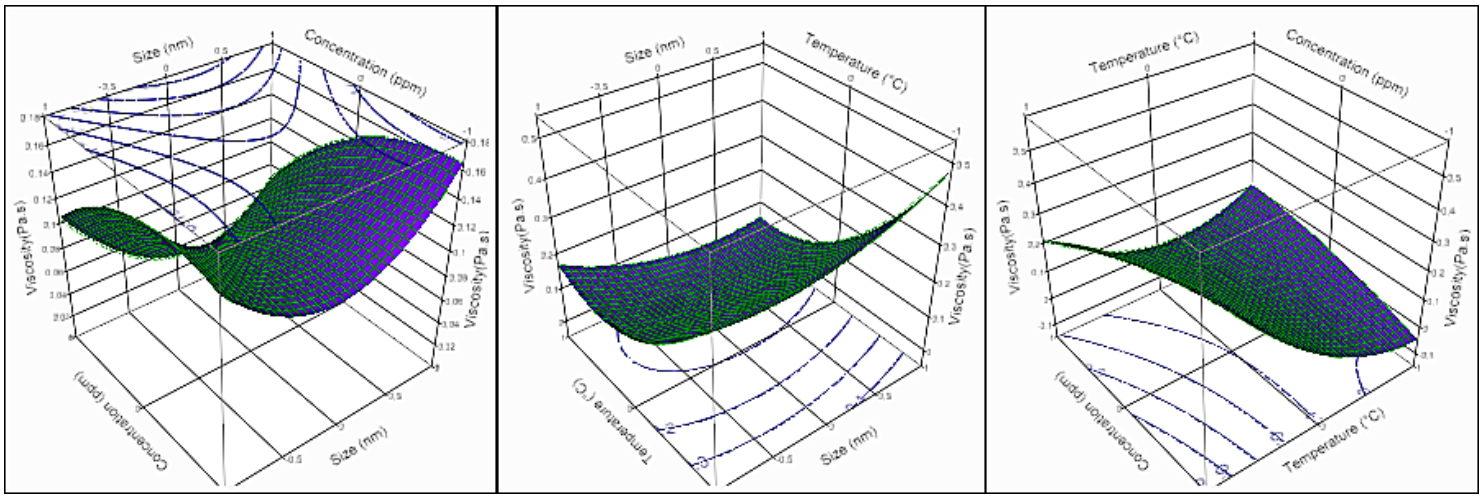

Figure II.12: Response surface contour (3D) of zero shear viscosity ($Pa.s^{-1}$) showing the combined effect of PSL size (nm); concentration (ppm) and temperature (°C)

Figure II.12.b illustrated the combined effect of PSL size and temperature at constant concentration of 50 ppm on the zero shear viscosity of HPAM/PSL solutions. It can be seen that zero shear viscosity increases as the temperature decreased from (80°C to 20 °C) at all particle sizes. Similarly, at fixed temperature, the viscosity slightly increases with particle size

Figure II.12.c shows the effect of concentration and temperature on the zero shear viscosity of solution at fixed size of 520 nm. It can be seen that at high temperature, increasing concentration leads to mild increase in the zero shear viscosity of solution. However, at low temperature, the shear viscosity decreases with concentration increase. Furthermore, at fixed concentration, increasing the temperature leads to decrease followed by increase in viscosity. The result indicated that the maximum zero shear viscosity achieved at lower temperature and concentration.

As expected, the temperature behavior follows the behavior of the polymer usually described in the literature, the viscosity decreases with temperature. The variations as a function of the concentration and the size of the microspheres are less obvious. The thickening effect is not directly related to an increase in particle concentration or size.

One of the explanations for this thickening behaviour is the adsorption of polymer chains

onto microspheres through interactions between the surface carboxylic functions of microspheres and the carbonyl functions of HPAM chains.

IV. Validation of the model & process optimization

One of the important reasons for this work was to find the optimal conditions in which the zero shear viscosity η_0 will be maximized. For this, the desirability function was used by Suich and Derringer in 1980 to solve the problems related to optimizing multiple responses related to industry that have been applied in many studies [167, 168].

From **figure II.13**, which shows the prediction profile of the zero shear viscosity η_0 as function of the studied parameters, It can be concluded that the optimum conditions were the use of PSL size (1000 nm) and concentration of 50 ppm at fixed temperature of 20°C for a predicted response (η_0=0.505383 Pa.s^{-1}) with a desirability value of 0.997604.

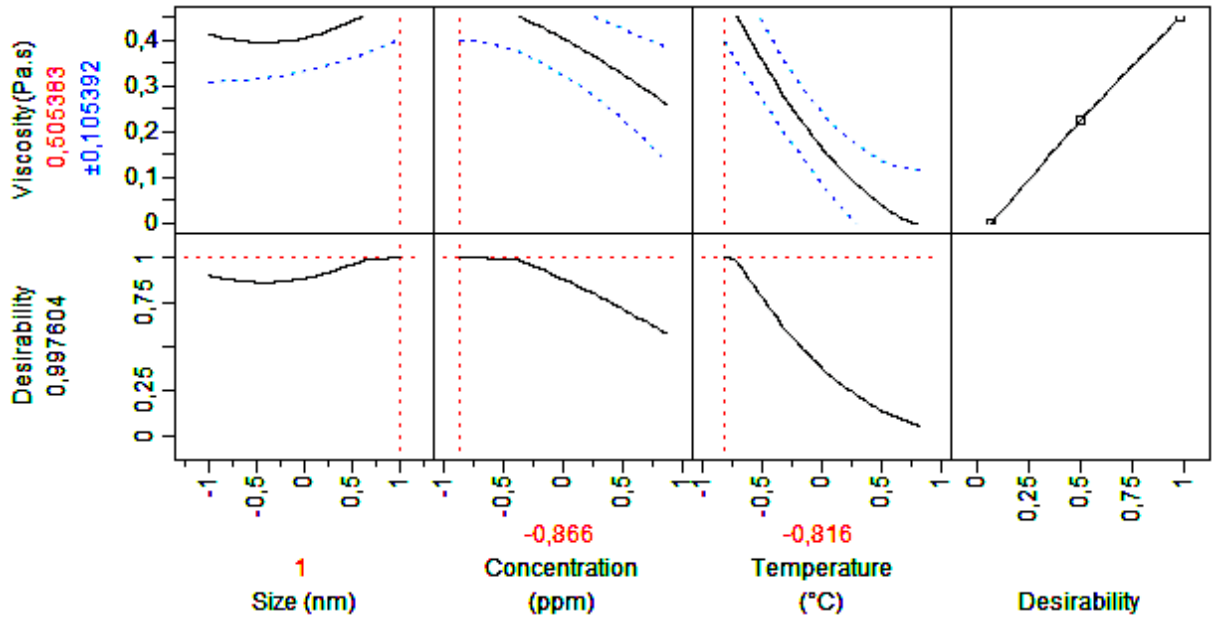

Figure II.13: Desirability function for optimizing the zero shear viscosity η_0 response

To verify the adequacy of the previous model, the experiment was performed and compared to the result given by the JMP8 software calculation; the results are collected in Table II.5. The experimental data obtained were in good agreement with the model values, which confirm the validity of the former.

Table II.5: Optimum conditions

Parameters	Size (nm)	Concentration (ppm)	Temperature (°C)	Zero shear viscosity η_0 (Pa.s^{-1})	
				Predicted	Experimental
Optimum conditions	1000	50	20	0.505383	0.56120

After the optimization process using design of experiments methodology, the formulation was tested on the laboratory based on the optimum conditions obtained**. Figure II.14** shows the results of microspheres incorporation on the solution viscosity at zero shear rate of polymer at 20°C in the range of shear rates (0.0001-1000 s^{-1}). The rheograms and the flow curves exhibit Newtonian behaviour followed by shear thinning behaviour over the shear rate range (0.1-1 s^{-1}) for an HPAM solution, without microspheres.

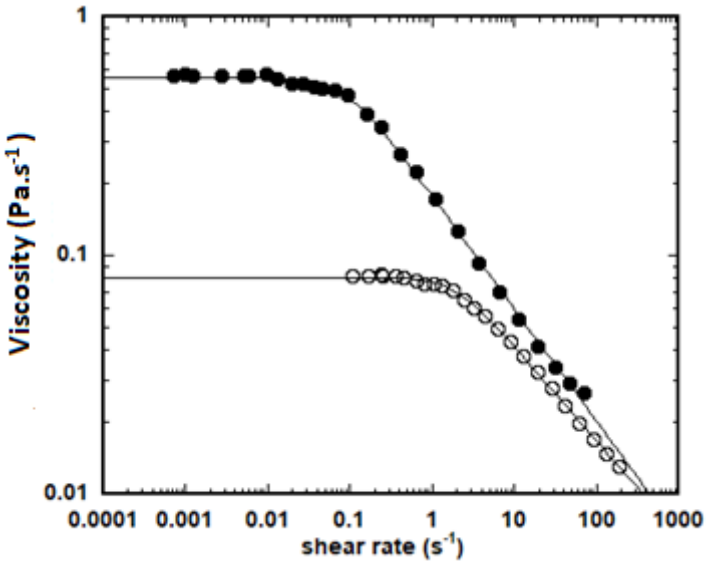

Figure II.14: Rheograms C_p=2 g/L C_{PSL} = 50ppm for. (○ HPAM without PSL; ● HPAM/ PSL (6g/L in NaCl; T=20°C; Size=1000 nm); the lines are fitted by eqII.1: carreau model

It was noted that the zero shear viscosity of HPAM solution η_0 (Pa.s^{-1}) =0.086 at 2 g/L was lower than the zero shear viscosity of HPAM/PSL formulation, which was η_0 (Pa.s^{-1}) = 0.56120. The zero shear viscosity at 50 ppm of HPAM/PSL is 8 times higher than that of HPAM solution at 2000 ppm. Our results suggest that the PSL microspheres interact with

polymers based on the adsorption phenomena which create a network with improved viscosity compared to the solution of HPAM [169, 170].

V. Conclusion

In this study, a thickening effect is highlighted in high molar mass of HPAM polymer in the presence of surface carboxylated polystyrene microsphere. Experimental and statistical investigations were established on the zero-shear viscosity of HPAM/Polystyrene microspheres formulations prepared in medium salinity of 6g/L NaCl in the range of temperature comprised of (20-80°C). The effects of microspheres size (50-1000 nm), concentration (50-500 ppm) and temperature on the viscosity at zero shear rate were evaluated through a three factor Doelhert matrix which allowed getting a second order mathematical model to correlate the experimental points of the response (zero shear viscosity) according to the independent effect and combinations of the three parameters studied. The statistical significance of the mathematical model was confirmed by the higher R^2-square value of (0.986) and ANOVA analysis. The most influential parameters were found, through their higher F-ratios and lower p-values ($p < 0.05$), to be the temperature, concentration and size of microspheres, respectively. Furthermore, the effect of different parameters on the zero shear viscosity was illustrated through 3D response surface contours.

In order to obtain an improved viscosity of HPAM with the best rheological properties, the response variables of the parameters studied were maximized using the desirability function. The formulation with concentration of 50 ppm polystyrene microspheres & sized 1000 nm at a solution temperature of 20°C as the optimum conditions to maximize the zero shear viscosity of HPAM polymer with improved rheological characteristics. At this optimal point, the response variables were obtained experimentally and compared with the model predictions as a validation test. The parameters studied have been promising to achieve viscosity with desirable properties for possible application in the chemical Enhanced Oil Recovery applications.

Interaction and Response Surface Methodology plots show that the thickening behavior observed for these composites is not obvious and will not be directly related by a volume fraction effect (size and concentration) of the microspheres, and an Arrhenius-type

temperature effect on the polymer matrix. This suggests that this thickening behaviour is due to the adsorption of polymer chains onto microspheres through interactions between the surface carboxylic functions of microspheres and the carbonyl functions of HPAM chains.

In this chapter, it was difficult to determine the surface functionality of polystyrene microspheres for lack of material, in order to introduce this parameter into the modeling. An alternative was to synthesize microspheres of similar size and different surface functionality to address the adsorption hypothesis. This work is the subject of the next chapter.

In perspective of these modeling works, it would have been interesting to apply the modeling on the relaxation time, and on all the rheological characteristics to model the effects on the parameters salinity, degree of hydrolysis and molar mass of the HPAM.

CHAPTER III: Rheological behaviour/ Adsorption phenomena of Hydrolyzed Polyacrylamide/Poly(Styrene-Acrylic-Acid) microspheres

CHAPTER III: Rheological behaviour/ Adsorption phenomena of Hydrolyzed Polyacrylamide/Poly(Styrene-Acrylic-Acid) microspheres

Résumé

Les propriétés en solution aqueuse de composites polymères-particules (PPC) dépendent de la taille et de la concentration des particules et des polymères ainsi que des interactions entre elles. Dans ce travail, le comportement rhéologique a été étudié dans un régime semi-dilué de polyacrylamide partiellement hydrolysé (HPAM) avec un rapport 2Rg /D et un paramètre de confinement (pc) supérieurs à 1. Rg est le rayon de giration du polymère et d le diamètre des particules. pc caractérise la distance entre particules (ID) en fonction de la taille du polymère (pc = ID / 2Rg) et dépend de la concentration et de la taille des particules. Nous avons mis en évidence les effets d'épaississement du PPC en fonction du nombre de fonctions carboxyliques à la surface des particules de polystyrène (PSL) obtenues par polymérisation en émulsion sans tensioactifs (0,16 à 1,2 mmol / g de COOH). L'épaississement augmente linéairement avec le pc inférieur à 10. Ce comportement a été mis en corrélation avec les interactions polymère-particule, ce qui a été démontré par les mesures d'adsorption en solution diluée (12–22 mg / g de HPAM sur PSL). L'adsorption a été quantifiée par des mesures de viscosité capillaire à cisaillement nul dans un dispositif microfluic. En revanche, un effet d'amincissement a été observé pour un pc supérieur à 10, ce qui est également lié aux études sur l'effet du sel (6-12 g / L dans NaCl).

I. Introduction

For several decades, significant theoretical and experimental attention has been devoted to colloidal particles in complex fluids, including polymer solutions, gels, and melts. These mixtures, known as polymer–particle composites (PPC), are interesting in many applications in the fields of material science, biophysics, and medicine, ect, [171-174]. The behaviour of these systems strongly depends on the length and time scale at which they are probed, and in certain conditions it is possible to observe interesting dynamic phenomena or viscoelastic properties[174, 175]. The rheological behaviour is mainly due to the large number of different scales present in the system, such as the diameter of the particles (d), the radius of the gyration of the polymer chains (Rg), the interactions between the particles and the polymer, and the polymer and particle concentration range [175]

When studying PPC, two main regimes can be identified as a function of the diameter of the particles (d): the "colloidal limit", where the size of the polymers is much smaller than the

particles ($2R_g/d \ll 1$), and the "protein limit" where the size of the polymers is greater than or comparable to that of the particles ($2R_g/d \gtrsim 1$) [176] In solution, the two main regimes are related to R_g: the diluted regime where the polymer concentration is lower than the overlap concentration called c*, and the semi-diluted regime where the concentration c is higher than c*. In terms of particle concentration, the two regimes can be distinguished according to a confinement parameter $p_c = ID/2R_g$. p_c characterizes the inter-particle distance (ID) with respect to the polymer size and depends on the concentration and size of the particles [177]. When $p_c>1$, the diffusion of the polymer chains tends towards the solution behaviour without particles, while $p_c<1$ defines the overcrowded particle regime. In the latter, the mobility of the polymer chains is reduced and can be subjected to a reduction in conformational entropy by being compressed between the closely spaced particles. The competition between the mobility and diffusion of both the colloidal particles and the polymer chains in these different regimes will impact their flow properties and thus their rheological behaviour [178]. The chemical structure of the components and their potential interactions, weak or strong, can also impact these properties.

In this context, the rheological behaviour of a partially hydrolysed polyacrylamide (HPAM) aqueous solution in the presence of particles is a recent development that can find interesting applications, for example, in oil and mining injection water [67, 179, 180].To date, some HPAM-based PPCs have been studied, including clay mineral [109, 162], graphene oxide [112] and metal oxide particles.[3, 4, 67, 105, 113, 181, 182]. These works are mainly carried out in a semi-diluted regime and result in a modification of the rheological properties as a function of the particle concentration. The authors generally explain these effects by a more or less strong hydrogen-bonding interaction between the particle and polymer chains without considering the effects of confinement or the dimensional ratio between the particles and polymer chains [3, 4, 67, 105, 109, 112, 113, 162, 181, 182].

Thus, it was interesting to study the hydrogen-bonding interactions effects between the particles and HPAM in a confinement domain with $p_c> 1$ as illustrated in figure III.1;

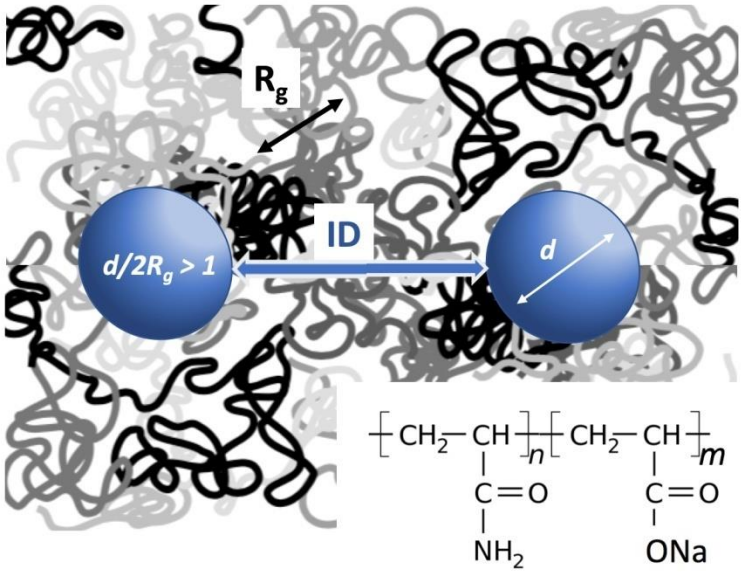

$M_w = 10^7$ g/mol, R_g = 300 nm, m=0.30, [NaCl] = 6 g/L, 350 < *d* < 500 nm

Figure III.1: Illustration of geometric consideration in this study: confinement parameter p_c= ID/2R_g (Rg : Gyration radius, ID: inter-particle distance);

This domain was chosen for potential applications using thickening effects at very low volume fractions of particles. In the present work, we developed the synthesis of polystyrene particles functionalized by carboxylic functions (COOH) on their surface. It was important to synthesize additive-free polystyrene particles and more particularly surfactant-free particles, because these additives could interact with polymer chains in complex fluid. Thus, the free soap emulsion polymerization of styrene and acrylic acid has been adopted to obtain batches of monodispersed particles of size ranging from 350 to 490 nm with different COOH contents. These polystyrene particles free of additives will be now called PSL. The study was done within the protein limit ($2R_g/d > 1$) by choosing a high molecular weight HPAM exhibiting a 300 nm radius of gyration in 6 g/L NaCl solution. The rheological properties were evaluated in a semi-diluted regime and interactions between PSL and HPAM were highlighted by the ability of PSL to adsorb onto the HPAM in diluted regime by zero-shear viscosity measurements in a microfluidic device. These works are completed by the effects of salinity (6–12 g/L in NaCl).

II. Materials and methods

II.1. Materials

Styrene (S, ≥ 99 %), acrylic acid (AA, 97%), ammonium persulfate (APS, ≥ 99 %), and salts (NaCl, ≥ 99 %) were purchased from Aldrich. Deionized water, with a resistivity of 18.3 MΩ·cm at 25°C, was filtered through a 0.22 µm Millipore filter prior to use. All chemicals were used as received. The polystyrene latex particle standards (PSLC, mass fraction of 1%) were manufactured by Thermo Scientific. The HPAM (FLOPAAM) with high molecular weight was kindly provided by "SNF Floerger-France". ^{13}C-NMR was employed to characterize the hydrolysis degree (HD) of HPAM. HD= 0.28 was determined as the ratio of the integrated areas under the peaks at 180 and 182 ppm, which corresponds to carbon in the carbonyl groups in the acrylamide and acrylate units, respectively[148].

$[\eta]$ = 4400 ml/g for HPAM, which corresponds to a mass average molecular weight $M_w = 10^7$g/mol and R_g = 300 nm calculated with the scale law $R_g = 0.022\ M_w^{0.59}$ and $[\eta] = 0.022\ M_w^{0.76}$ established in the laboratory on the model HPAM (see Figure II.4 in the chapter 2. The molecular weight was determined from an intrinsic viscosity measurement which does not provide the dispersity index (see **figure III.9**), however as it is expected high for this industrial sample.

II.2. PSL synthesis

All syntheses were performed using a soap-free emulsion copolymerization process using ammonium persulfate (APS) as the initiator. A representative synthesis is as follows: styrene, acrylic acid and deionized water were degassed by nitrogen separately for 20 min. Styrene (16.5 mL, 0.14 mol) and acrylic acid (2.14 mL, 0.03 mol) were added to 140 mL of deionized water in a glass reactor equipped with a mechanical stirrer (350 rpm). The reactive medium was then stabilized at 70°C via an external water circulator before adding the APS solution (75 mg, 0.32 mmol in 10 mL of deionized water). After 10 hours under stirring at 70°C, the reaction mixture was cooled down to room temperature. Water dispersed PSLs were purified by 5–6 centrifugation cycles at 12000 rpm for 30 min. After each centrifugation step, the supernatant was replaced by an equal volume of deionized water until its conductivity was close to that of deionized water (< 40 µS/cm). The yield of the overall synthetic

process was determined using a gravimetric method taking the aggregates apart and was equal to 82, 89, 90 and 97 wt% for PS9, 13, 18 and 22, respectively.

II.3. Characterizations

a) Dynamic light scattering (DLS) and Zeta potential: Hydrodynamic diameters and PDI were determined using a contactless (in situ) DLS probe (Vasco flex) from Cordouan Technologies at 170°. The intensity fluctuations as a function of time were processed as an autocorrelation function. Cumulant algorithms were used to fit this function in order to obtain a size distribution. The zeta potential of Latex samples was measured with Malvern Zetasizer nano Series ZS. Before the tests, the cell was rinsed carefully with alcohol and deionized water to ensure the accuracy of the measured data; the measurements were repeated five times. The concentration used for each latex was 10 ppm.

b) Titration measurement: The COOH of the surface of the PSL (4 g/L) was titrated with a Titrando 888 equipped with a stirrer 728 and a combined pH glass electrode (pH: 0–14; 0–80°C; KCl: 3 M). All components were purchased from Metrohm. The software used was Tiamo 2.5. NaOH at 0.10 M and HCl at 6.58 x 10^{-3} M were used for all experiments.

c) Rheology measurements: Concentrated stock polymer solutions were prepared by the dissolution of an appropriate amount of polymer powders in PSL aqueous solution under gentle magnetic stirring for 2 days at room temperature. NaCl powder was directly poured into these solutions and the solution was stirred using a magnetic stirrer at300 rpm and room temperature for 1 day. Before the measurements, these solutions were kept standing overnight to reach equilibrium.

The steady shear rheological properties of PPC in semi-dilute solutions were measured using a Bohlin CVOR150 rheometer equipped with a bob-cup system (inner radius 25.0 mm, height 37.5. mm and outer radius 27.5 mm). This apparatus works with controlled shear stress. All of these measurements were performed at 20°C. The systems were allowed to reach a steady state at each shear stress prior to registering the obtained values. The measurement of viscosity for the dilute solutions was carried out on a capillary viscosimeter**.** The technique used is based on the measurement of the pressure drop (ΔP) of a polymer in a known

internal diameter polyether ether ketone (PEEK) tubing and a known fixed flow rate (Q) by a syringe pump (Nemesys mid pressure syringe pump) at 20°C according to the protocol reported elsewhere [150]. Calculations of zero-shear rate viscosity were made with the Rabinowitsch-Mooney equation [183]. The intrinsic viscosity of HPAM in 6 g/L NaCl at 20°C equal to 4400 ±200 mL/g was determined according to the calculation and protocol reported elsewhere

d) Microscopy: Latex was analyzed on 150 µL sample deposited by spin coating (2000 rpm, 60 s) onto a silica wafer. Scanning electron microscopy (SEM) images were taken using a Hirox© SH-3000 device. Atomic force microscopy (AFM) images were obtained using MultiMode 8 Atomic Force Microscope (AFM) from Bruker in PeakForce QNM (Quantitative NanoMechanics) mode[184] . This part was conducted by our laboratory members and the article was published by Pessoni et al.[184] in the journal of Environmental Science: Nano.

III. Results and discussions

III.1. PSL synthesis and characterization

Monodispersed polymer latexes obtained via emulsion polymerization are generally assisted by surfactants acting as emulsifiers. The latter may affect the final latex properties, i.e., an adsorbed surface layer generating a defect in the size, stability and electrophoresis measurements. The removal of the surfactant after an emulsion polymerization can lead to irreversible coagulation or flocculation. Unlike a hazardous post synthesis removal, the challenge was the preparation of latexes using soap-free emulsion polymerization with control in terms of particle size, size distribution and surface functionalization. In the present work, a PSL model has been synthesized using a water dispersed process and a soap-free emulsion polymerization of styrene (S) and acrylic acid (AA) monomers [185] illustrated in the **figure III.2**. The experimental conditions and yields optimized for the four PSL formulations are given in **Table III.1**. By adjusting the experimental conditions of the synthesis, PSLs exhibiting a z-average size ranging from 350 to 490 nm will have a particle surface functionality measured in mol of COOH per gram of PSL between 0.16 and 1.2 mmol/g. All PSL samples have been characterized using dynamic light scattering (DLS). The PSLs present a low polydispersity with a polydispersity index (PDI) determined by a DLS of less than 0.05, which corresponds to the characteristics of highly monodispersed samples,

and this was obtained regardless of the surface functionality.

Table III.1: Experimental conditions for soap-free PSL synthesis with S: styrene, AA: acrylic acid and main principal characteristics ([S]+[AA]=1.2 M, [APS]= 2.3 mM, yield > 80%, T=70°C)

Sample name	AA[a]	Solid content (%)	Z-average / *PDI*	ζ[b] (mV)	COOH[d] (mmol/g)
PSL 9	9.1	8.0	380± 20 0.007	-42± 2	0.16 ±0.02
PSL 13	12.9	7.9	350± 20 0.008	-46± 2	0.19 ±0.02
PSL 18	18.2	8.3	390± 20 0.003	-42± 2	0.92 ±0.1
PSL 22	21.8	9.2	490± 30 0.009	-46± 2	1.2 ±0.2
PSL [c]	n.d.	1	300±10 0.01	-36± 1	n.d.

a: concentration (mol-% vs. styrene); b: ζ-potential at pH =7.0; c: commercial product; d: COOH groups per PSL

The PDI results may be compared to the PDI results of NIST certified particle standards. Under the same DLS conditions (analysis and data processing), the PDI of a NIST certified and a commercial nanoparticle sample 300 nm in diameter is 0.01 (PSLC in **Table III.1**).

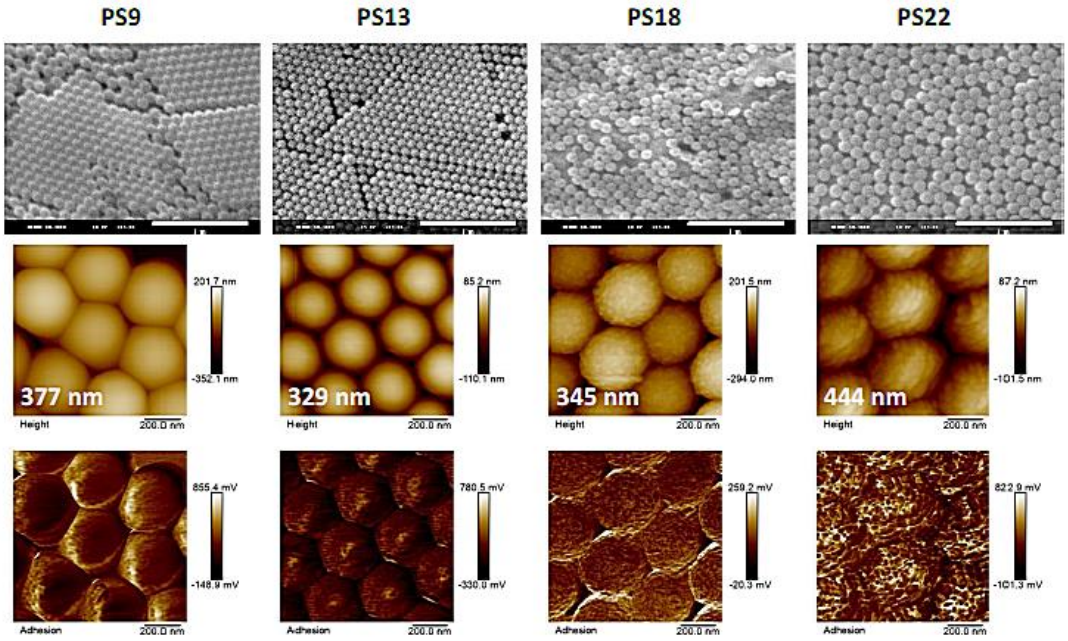

Figure III.2: Synthesis of different Poly (Styrene-Acrlylic Acid) functionality, first line SEM

photos of (Right to Left PSL 22; PSL 18; PSL 13; PSL 9), Second line, AFM characterization, third line, Adhesion of microspheres. [184]

III.2.Effect of microspheres charge on the rheological behaviour of HPAM solution

The influence of PSL concentrations at different shear rates was investigated with a rotational viscometer. A polymer solution without PSL and eight PSL-HPAM composite dispersions were prepared at different concentrations of PSL, i.e., from 50 to 500 mg/L in 2g/L of HPAM solution at room temperature (pH=6.2±0.2, 6 g/L in NaCl). Note that c* = 225 mg/L for HPAM is calculated from the intrinsic viscosity of the HPAM ($c^* \approx 1/[\eta]$) The initial HPAM aqueous solution at room temperature is transparent while the HPAM/Polystyrene aqueous solution turns into translucent. These samples are stable, homogeneous and no visible macroscopic phase separation is observed over time at room temperature as shown in the figure **III.3**.

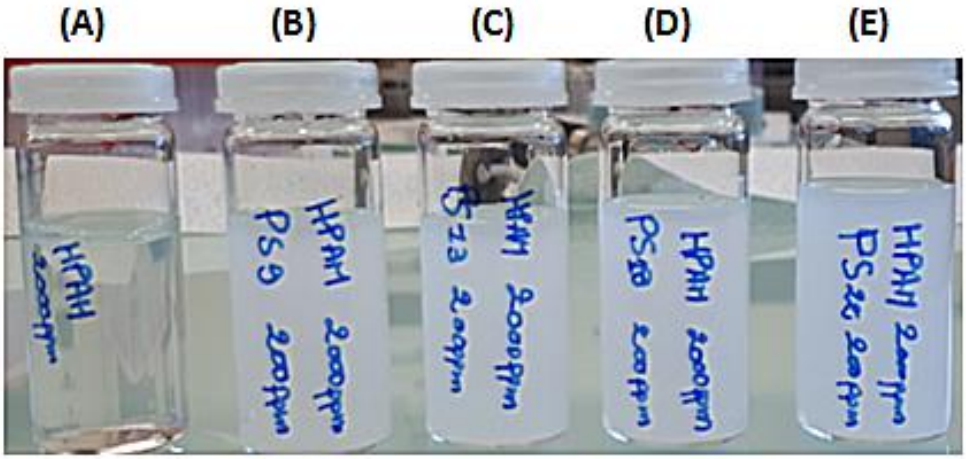

Figure III.3: Appearances of (A) HPAM and (B) HPAM/PS 9; (C) HPAM/PS 13 (D) HPAM/PS 18; (E) HPAM/PS 22 (T=20°C ; $C_{polymer}$=2000ppm ; C_{PSL}= 200ppm ; C_{NaCl} = 6 g/L)

The stability of the PSLs in the formulation has been confirmed by DLS measurements where the autocorrelation functions of the mixtures do not show any evolution over time (2 months) as shown in the figure **III.4**.

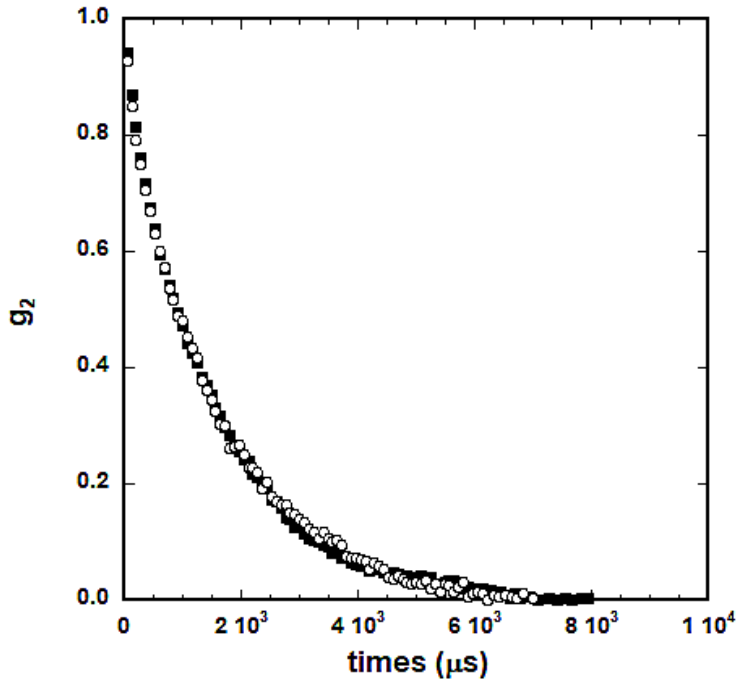

Figure III.4: Autocorrelation functions for HPAM/PSL22 formulation after 2 days (empty circle) and 2 months (full square) of preparation. Autocorrelation functions were obtained by using a contactless (in situ) DLS probe (Vasco flex) applied directly to the samples

Figure III.5 shows a representative example of the rheogram for both the PSL-HPAM mixtures and the HPAM alone. Both the mixture and the HPAM samples showed classical rheological behavior as expected for a polymer in solution, i.e., a Newtonian plateau following by a shear thinning effect. It should be noted that all flow curves converged at a high shear rate, which indicates that the rheological properties of the PSL-HPAM samples depend mainly on the viscoelastic character of the matrix polymer. Each flow curve is modelled by the Carreau equation, and this model describes both the Newtonian and the shear thinning behaviours (eq. III.1) [44].

$$\eta = \eta_{inf} + (\eta_0 - \eta_{inf})(1 + (\lambda\dot{\gamma})^2)^{(n-1)/2} \quad \text{(III.1)}$$

Where η_0 and η_{inf} the viscosity are at zero and infinite shear rate (Pa.s), λ is the relaxation time (s) and *n* is a power index.

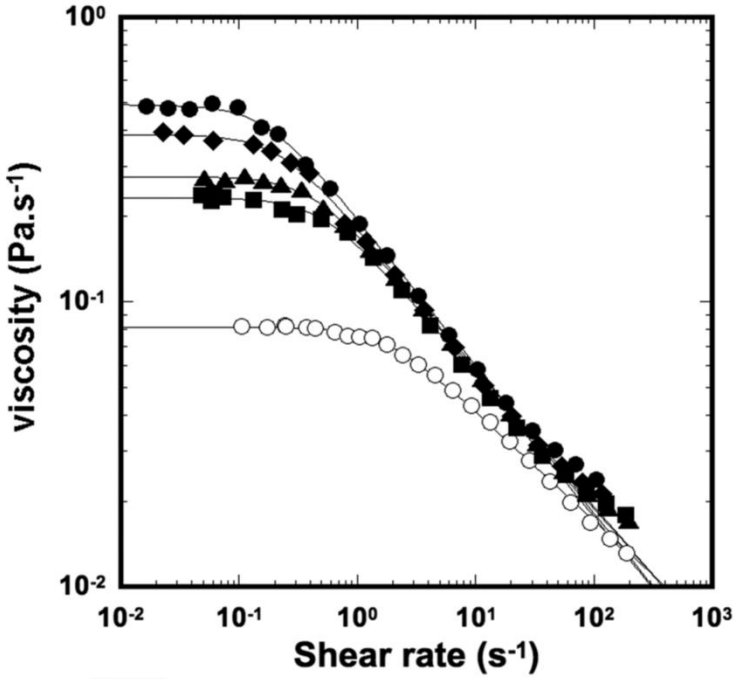

Figure III.5: Rheograms. C_p = 2 g/L and C_{PSL} = 400 mg/L for ● PSL22 ◆PSL18 ▲PSL13 and ■ PSL9. ○ HPAM without PSL. (6 g/L in NaCl, pH = 6.2, T=20°C). The lines are the fits by eq. 1. (Carreau model).

As shown in **figure III.6**, with increasing of Polystyrene microspheres functionnality and concentrations, the zero shear viscosity of HPAM/PSL mixtures increases to a maximum and reaching a plateau when Polystyrene concentration is 200-500 ppm for all different functionnality. The increase of zero shear viscosity in the range of (50-200ppm) may come from the increasing volume fraction of dispersed phase (polymer and microspheres). Another explication could be the existence of strong interactions between the polyacrylamide chains and PSL resulting in large effective particle size and therefore higher viscosity [186, 187].

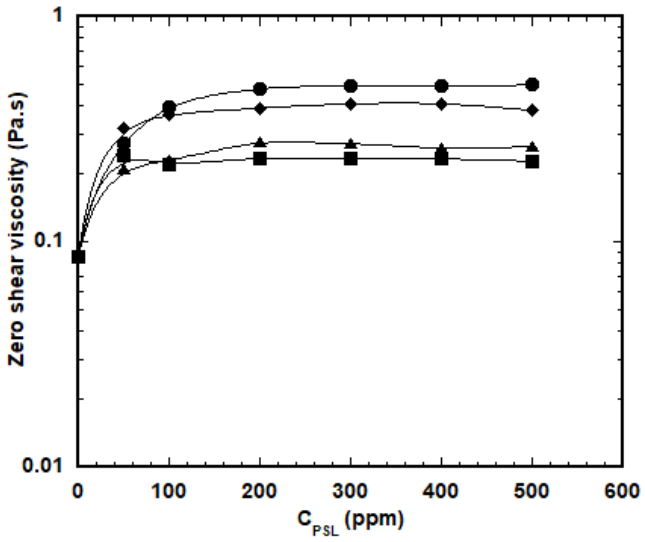

Figure III.6: Zero shear viscosity of HPAM/PSL charges samples as a function of (● PSL22 ◆PSL18 ▲PSL13 ■ PSL9. C_p = 2 g/L., 6 g/L in NaCl, pH = 6.2, T=20°C; shear rates of 0.001 to 100 s^{-1} The lines are guides for the eyes

Below the 200ppm, the variation of η_0 is constant and reached a plateau which proves that the possible mechanism could be an adsorption interaction of HPAM molecules on the surface of Polystyrene microspheres which present in the liquid. The adsorption interaction of HPAM molecules is caused by hydrogen bonding between HPAM molecules and the surface of the PSL which can be either electrostatic or hydrophobic [111, 188-190]. It should be mentioned that the effective PSL concentration of NPs-HPAM dispersion depends on HPAM concentration in the dispersion and varies from one experiment to another.

The relative zero-shear viscosity is plotted as a function of the confinement parameter $p_c=ID/2R_g$ (**Figure III.7**). Given that the particles are well-dispersed in the polymer matrix solution, *ID* can be calculated under the assumption that particles are randomly distributed as reported within eq. (III.2) [177, 191].

$$ID = d\left[\left(\frac{2}{\pi C_{PSL}}\right)^{1/3} e^{ln(1+PDI)^2} - 1\right] \qquad \text{(III.2)}$$

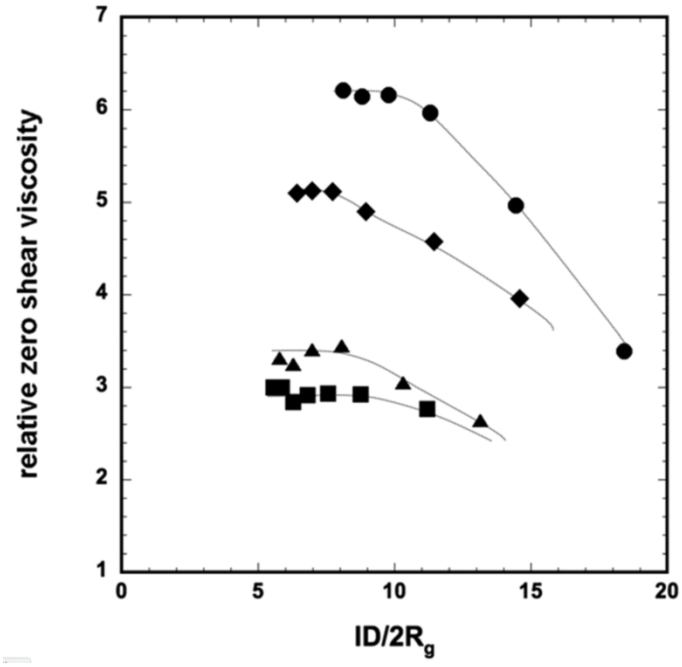

Figure III.7: Relative zero-shear rate viscosity ($\eta_{0,rel}$) *vs* confinement parameter. p_c= $ID/2R_g$ for ● PSL22 ◆PSL18 ▲PSL13 ■ PSL9. C_p = 2 g/L., 6 g/L in NaCl, pH = 6.2, T=20°C. The lines are guides for the eyes

Figure III.8 shows the variation of relative zero-shear viscosity ($\eta_{0,rel}$) as a function of the confinement parameter p_c. $\eta_{0,rel}$ is constant before decreasing to converge with the data of the polymer solution without particles. The value of $\eta_{0,rel}$ at the plateau increases with the COOH functionalization of the PSL. The thickening effect varies as a function of the number of carboxylic functions on the surface of the polystyrene particles (PSL). This dependency is the amide function (NH_2) of the main chain and carbonyl functions of PSL. To go further, the adsorption of HPAM chains on the PSLs with the lowest and highest functionality, i.e., 0.16 and 1.2mmol/g (PSL 9 and PSL 22, respectively) has been studied.

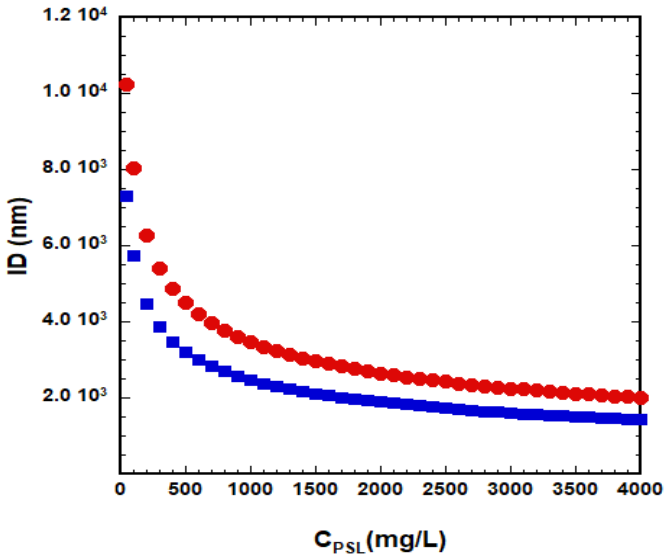

Figure III.8: ID versus PSL concentrations: ●PSL22 (z-average = 490 nm), and ■PSL13 (z average = 350 nm).

As a result, *ID* depends on particle size (*d* in nm), particle concentration (C_{PSL} in g/mL)), and particle size polydispersity (*PDI*). It should be noted that *ID* increases rapidly with low particle loading (see **Figure III.8**).

III.3. Adsorption phenomena

In general, measurements of polymer chain adsorption on colloidal particles are carried out by the classical depletion method, i.e., the particles and the non-absorbed polymer are separated by centrifugation or filtration [178] while IR spectroscopy was previously used for silica or titanium particles [192].We developed an original method within this work based on zero shear gradient capillary viscosity measurements adapted for very diluted solutions for both the particle and polymer. The microfluidic device used can measure relative zero-shear viscosity between 1.05 and 2.0 with a precision on the order of 5%. The principle of the adsorption method is based on an intrinsic viscosity discrepancy between the colloidal particles and a polymer solution. Indeed, Einstein's relationship for a volume fraction less than 0.02 is as described within eq. III.3. [193]

$$\eta_{0,spc} = [\eta] * C \qquad \text{(III.3)}$$

Where C is the concentration of particles or polymer, $\eta_{0,spc}$ is the specific viscosity ($\eta_{0,rel}$-*1*), and [η] is the intrinsic viscosity of the solute that depends on its chemical composition, the solvent and the temperature. For solid and spherical particles, [η] is 2.5 mL/g [193]. For colloidal particles, slightly higher values were observed (3–16 mL/g for example) [194]. For this work, the [η] determined for PSL 9 and PSL 22 were 5 and 10 mL/g, respectively. The polymer has an [η] of 4400 mL/g, which is a value 400 times higher than that of the particles. Thus, the monitoring of the $\eta_{0,spc}$ of the composite particle solution as a function of the polymer concentration for a fixed particle concentration is used to show the contribution of the adsorption and the free polymer. For a polymer concentration lower than the equilibrium adsorption concentration ($C_{p,abs}$), the variation of $\eta_{0,spc}$ is linear with a slope of approximately 2.5, then at $C_p > C_{p,abs}$ the $\eta_{0,spc}$ will grow linearly with a much sharper slope corresponding to the contribution of the free polymer and the adsorbed particles. In order to understand the adsorption mechanism, we have chosen to work in the diluted regime of polymer (c<*c) using the intrinsic viscosity of HPAM and HPAM/PSL formulations which are prepared using (6g/l NaCl water) and to determine the amount adsorbed. To do this, the polymer concentration was varied for high and low functionality of microspheres charge at constant concentration of microspheres (4000 ppm).

Figure III.9 shows an example of the variation of $\eta_{0,spc}$ as a function of C_p with C_{PSL}=4 g/L using both PSL9 and PSL22. Note that the confinement parameter must be greater than 1; 2.8 and 3.7 have been tested for PSL9 and PSL22, respectively. The intersection of the lines corresponding to the two concentration limits below and above $C_{p,\text{aps}}$ are used to determine this value, which is 48±5 and 95±5 mg/L of HPAM. In this case, the quantities of the adsorbed HPAM chain ($Q_{p,abs}$) are 12±1 and 22±2 mg/g for PSL9 and PSL22, respectively.

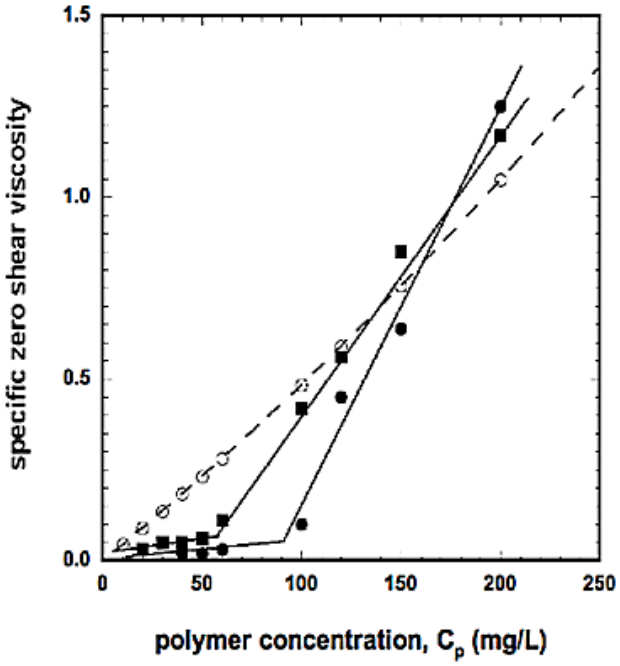

Figure III.9: Adsorption measurement. C_{PSL} = 4000 mg/L for ● PSL22 ■PSL9. ○ HPAM without PSL. Slope break = $C_{p,abs}$.

These results demonstrate the interaction of HPAM chains and PSL and the adsorbed HPAM amount depends on the PSL functionality density. It is worth mentioning that the $\eta_{0,rel}$ variations at the plateau reported above within Figure 3 should be correlated to the functionality of PSLs. It would seem there is a linear correlation with the functionalization of PSLs as shown in **Figure III.10**.

Taking into account the confinement parameter ($5 < p_c < 8$), the viscosity increase cannot be explained any self-crosslinking PSL occurring via the HPAM chains since the distance between the particles is greater than the size of the HPAM chains with $10R_g < ID < 16R_g$. However, the adsorbed HPAM layer may be seen as a shell over the PSL leading as the occurrence of bulkier final particles.

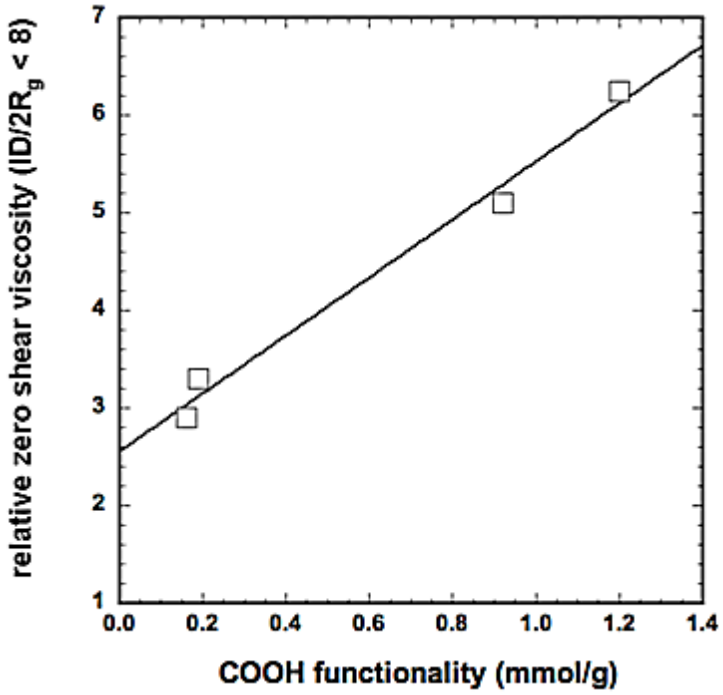

Figure III.10: Correlation between relative zero-shear viscosity at p_c< 8 and COOH functionality.

Figure III.5 reports the results of a mixture of HPAM with 20wt% of PSL with four different functionalities. In a first approach, the viscosity increase may be explained by the increase of the volume fraction of adsorbed very high molar mass HPAM as a function of the particle surface functionality. Nevertheless, considering this sole effect, a gradual decrease of the viscosity as a function of the confinement parameter should have been obtained instead of a plateau as observed in Figure III.7. At a HPAM concentration of 2 g / L, the polymer chains onto PSL decreases with pc. Other parameters should be thus taken into account to explain the behaviour observed within Figure III.7; the entanglement of adsorbed and free HPAM chains must certainly play a significant role both on the additivity effect and on the rheological effects. Furthermore, the entanglement should be of different level if we consider the one of the adsorbed HPAM onto PSLS and the one of adsorbed and free HPAM chains creating an outer layer. Under constraint as obtained during the rheological experiments, the layer composed of interaction between adsorbed and free HPAM chain is the first to be affected leading then to a shift of the adsorbed layer structure.

As a conclusion, higher viscosity is obtained with the highest volume fraction of adsorbed HPAM obtained by using PSL with the highest density of functionality. At the same time, the entanglement of adsorbed and free HPAM is the greatest. Under shearing, the outer layer is the first to be modified; the shell of the PSL made of adsorbed HPAM may be then affected with a decrease of its volume fraction and thus the viscosity value.

The flow thinning effects as a function of geometric parameters p_c is not easily interpreted (**Figure III.8**). It would appear that the effect of the HPAM-coated particles does affect the viscosities of the medium up to a critical p_c at which point the effects are reduced. There is no obvious correlation of this critical concentration with the surface functionality of PSLs. The general trend for the entire results shows a flow thinning effect for concentrations below 0.2 g/L in PSL (C_p = 2 g/L), i.e., a confinement parameter higher than 10. These fluidization effects can also be identified by varying the salt concentration of the medium.

Table III.2: Salinity effect on relative zero shear viscosity (Cp=2g/L; CPSL=0.2 g/L)

PSL	C NaCl (g/L)	$\eta_{0;rel}$
PSL 9	6	3.2± 0.1
	12	2.6± 0.1
PSL 22	6	5.6±0.1
	12	4.0 ± 0.1

The variation of the relative viscosity as a function of the salinity (6 and 12 g/Lin NaCl) for mixtures of PSL 9 and PSL 22 at 0.2 g/L1 (Cp = 2 g/L). The increase in salinity affects the macromolecular dimensions of the HPAM chain, also known as the polyelectrolyte effect. The radius of gyration decreases with the salinity and thus increases the confinement parameter. This leads to a decrease in viscosity.

IV. Conclusion

In the context of PPC, this chapter highlights the thickening effects related to the surface functionality of particles for a semi-diluted polymer regime, a "protein limit" regime (R_g/d > 1), depending on the confinement parameter that characterizes the inter-particle distance to the polymer size. Thickening increases linearly with surface functionality for a p_c< 10. This rheological behaviour is explained by the polymer-particle interactions that were observed in diluted conditions using zero shear capillary viscosity measurements. For p_c> 10, a fluidizing effect is detected as in salt solutions. This work opens interesting perspectives both for polymer adsorption studies on colloidal particles and the establishment of adsorption isotherm, studies of nano-rheological effects for particle sizes less than 100 nm with variable functionality.

CHAPTER VI: Thermal and mechanical behaviour of formulations based on HPAM/PSL microspheres

Résumé

Dans ce chapitre, une étude préliminaire a été réalisée sur le comportement des formulations de HPAM et HPAM/PSL microsphères. L'influence de la température sur la viscosité à cisaillement nulle des formulations a été étudié en régime semi-dilué. Dans une seconde partie, l'influence sur les masses molaires d'un cisaillement élongationel dans une contraction tubulaire en régime dilué du polymère a été étudiée.

L'effet en température montre un comportement légèrement diffèrent en fonction de la fonctionnalité de surface des microsphères (PSL9 et PSL22). Dans les deux cas, l'effet d'épaississent est conservé sur la plage de température 20-80°C mais avec des énergies d'activation légèrement plus élevées dans le cas de PSL 22 : E_a = 18.6, 18.8, 29.0 kJ/mol pour respectivement HPAM seul, HPAM/PSL 9 et HPAM/PSL 22. Il semblerait que la fonctionnalité influence légèrement le maintien de l'effet épaississant en température.

Pour comprendre le comportement des formulations soumises à des écoulements transitoires d'élongationel en régime laminaire à température ambiante (T=20°C), le viscosimètre capillaire a été modifié pour générer une dégradation mécanique contrôlée dans une contraction (R=4).L'évolution de la perte en viscosité en fonction du cisaillement (0-100000 s^{-1}) a été évaluée par une mesure de viscosité intrinsèque en régime dilué en se basant sur une méthode « single point » et par la suite déterminer l'évolution de la masse molaire Mw . Cette étude fournit des conclusions intéressantes telles que la contribution des microsphères ne modifient pas la dégradation mécanique à forts cisaillements des chaine de HPAM en solution dans le domaine de concentration et régime bien définis (200 ppm en HPAM, 20 ppm en PSL 9 et PSL22).

I- Introduction

Solutions of Hydrolyzed Polyacrylamide polymers commonly used in EOR applications are known to be sensitive to the temperature and mechanical degradation [33, 69, 195, 196]. For polymer systems in oilfields, it is important to quantify the effect of temperature on the stability of HPAM polymers. When the temperature is lower, the polymer is thermally stable [60], but when the elevation of temperature is important, the amide group present in the

polymer backbone start to hydrolyse [61]. For example, Davison and Mentzer [66] studied the viscosity measurements of several polymers at 90 ° C for possible application in the oil fields of the North Sea. Their results indicate that the viscosity of polyacrylamide is particularly poor at high temperature and precipitation of the polymer was observed. To overcome this problem, the nanotechnology approach has been used to increase the efficiency of polymer at high temperatures using different surfaces of nanoparticles. Sebastián Llanos et al. evaluated the effect of SiO_2 by surface modification (functionalization) based on different loadings of sodium oleate on HPAM viscosity[197]. In the same context, Corredor-Rojas et al. Examined the viscosity of HPAM based on the surface modification of silica with carboxylic acid and silane groups (3-methacryloxypropyltrimethoxysilane, octyltriethoxysilane, and oleic acid) at different concentrations and temperatures**[198].** Both of works suggest that surface functionality improve the viscosity of HPAM polymer and can tolerate to ion degradation at high temperature based on the formation of a three-dimensional networks between the polymer chains and nanoparticle used.

On the other side, the mechanical degradation of the polymers is also an irreversible phenomenon which leads to a breakdown of polymer chains and a decrease in the molar mass and viscosity. This type of degradation can occur at various stages, from the preparation of the polymer solution to the polymer injection process through surface installations (pumping systems, valves, contractions, etc.), but also in the porous medium. During mechanical degradation, the polymer chains in solutions are subjected to elongation phenomena that can lead to their breakage if the force applied is too important. Two types of flow can generally describe these elongation phenomena: transient and stationary elongational flow

There are many systems described in the literature for mechanically degrading polymer solutions in a controlled manner. We can cite for example the "API system (American Petroleum Institute)" which allows to estimate the sensitivity of the degradation of a polymer solution using a porous mass (carrot) or a capillary device [199] according to RP63 [200] [API-RP-63, 1990]. According to this standard, the polymer solutions pass through a capillary under the action of a pressure of between 0.5 and 20 bars. The flow created by this device is realized in the way following: at the inlet of the capillary, the contraction induces a

strong elongational component of the rate of deformation, whereas in the capillary, the solution is subjected to a stress in shear. By analogy with these principles, it seemed appropriate to adapt the capillary rheology assembly to the study of the mechanical stability of the formulations based on Hydrolyzed Polyacrylamide (HPAM) and different functionnality of poly (styrene-acrylic acid) microspheres. To do this, we have improved the measuring device of capillary rheology by adding a system allowing shearing in a controlled way polymer solutions in order to study their mechanical stabilities by analyzing their rheological and molar mass proprieties.

However, based on the thickening effects shown in the previous chapters, it was important to characterize the behavior of these systems in temperature and mechanical solicitation according to the surface function of PSL microspheres. This chapter presents the preliminary results for which a) the temperature range (20-80 ° C) was chosen according to the Hassi Messaoud Algerian oil field characteristic and b) the mechanical solicitation applied on diluted solution in a tubular contraction "mimicking" high shear stress (<100 000 s^{-1}).

II. Materials & methods

II.1. Materials

The reactants of this chapter (Polymer and PSL microspheres) were well characterized in the chapter 3). An HPAM with high molar mass of 10^7 g/mol and hydrolysis degree of 30%, PSL microspheres with High and Low functionality (PSL22 & PSL 9) were used for this study. The formulations based on HPAM / PSL were prepared in medium salinity of 6 g / L NaCl according to the protocol described also in chapter 3.

II.2. Protocol and measurement of the mechanical degradation of polymers in a tubular contraction

Mother solutions of HPAM polymer; HPAM/PSL (high functionality: PSL22 & low functionality: PSL9) formulations were prepared at a concentration of 2000 ppm HPAM which is under semi-dilute regime, and a concentration of 200 ppm PSL microspheres. Dilutions were carefully performed to obtain a final concentration of 200ppm which is at the diluted regime of polymer and a final concentration of 20 ppm for PSL microspheres.

Then, the formulation have been subjected to transient elongational flows in order to study their mechanical stability under medium salinity of 6 g/L NaCl and pH=6.2 at ambient temperature (20°C). To do this, the formulations were injected into a tube of radius (R_1 = 1 mm) followed by a passage of the solutions in smaller tube with a radius (R_2 = 0.125 mm) and a length of 7 cm. Note that the contraction is the ration of radius. In our case $R=R_1/R_2$ = 4. At the outlet, the degraded solution was collected into a becker. The scheme was illustrated in the figure IV.1.

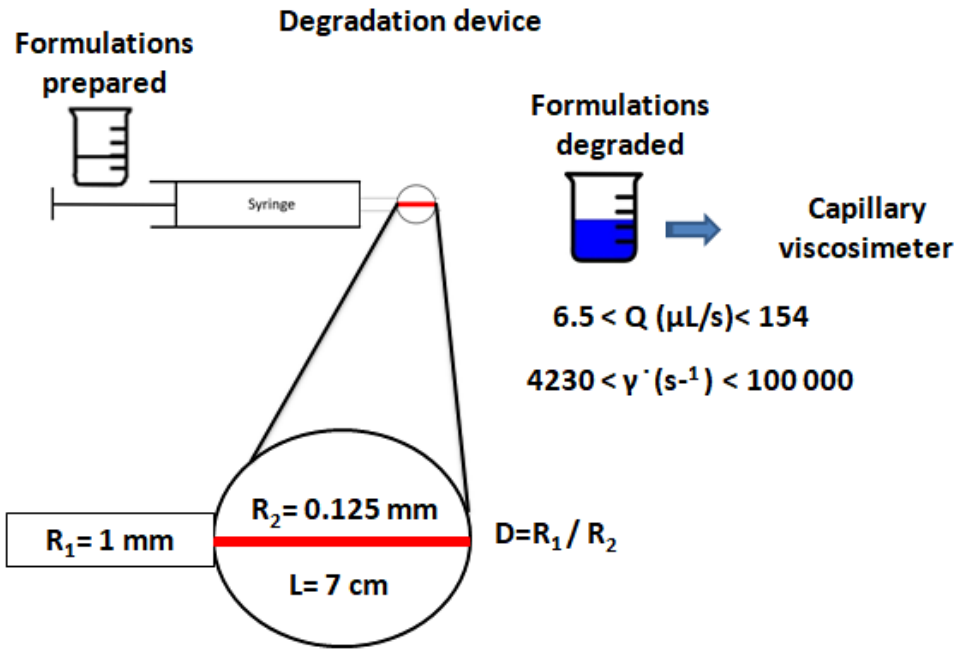

Figure IV.1: Scheme of degradation device of our formulations

A volume of 12 mL different formulations based on HPAM/PSL microspheres was passed through the device at different flow rates in order to obtain shear rates between 0 to 10^5 s^{-1} calculated using the Poiseuille's law (eq IV.1) :

$$\dot{\gamma} = \frac{4\,Q}{\pi\,R^3} \qquad \text{(IV.1)}$$

Where Q is the injection rate fixed by the operators, R= 0.125 mm is the internal radius of the tube 2 after the contraction. Table IV.1 illustated the values obtained of shear rates ($\dot{\gamma}$) as function of Q in (uL/s)

Table IV.1: values of Shear rates ($\dot{\gamma}$) as function of Q (µL/s)

Q (µL/s)	Shear rates ($\dot{\gamma}$)
6.51	4231.5
9.02	5859.4
12.03	7812.5
19.25	12 500
38.4	25 000
76.7	50 000
115	75 000
154	100 000

Note that to study the injection of previously degraded systems, it must be avoided that this solution undergoes degradation before the restriction. To verify that in is the case; we measured the viscosity before and after injection in the same experimental configuration without the restriction and the tube 2. The viscosity remains the same regardless of the flow rate imposed (6-154 uL/s). Since the polymer solution does not undergo mechanical degradation during its passage, it is then possible to determine the consequences of the mechanical degradation undergone by an HPAM solution in the presence and absence of the PSL microspheres in the tubular contraction.

The degraded solutions of HPAM and HPAM/ PSL microspheres were then collected in the beaker and injected in second time inside the capillary viscosimeter device (see chapter 2) to evaluate the viscosity based on the relation (IV.2):

$$\eta = \frac{\sigma}{\dot{\gamma}} = \frac{\Delta P\ \pi R^4}{2\ L\ Q\ (m+3)} \qquad \text{(IV.2)}$$

Where, η is the absolute viscosity of the polymer solution, R is the capillary tube radius, Q is the injection flow rate, L is the length of the tube between the two pressure sensor terminals, and m is a corrective factor taking consider the non-Newtonian character of the polymer solution. This value is equal to 1 in the case of a diluted solution (Newtonian behavior) and is greater than or equal to 1 in the case of a semi-diluted solution.

The value of relative viscosity measurement makes it possible to determine the intrinsic viscosity based on the single point method which can determined the molecular weight of

our polymer.

II.3. Measurement of intrinsic viscosity & molar mass using a single point approach

After achieving the mechanical degradation of polymer solutions in the contraction, in-line viscosity measurements and intrinsic viscosities at 20 ° C were performed at 1 round trip.

Intrinsic viscosity measurements [η] were carried out only in a diluted in this degradation system in order to evaluate the impact of mechanical degradation on the molar mass of the Hydrolyzed Polyacrylamide (HPAM). Intrinsic viscosity can be determined using two approaches: the "classic" approach and approach single point ".Unlike the "classical" approach where the measure of [η] requires several dilutions and 4 - 5 measurements of reduced viscosity, the use of the “single point" approach makes it possible to estimate the intrinsic viscosity directly online for each round trip, by a single viscosity measurement, which is not possible with the "classical" approach where one is obliged to perform several off-line measurements.

In our case, we decided to use the Huggins relationship (because already used in the "classical" approach) to achieve the "IV in one point" approach. Indeed, we can notice that the relation of Huggins (IV.3) is equivalent to a second-order equation whose resolution allows determine the intrinsic viscosity with the value of k_H set at 0.5.

$$\eta_{red} = \frac{\eta_r - 1}{C} = [\eta] + k_H[\eta]^2 C \qquad \text{(IV.3)}$$

Where [η] is the intrinsic viscosity, η_r is the relative viscosity, k_H is the constant of Huggins and C is the concentration of polymer. Based on the relation of Mark-Houwink determined in the chapter, the molar mass of our polymer can be so determined for each sheared solution.

III. Results and discussions

This section is organized as follows: In a first step, the formulation based on HPAM/ PSL microspheres was evaluated by studying the effect of operational parameters such as temperature in semi dilute regime. Furthermore, we have focused on the novelty which is

the study of the mechanical stability of the HPAM/PSL microspheres (dilute regime) in one contraction geometry which was used under different shears in order to compare the mechanical stability of polymer in presence and absence of PSL microspheres.

III.1.Effect of temperature on the formulations of HPAM/PSL microspheres

The loss of Hydrolyzed Polyacrylamide viscosity and its derivative at elevated temperature is one of the drawbacks for its use in high pressure-high temperature environment. The effect of temperature on HPAM and HPAM/ PSL (low and high functionality) in 6g/L NaCl has been studied and results are presented in the figure IV.2. Furthermore the effect of temperature on viscosity can be correlated by Arrhenius equation given by eq. (IV.4).

$$\eta_0 = A.exp\left(\frac{E_a}{RT}\right) \qquad \text{(IV.4)}$$

Where, η_0 is the zero shear viscosity in (cp), A is the constant, Ea is the activation energy (kJ/mole), R is the universal gas constant (0.008314 kJ/mole- K), T is the temperature (Kelvin). The variations of viscosity (ln η_0) as the function of inverse of temperature (1/T) for the different formulations based on HPAM/ Polystyrene at zero shear rates (s^{-1}) are shown in figure IV.3.

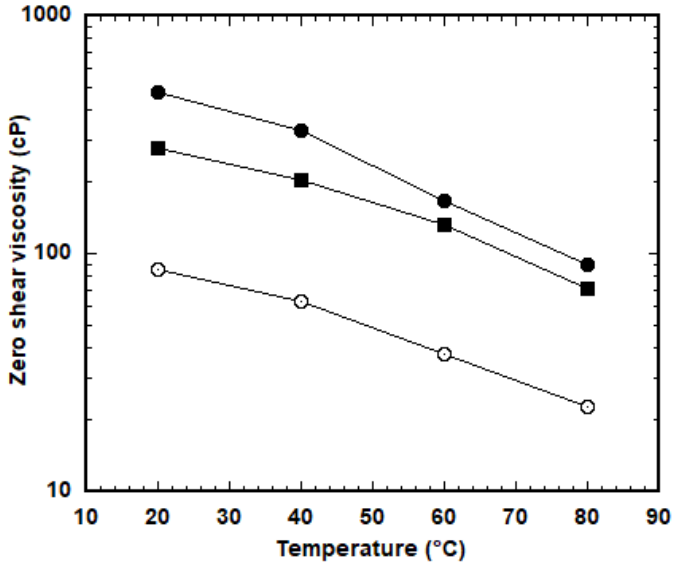

Figure IV.2: Temperature effect on the zero shear viscosities of formulations (● PSL22 ■ PSL9 ○HPAM without PSL. C_p = 2 g/L, C_{PSL}=0.2 g/L, pH = 6.2, T=20°C. (Shear rates of 0 to 1000 s^{-1}). The lines are guides for the eyes

It was found that the zero shear viscosities for all samples decreased in presence of absence

of PSL microspheres at elevated temperature. Compared with the pure HPAM solution, the HPAM/PSL 22 hybrids still maintained ~5 fold higher effective viscosities in the whole temperature range studied. The same tendency was observed for the PSL9 which maintain the viscosity ~3.

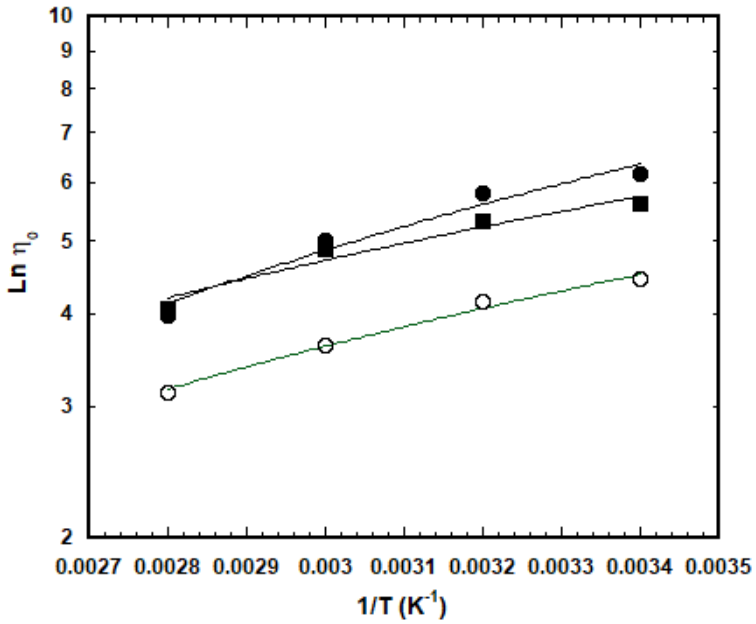

Figure IV.3: Variation of Ln η_0 versus temperature inverse of different formulations (● PSL22 ■ PSL9. C_p = 2 g/L., 6 g/L in NaCl, pH = 6.2, T=20°C. C_{PSL}=0.2 g/L).

Using Eq. 1, the ln η_0 and temperature reciprocal shows a straight line relationship with a slope of $\Delta E\eta_0$ / R. The graph showing the straight line relationship between ln η_0 and 1/T of different HPAM, HPAM /PSL 22 & HPAM/PSL 9 for zero shear rates (s^{-1}) is shown in figure IV.3. A good fit of the three formulations (R^2>90%) was observed with activation energy of 18.6, 18.8, 29.0 kJ/mol for HPAM, HPAM/PSL 9 and HPAM/PSL 22 respectively**.** In the case of high functionality, it seems that there is an effect of functionality which translates that the thickening effect will decrease with the increase of the temperature.

III.2.Effect of elongational flow on the HPAM/PSL formulations

In the last part of this chapter, we have focused on the effect of elongational flow on the HPAM/PSL formulations. Figure IV.4 illustrated the viscosity loss of HPAM and HPAM/ PSL under the effect of different shear rates. We can notice first of all that the relative viscosity is directly affected by the mechanical degradation and drops sharply between 10^4- $8*10^4$ s^{-1} and then stabilizes betwwen $8*10^4$ – 10^5 s^{-1} .

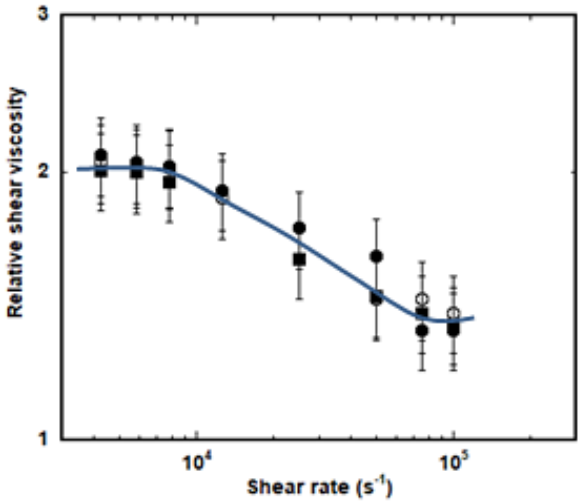

Figure IV.4: Degradation of HPAM polymer under different shear rates (○ HPAM without PSL, ● HPAM/PSL22 ■ HPAM/PSL 9; 6 g/L in NaCl, pH = 6.2, T=20°C). The line is guide for eyes

At high injection speeds, there is a significant decrease in relative shear viscosity. By way of example, for an injection speed of 154 ml /s corresponded to shear rate of 100 000 s^{-1}, the viscosity of the degraded solution is three times lower than that of the initial solution. This will allow the injection of the polymer to apply lower pressures provided that the polymer is previously degraded.

The figure IV.5 illustrated the same tendency of the drop in the molar mass of polymer used as a function of shear rates in the presence and absence of PSL microspheres. A rapid decrease was observed between 10^4- 8*10^4 s^{-1} and then stabilized between 8*10^4 - 10^5 s^{-1}.

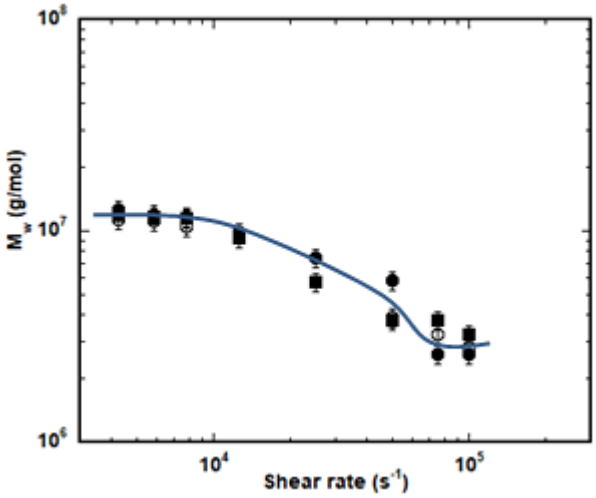

Figure IV.5: Evolution of molar mass distribution of different formulations (○ HPAM without PSL, ● HPAM/PSL 22 ■ HPAM/PSL 9; 6 g/L in NaCl, pH = 6.2, T=20°C). The line is guide for eyes

These results are consistent with those from the literature which have studied the degraded polystyrene solutions in dilute regime after a single passage through a narrow contraction [201, 202].

From a comparative point of view with polymer used, and based on the literature concerning the work related to the degradation of the HPAM polymer, the work was carried out under a semi-diluted regime, which made the comparison of the results very complicated.

In the shear rate range where the high molecular HPAM undergoes mechanical degradation in the dilute regime, the incorporation of the microsphere does not affect this elongational degradation of the HPAM chain in solution, that corresponding to the matrix. For the chains of adsorbed HPAM corresponding here to a very small fraction of HPAM, the results do not make it possible to conclude on their possible degradations and desorption. The question remains and a study in semi-diluted regime could bring clarification on these last points.

IV. Conclusion

This chapter has been the subject of a preliminary study on the thermal and mechanical behavior of HPAM and HPAM / PSL formulations in a semi-dilute (cp > c*) and dilute (cp < c*) regimes respectively. The temperature effect shows a slightly different behavior depending on the surface functionality of the microspheres (PSL9 and PSL22). In both cases, the effect of thickening is maintained over the temperature range 20-80 ° C but with slightly higher activation energies in the case of PLS22.

Because of their conformations of flexible chain of large molar masses, these types of polymers are known to be sensitive to mechanical degradation via elongation phenomena that can lead to their rupture if the forces applied are too important. To understand the behavior of formulations subjected to transient elongational flows in laminar and ambient temperature, capillary viscosimeter was modified to generate controlled mechanical degradation through contraction. The evolution of the degradation was evaluated following an intrinsic viscosity measurement in dilute regime.

This preliminary study provides an interesting conclusions such as that the contribution of the PSL microspheres to the formulation of HPAM/PSL does not modify the degradation behaviour in the concentration and shear regime of diluted solutions (cp < c*) and $\dot{\gamma} < 100000\ s^{-1}$.

It would have been interesting to deepen the subject by studying the influence of other parameters including the effect of : (i) mechanical degradation at high temperature (50 ° C & 80 ° C), (ii) Influence of water salinity ($CaCl_2$, $MgCl_2$ ...ect) (Solvents), (iii) the influence of the length of the tubular and different diameter of contractions and functionality of microspheres.

Conclusion Générale

CONCLUSION GENERALE

Une des méthodes de récupération assistée du pétrole les plus utilisées est l'injection de polymères (polymer flooding). L'efficacité de cette méthode est attribuée principalement à la réduction de la mobilité de la phase aqueuse et à la viscoélasticité des polymères. Cette efficacité dépend de plusieurs paramètres comme la perméabilité, la température, la salinité, l'hétérogénéité, la mouillabilité, le nombre capillaire, etc. De nombreuses connaissances ont été accumulées s'agissant du rôle des polymères dans la récupération du pétrole. Le principal but des travaux de cette thèse est d'étudier de nouvelles formulations aqueuses basées sur des mélanges de type polymères/microparticules afin d'améliorer les comportements rhéologiques classiques de polymère décris dans la littérature en vue d'une application à la récupération assistée du pétrole par la méthode chimique. Ces formulations ont été étudiées et optimisées dans des conditions de salinité et de température simulés à un réservoir pétrolier Algérien (6 g/L NaCl et 20-80 °C).

L'étude bibliographique a montré l'intérêt de combiner des nanomatériaux au polyacrylamide en solution pour améliorer les taux de récupération, la tenue en température et leurs rôles comme fluide de fracturation. L'attrait de ces systèmes est lié au comportement rhéologique particulier de ces mélanges dénommés composites polymère-particule qui peuvent développer une recrudescence d'effets viscosifiants. Ces effets sont principalement dûs aux différentes caractéristiques physico-chimiques présentes dans le système, telles que le diamètre des particules (d), le rayon de giration des chaînes de polymères (Rg), les interactions entre les particules et le polymère, la plage de concentration du polymère et des particules.

L'ensemble des travaux exposé dans ce manuscrit ont permis de préciser le rôle de quelques unes de ces caractéristiques physico-chimiques sur les effets d'épaississement mis en évidence sur des composites polymère-particule à base de polyacrylamide hydrolysé (HPAM, 30%) de forte masse molaire (Mw = 10^7 g/mol) et de particule bien définie en termes de taille, dispersité, et fonctionnalité. Le choix du HPAM s'est orienté sur un polyacrylamide commercial (SNF Floerger) connu pour son utilisation en « polymer flooding », le choix des particules vers des latex, i.e. des émulsions aqueuses industrialisable de microsphères de polystyrène fonctionnalisées en surface par des fonctions acide carboxylique (PSL).

La minimisation et l'optimisation des expériences via l'utilisation d'un plan d'expérience de Doehlert a montré l'effet de trois caractéristiques physico-chimiques : la taille et

concentration des microsphères, et la variation de la température sur la viscosité newtonienne (η0) de composites HPAM-PSL. Les résultats montrent que la taille et la température ont été les facteurs les plus influents et que les paramètres optimaux du procédé sont les suivants: 20 ° C (température); 50 ppm (concentration en microsphères); 1000 nm (taille). La méthodologie de surface de réponse (RSM) montre que les comportements d'épaississement observé pour ces composites n'est pas évidente et ne serai pas relié directement par un simple effet de la contribution de la fraction volumique (taille et concentration) des microsphères sur la matrice HPAM. Ces travaux ont mis en évidence le rôle de la fonctionnalité de surface des particules (0,16 à 1,2 mmol / g de COOH) sur les effets d'épaississement pour un régime semi-dilué, un régime "limite protéique" (Rg/d > 1), en fonction du paramètre de confinement (pc) qui caractérise la distance inter-particules à la taille du polymère. L'épaississement augmente linéairement avec la fonctionnalité de surface pour un p_c < 10. Ce comportement rhéologique s'explique par les interactions polymère-particules qui ont été observées dans des conditions diluées en utilisant des mesures de viscosité capillaire. Pour pc > 10, un effet contraire apparait, une fluidification est observée. Pour p_c<10, la fonctionnalité impacte légèrement les effets d'épaississement à plus haute température. Il est conservé sur la plage de température 20-80°C mais avec des énergies d'activation légèrement plus élevées dans le cas de PSL les plus fonctionnalisés (Ea = 18.8 kJ/mol pour 0,16 mmol/g et Ea = 29 kJ/mol pour 1,2 mmol/g de COOH).

En perspective aux applications EOR, une étude préliminaire a démontré que la fonctionnalité des microsphères ne modifie pas la dégradation mécanique à forts cisaillements (10^5 s^{-1}) des chaines de HPAM en solution soumises à des écoulements transitoires élongationels en régime laminaire dans une contraction tubulaire, dans le domaine de concentration et régime bien définis : 200 ppm en HPAM, 20 ppm en microsphère.

L'approche expérimentale de ces travaux est basée sur la synthèse de microsphère modèle de fonctionnalité contrôlé, d'une caractérisation fine de tous les paramètres d'étude et de mesure rhéologique dont la viscosimétrie capillaire qui nous a permis de développer une méthodologie originale pour déterminer la quantité de polymère adsorber sur des nanomatériaux. Ces travaux ouvrent des perspectives intéressantes tant pour l'étude de

l'adsorption des polymères sur les particules colloïdales que pour l'établissement d'isotherme d'adsorption, l'étude des effets nanorhéologiques des particules de taille inférieure à 100 nm à fonctionnalité variable.

La perspective à l'objectif principale de ce travail de thèse serait d'étendre les caractéristiques physico-chimiques à la concentration et masse molaire du polymère, sa composition chimique ainsi que la nature de la fonctionnalisation des microsphères PSL, la salinité (concentration et valence du sel). A l'ensemble de ces paramètres, il serait intéressant de suivre leurs effets sur la viscosité au plateau newtonien mais aussi sur le temps de relaxation. Au niveau application EOR, le comportement en milieu poreux est primordial pour valider le concept à l'utilisation industriel de ces composite HPAM/PSL, ainsi que leur comportement en adsorption sur des roches modèles.

References

REFERENCES

1. Thomas, A., *Essentials of Polymer Flooding Technique*2019: Wiley.
2. Gbadamosi, A.O., et al., *Hybrid suspension of polymer and nanoparticles for enhanced oil recovery.* Polymer Bulletin, 2019: p. 1-38.
3. Zheng, C., et al., *Suspension of surface-modified nano-SiO2 in partially hydrolyzed aqueous solution of polyacrylamide for enhanced oil recovery.* Colloids and Surfaces A: Physicochemical and Engineering Aspects, 2017. **524**: p. 169-177.
4. Giraldo, L.J., et al., *The effects of SiO2 nanoparticles on the thermal stability and rheological behavior of hydrolyzed polyacrylamide based polymeric solutions.* Journal of Petroleum Science and Engineering, 2017. **159**: p. 841-852.
5. Green, D.W. and G.P. Willhite, *Enhanced oil recovery*. Vol. 6. 1998: Henry L. Doherty Memorial Fund of AIME, Society of Petroleum Engineers ….
6. Sen, R., *Biotechnology in petroleum recovery: the microbial EOR.* Progress in energy and combustion Science, 2008. **34**(6): p. 714-724.
7. Bavière, M., *Basic concepts in enhanced oil recovery processes*. Vol. 33. 1991: SCI.
8. Buridant, J., et al., *Histoire des faits economiques*2007: Editions Bréal.
9. Avendano, J., *Viscoélasticité et récupération améliorée du pétrole*, 2012.
10. Thomas, S., *Enhanced oil recovery-an overview.* Oil & Gas Science and Technology-Revue de l'IFP, 2008. **63**(1): p. 9-19.
11. Lake, L.W., *Enhanced oil recovery*1989: Prentice Hall.
12. Greaser, G.R. and J.R. Ortiz. *New Thermal Recovery Technology and Technology Transfer for Successful Heavy Oil Development*. in *SPE International Thermal Operations and Heavy Oil Symposium*. 2001. Society of Petroleum Engineers.
13. Blackwell, R., J. Rayne, and W. Terry, *Factors influencing the efficiency of miscible displacement.* 1959.
14. Christie, M. and D. Bond, *Detailed simulation of unstable processes in miscible flooding.* SPE Reservoir Engineering, 1987. **2**(04): p. 514-522.
15. Claridge, E., *Prediction of recovery in unstable miscible flooding.* Society of Petroleum Engineers Journal, 1972. **12**(02): p. 143-155.
16. Stone, P., B. Steinberg, and J. Goodson, *Completion design for waterfloods and CO2 floods.* SPE Production Engineering, 1989. **4**(04): p. 365-370.
17. Sandiford, B., *Laboratory and field studies of water floods using polymer solutions to increase oil recoveries.* Journal of Petroleum Technology, 1964. **16**(08): p. 917-922.
18. Gogarty, W. and W. Tosch, *Miscible-type waterflooding: oil recovery with micellar solutions.* Journal of Petroleum Technology, 1968. **20**(12): p. 1,407-1,414.
19. Hill, H., J. Reisberg, and G. Stegemeier, *Aqueous surfactant systems for oil recovery.* Journal of Petroleum Technology, 1973. **25**(02): p. 186-194.
20. Shutang, G., et al., *Alkaline/surfactant/polymer pilot performance of the west central Saertu, Daqing oil field.* SPE Reservoir Engineering, 1996. **11**(03): p. 181-188.
21. Vargo, J., et al. *Alkaline-surfactant-polymer flooding of the Cambridge Minnelusa field*. in *SPE Rocky Mountain Regional Meeting*. 1999. Society of Petroleum Engineers.
22. Stoll, M., et al. *Alkaline-surfactant-polymer Flood–From the Laboratory to the Field*. in *IOR 2011-16th European Symposium on Improved Oil Recovery*. 2011.
23. Gao, C.H. *Advances of polymer flood in heavy oil recovery*. in *SPE heavy oil conference and exhibition*. 2011. Society of Petroleum Engineers.
24. Sheng, J., *Modern chemical enhanced oil recovery: theory and practice*2010: Gulf Professional Publishing.
25. Salager, J.L., *Physico-chemical properties of surfactant-water-oil mixtures: phase behavior, micro-emulsion formation and interfacial tension*, 1977, Citeseer.
26. Foster, W., *A low-tension waterflooding process.* Journal of Petroleum Technology, 1973. **25**(02): p. 205-210.
27. Healy, R.N. and R.L. Reed, *Physsicochemical aspects of microemulsion flooding.* Society of Petroleum Engineers Journal, 1974. **14**(05): p. 491-501.
28. Lefebvre du Prey, E., *Factors affecting liquid-liquid relative permeabilities of a consolidated*

porous medium. Society of Petroleum Engineers Journal, 1973. **13**(01): p. 39-47.
29. Taber, J., *Dynamic and static forces required to remove a discontinuous oil phase from porous media containing both oil and water.* Society of Petroleum Engineers Journal, 1969. **9**(01): p. 3-12.
30. Delshad, M., et al. *Effect of capillary number on the residual saturation of a three-phase micellar solution*. in *SPE enhanced oil recovery symposium*. 1986. Society of Petroleum Engineers.
31. Ali, S. and S. Thomas, *A realistic look at enhanced oil recovery.* Sci. Iran, 1994. **1**: p. 219-230.
32. Tognisso, D.E., *Écoulements de fluides complexes en milieu poreux: utilisation de micelles géantes pour la Récupération Améliorée du Pétrole*, 2011, PhD thesis, Bordeaux 1.
33. Sorbie, K., *Polymer-Improved Oil Recovery, 115 Glasgow.* Scotland: Blackie & Son, 1991: p. 126-163.
34. Barreau, P., *Modifications des propriétés poly-phasiques d'un milieu poreux en présence d'une couche de polymère adsorbe: études expérimentale et numérique*, 1996, Paris, ENSAM.
35. Wang, D., et al., *Key aspects of project design for polymer flooding at the Daqing Oilfield.* SPE Reservoir Evaluation & Engineering, 2008. **11**(06): p. 1,117-1,124.
36. Needham, R.B. and P.H. Doe, *Polymer flooding review.* Journal of Petroleum Technology, 1987. **39**(12): p. 1,503-1,507.
37. Seright, R.S., A. Campbell, and P. Mozley. *Stability of partially hydrolyzed polyacrylamides at elevated temperatures in the absence of divalent cations*. in *SPE International Symposium on Oilfield Chemistry*. 2009. Society of Petroleum Engineers.
38. Osterloh, W. and E. Law. *Polymer transport and rheological properties for polymer flooding in the north sea*. in *SPE/DOE Improved Oil Recovery Symposium*. 1998. Society of Petroleum Engineers.
39. Zirnsak, M., D. Boger, and V. Tirtaatmadja, *Steady shear and dynamic rheological properties of xanthan gum solutions in viscous solvents.* Journal of Rheology, 1999. **43**(3): p. 627-650.
40. Kohler, N. and G. Chauveteau, *Xanthan polysaccharide plugging behavior in porous media-preferential use of fermentation broth.* Journal of Petroleum Technology, 1981. **33**(02): p. 349-358.
41. Williams, P.A., *Handbook of industrial water soluble polymers*2008: John Wiley & Sons.
42. Bird, R.B., R.C. Armstrong, and O. Hassager, *Dynamics of polymeric liquids. Vol. 1: Fluid mechanics.* 1987.
43. Jouenne, S., et al. *Universal Viscosifying Behavior of Acrylamide-based Polymers Used in EOR-Application for QA/QC, Viscosity Predictions and Field Characterization*. in *IOR 2019–20th European Symposium on Improved Oil Recovery*. 2019.
44. Carreau, P.J., *Rheology of polymeric systems: principles and applications.* 1997.
45. Teraoka, I., *Polymer solutions: an introduction to physical properties*2002: John Wiley & Sons.
46. Flory, P.J., *Principles of polymer chemistry*1953: Cornell University Press.
47. Kamal, M.S., et al., *Review on polymer flooding: rheology, adsorption, stability, and field applications of various polymer systems.* Polymer Reviews, 2015. **55**(3): p. 491-530.
48. Ghoumrassi-Barr, S. and D. Aliouche, *A Rheological Study of Xanthan Polymer for Enhanced Oil Recovery.* Journal of Macromolecular Science, Part B, 2016. **55**(8): p. 793-809.
49. Wu, Y., et al. *Development of new polymers with better performance under conditions of high temperature and high salinity*. in *SPE EOR conference at oil and gas West Asia*. 2012. Society of Petroleum Engineers.
50. Al-Saadi, F.S., et al. *Polymer Flooding in a large field in South Oman-initial results and future plans*. in *SPE EOR Conference at Oil and Gas West Asia*. 2012. Society of Petroleum Engineers.
51. Mogollon, J.L. and T. Lokhandwala. *Rejuvenating viscous oil reservoirs by polymer injection: lessons learned in the field*. in *SPE Enhanced Oil Recovery Conference*. 2013. Society of Petroleum Engineers.
52. Pu, H. *An update and perspective on field-scale chemical floods in Daqing oilfield, China*. in *SPE Middle East Oil and Gas Show and Conference*. 2009. Society of Petroleum Engineers.

53. Pratap, M. and M. Gauma. *Field implementation of alkaline-surfactant-polymer (ASP) flooding: a maiden effort in India*. in *SPE Asia Pacific oil and gas conference and exhibition*. 2004. Society of Petroleum Engineers.
54. Hryc, A., et al. *Design and execution of a polymer injection pilot in Argentina*. in *SPE Annual Technical Conference and Exhibition*. 2013. Society of Petroleum Engineers.
55. Pitts, M.J., et al. *Alkaline-surfactant-polymer flood of the Tanner Field*. in *SPE/DOE symposium on improved oil recovery*. 2006. Society of Petroleum Engineers.
56. Watson, A., G.A. Trahan, and W. Sorensen. *An interim case study of an alkaline-surfactant-polymer flood in the Mooney Field, Alberta, Canada*. in *SPE Improved Oil Recovery Symposium*. 2014. Society of Petroleum Engineers.
57. Delamaide, E., et al. *Chemical EOR for heavy oil: The Canadian experience*. in *SPE EOR Conference at Oil and Gas West Asia*. 2014. Society of Petroleum Engineers.
58. Levitt, D. and G.A. Pope. *Selection and screening of polymers for enhanced-oil recovery*. in *SPE Symposium on Improved Oil Recovery*. 2008. Society of Petroleum Engineers.
59. Chauveteau, G. and A. Zaitoun. *Basic rheological behavior of xanthan polysaccharide solutions in porous media: effects of pore size and polymer concentration*. in *Proceedings of the first European symposium on enhanced oil recovery, Bournemouth, England, Society of Petroleum Engineers, Richardson, TX*. 1981.
60. Ryles, R. *Elevated temperature testing of mobility control reagents*. in *SPE Annual Technical Conference and Exhibition*. 1983. Society of Petroleum Engineers.
61. Caulfield, M.J., G.G. Qiao, and D.H. Solomon, *Some aspects of the properties and degradation of polyacrylamides.* Chemical reviews, 2002. **102**(9): p. 3067-3084.
62. Rashidi, M., A.M. Blokhus, and A. Skauge, *Viscosity and retention of sulfonated polyacrylamide polymers at high temperature.* Journal of Applied Polymer Science, 2011. **119**(6): p. 3623-3629.
63. Mungan, N., *Rheology and adsorption of aqueous polymer solutions.* Journal of Canadian Petroleum Technology, 1969. **8**(02): p. 45-50.
64. Sheng, J., *Polymer flooding.* Modern chemical enhance oil recovery, 2011: p. 101-206.
65. Drumeanu, A. *Some considerations concerning four-ball machine testing of the polyacrylamide solutions*. in *IOP conference series: materials science and engineering*. 2017. IOP Publishing.
66. Davison, P. and E. Mentzer, *Polymer flooding in North Sea reservoirs.* Society of Petroleum Engineers Journal, 1982. **22**(03): p. 353-362.
67. Hu, Z., et al., *Rheological properties of partially hydrolyzed polyacrylamide seeded by nanoparticles.* Industrial & Engineering Chemistry Research, 2017. **56**(12): p. 3456-3463.
68. Sorbie, K.S., *Polymer-improved oil recovery*2013: Springer Science & Business Media.
69. Zaitoun, A., et al., *Shear stability of EOR polymers.* Spe Journal, 2012. **17**(02): p. 335-339.
70. Afolabi, R.O., *Effect of surfactant and hydrophobe content on the rheology of poly (acrylamide-co-N-dodecylacrylamide) for potential enhanced oil recovery application.* American Journal of Polymer Science, 2015. **5**(2): p. 41-46.
71. Willhite, G.P. and J.G. Dominguez, *Mechanisms of polymer retention in porous media*, in *Improved oil recovery by surfactant and polymer flooding*1977, Elsevier. p. 511-554.
72. Lai, N., et al., *Shear Resistance Properties of Modified Nano-SiO2/AA/AM Copolymer Oil Displacement Agent.* Energies, 2016. **9**(12): p. 1037.
73. Seright, R., et al. *Rheology and mechanical degradation of EOR polymers*. in *SPE/British Society of Rheology Conference on Rheology in Crude Oil Production*. 1983.
74. Zhang, L.-h., D. Zhang, and B. Jiang, *The rheological behavior of salt tolerant polyacrylamide solutions.* Chemical Engineering & Technology: Industrial Chemistry-Plant Equipment-Process Engineering-Biotechnology, 2006. **29**(3): p. 395-400.
75. Liu, P., et al., *Experimental study of rheological properties and oil displacement efficiency in oilfields for a synthetic hydrophobically modified polymer*. Scientific reports, 2017. **7**(1): p. 8791.
76. Shupe, R.D., *Chemical stability of polyacrylamide polymers.* Journal of Petroleum Technology, 1981. **33**(08): p. 1,513-1,529.
77. Yang, S. and L. Treiber. *Chemical stability of polyacrylamide under simulated field*

conditions. in *SPE Annual Technical Conference and Exhibition*. 1985. Society of Petroleum Engineers.

78. Lee, K.S., *Performance of a polymer flood with shear-thinning fluid in heterogeneous layered systems with crossflow.* Energies, 2011. **4**(8): p. 1112-1128.
79. Alomair, O.A., K.M. Matar, and Y.H. Alsaeed, *Experimental study of enhanced-heavy-oil recovery in Berea sandstone cores by use of nanofluids applications.* SPE Reservoir Evaluation & Engineering, 2015. **18**(03): p. 387-399.
80. Hendraningrat, L. and O. Torsaeter. *Unlocking the potential of metal oxides nanoparticles to enhance the oil recovery*. in *offshore technology conference-Asia*. 2014. Offshore Technology Conference.
81. Ogolo, N., O. Olafuyi, and M. Onyekonwu. *Enhanced oil recovery using nanoparticles*. in *SPE Saudi Arabia section technical symposium and exhibition*. 2012. Society of Petroleum Engineers.
82. Ogolo, N.C., O.A. Olafuyi, and M. Onyekonwu. *Effect of nanoparticles on migrating fines in formations*. in *SPE International Oilfield Nanotechnology Conference and Exhibition*. 2012. Society of Petroleum Engineers.
83. Ogolo, N.A. *The trapping capacity of nanofluids on migrating fines in sand*. in *SPE Annual Technical Conference and Exhibition*. 2013. Society of Petroleum Engineers.
84. Ogolo, N., O. Olafuyi, and M. Onyekonwu. *Impact of hydrocarbon on the performance of nanoparticles in control of fines migration*. in *SPE Nigeria Annual International Conference and Exhibition*. 2013. Society of Petroleum Engineers.
85. Yan, C., et al. *Synthesis and size control of monodispersed Al-Sulphonated Polycarboxylic Acid (Al-SPCA) nanoparticles with improved squeeze performance and their transport in porous media*. in *SPE International Oilfield Nanotechnology Conference and Exhibition*. 2012. Society of Petroleum Engineers.
86. Yan, C., et al. *Boehmite Based Sulphonated Polymer Nanoparticles with ImprovedSqueeze Performance for Deepwater Scale Control*. in *Offshore Technology Conference*. 2013. Offshore Technology Conference.
87. Yan, C., et al., *Synthesis and size control of monodispersed Al-sulfonated polycarboxylic acid nanoparticles and their transport in porous media.* Spe Journal, 2013. **18**(04): p. 610-619.
88. Alaskar, M.N., et al., *Nanoparticle and Microparticle Flow in Porous and Fractured Media--An Experimental Study.* Spe Journal, 2012. **17**(04): p. 1,160-1,171.
89. Sun, X., et al., *Application of nanoparticles in enhanced oil recovery: a critical review of recent progress*. Energies, 2017. **10**(3): p. 345.
90. Maghzi, A., et al., *The impact of silica nanoparticles on the performance of polymer solution in presence of salts in polymer flooding for heavy oil recovery*. Fuel, 2014. **123**: p. 123-132.
91. Maghzi, A., et al., *An experimental investigation of silica nanoparticles effect on the rheological behavior of polyacrylamide solution to enhance heavy oil recovery*. Petroleum Science and Technology, 2013. **31**(5): p. 500-508.
92. Bera, A. and H. Belhaj, *Application of nanotechnology by means of nanoparticles and nanodispersions in oil recovery-A comprehensive review*. Journal of Natural Gas Science and Engineering, 2016. **34**: p. 1284-1309.
93. Manan, M., et al., *Effects of nanoparticle types on carbon dioxide foam flooding in enhanced oil recovery.* Petroleum Science and Technology, 2015. **33**(12): p. 1286-1294.
94. Nazari Moghaddam, R., et al., *Comparative study of using nanoparticles for enhanced oil recovery: wettability alteration of carbonate rocks.* Energy & Fuels, 2015. **29**(4): p. 2111-2119.
95. Sharma, T., G.S. Kumar, and J.S. Sangwai, *Comparative effectiveness of production performance of Pickering emulsion stabilized by nanoparticle–surfactant–polymerover surfactant–polymer (SP) flooding for enhanced oil recoveryfor Brownfield reservoir*. Journal of Petroleum Science and Engineering, 2015. **129**: p. 221-232.
96. Singh, R. and K.K. Mohanty, *Foams stabilized by in-situ surface-activated nanoparticles in bulk and porous media.* Spe Journal, 2016. **21**(01): p. 121-130.
97. Abhishek, R., G.S. Kumar, and R. Sapru, *Wettability alteration in carbonate reservoirs using nanofluids.* Petroleum Science and Technology, 2015. **33**(7): p. 794-801.

98. Nguyen, B.D., et al., *The impact of graphene oxide particles on viscosity stabilization for diluted polymer solutions using in enhanced oil recovery at HTHP offshore reservoirs.* Advances in Natural Sciences: Nanoscience and Nanotechnology, 2014. **6**(1): p. 015012.
99. Yousefvand, H. and A. Jafari, *Enhanced oil recovery using polymer/nanosilica.* Procedia Materials Science, 2015. **11**: p. 565-570.
100. Cheraghian, G. and L. Hendraningrat, *A review on applications of nanotechnology in the enhanced oil recovery part A: effects of nanoparticles on interfacial tension.* International Nano Letters, 2016. **6**(2): p. 129-138.
101. Tang, J., et al., *Polyimide-silica nanocomposites exhibiting low thermal expansion coefficient and water absorption from surface-modified silica.* Journal of Applied Polymer Science, 2007. **104**(6): p. 4096-4105.
102. Ponnapati, R., et al., *Polymer-functionalized nanoparticles for improving waterflood sweep efficiency: Characterization and transport properties.* Industrial & Engineering Chemistry Research, 2011. **50**(23): p. 13030-13036.
103. Barati, N., M. Zargartalebi, and R. Kharrat, Rheological behavior of nanosilica suspensions and the potential to enhance polymer flooding performance. Special Topics & Reviews in Porous Media: An International Journal, 2013. **4**(4).
104. Sharma, T. and J.S. Sangwai, *Silica nanofluids in polyacrylamide with and without surfactant: Viscosity, surface tension, and interfacial tension with liquid paraffin.* Journal of Petroleum Science and Engineering, 2017. **152**: p. 575-585.
105. Abdullahi, M.B., et al., *Appraising the impact of metal-oxide nanoparticles on rheological properties of HPAM in different electrolyte solutions for enhanced oil recovery.* Journal of Petroleum Science and Engineering, 2019. **172**: p. 1057-1068.
106. Cheraghian, G., *Effect of nano titanium dioxide on heavy oil recovery during polymer flooding.* Petroleum Science and Technology, 2016. **34**(7): p. 633-641.
107. Lima, M.C.F.S., et al., *Aqueous suspensions of carbon black with ethylenediamine and polyacrylamide-modified surfaces: Applications for chemically enhanced oil recovery.* Carbon, 2016. **109**: p. 290-299.
108. Cheraghian, G., *An experimental study of surfactant polymer for enhanced heavy oil recovery using a glass micromodel by adding nanoclay.* Petroleum Science and Technology, 2015. **33**(13-14): p. 1410-1417.
109. Rezaei, A., et al., *Using surface modified clay nanoparticles to improve rheological behavior of Hydrolized Polyacrylamid (HPAM) solution for enhanced oil recovery with polymer flooding.* Journal of Molecular Liquids, 2016. **222**: p. 1148-1156.
110. Khalilinezhad, S.S., et al., *Characterizing the role of clay and silica nanoparticles in enhanced heavy oil recovery during polymer flooding.* Arabian Journal for Science and Engineering, 2016. **41**(7): p. 2731-2750.
111. Zeyghami, M., R. Kharrat, and M. Ghazanfari, *Investigation of the applicability of nano silica particles as a thickening additive for polymer solutions applied in EOR processes.* Energy Sources, Part A: Recovery, Utilization, and Environmental Effects, 2014. **36**(12): p. 1315-1324.
112. Haruna, M.A., et al., *Improved rheology and high-temperature stability of hydrolyzed polyacrylamide using graphene oxide nanosheet.* Journal of Applied Polymer Science, 2019: p. 47582.
113. Aliabadian, E., et al., *Prevention of network destruction of partially hydrolyzed polyacrylamide (HPAM): Effects of salt, temperature, and fumed silica nanoparticles.* Physics of Fluids, 2019. **31**(1): p. 013104.
114. Kumar, R.S. and T. Sharma, *Stability and rheological properties of nanofluids stabilized by SiO2 nanoparticles and SiO2-TiO2 nanocomposites for oilfield applications.* Colloids and Surfaces A: Physicochemical and Engineering Aspects, 2018. **539**: p. 171-183.
115. Kadhum, M.J., et al., *Polymer-stabilized multi-walled carbon nanotube dispersions in high-salinity brines.* Energy & Fuels, 2017. **31**(5): p. 5024-5030.
116. Cheraghian, G., et al., *Adsorption polymer on reservoir rock and role of the nanoparticles, clay and SiO 2.* International Nano Letters, 2014. **4**(3): p. 114.
117. Khalilinezhad, S.S., et al., *Improving heavy oil recovery in the polymer flooding process by*

utilizing hydrophilic silica nanoparticles. Energy Sources, Part A: Recovery, Utilization, and Environmental Effects, 2017: p. 1-10.

118. AlamiNia, H. and S.S. Khalilinezhad, *Application of hydrophilic silica nanoparticles in chemical enhanced heavy oil recovery processes.* Energy Sources, Part A: Recovery, Utilization, and Environmental Effects, 2017: p. 1-10.
119. Bagaria, H.G., et al., *Iron oxide nanoparticles grafted with sulfonated copolymers are stable in concentrated brine at elevated temperatures and weakly adsorb on silica.* ACS applied materials & interfaces, 2013. **5**(8): p. 3329-3339.
120. Wiśniewska, M., et al., *Impact of anionic polyacrylamide on stability and surface properties of the Al 2 O 3–polymer solution system at different temperatures.* Colloid and Polymer Science, 2016. **294**(9): p. 1511-1517.
121. Wiśniewska, M., S. Chibowski, and T. Urban, *Modification of the alumina surface properties by adsorbed anionic polyacrylamide—impact of polymer hydrolysis.* Journal of Industrial and Engineering Chemistry, 2015. **21**: p. 925-931.
122. Zhu, D., et al., *Enhancing rheological properties of hydrophobically associative polyacrylamide aqueous solutions by hybriding with silica nanoparticles.* Journal of Applied Polymer Science, 2014. **131**(19).
123. Zhu, D., et al., *Aqueous hybrids of silica nanoparticles and hydrophobically associating hydrolyzed polyacrylamide used for EOR in high-temperature and high-salinity reservoirs.* Energies, 2014. **7**(6): p. 3858-3871.
124. Haruna, M.A., et al., *Improved rheology and high-temperature stability of hydrolyzed polyacrylamide using graphene oxide nanosheet.* Journal of Applied Polymer Science, 2019. **136**(22): p. 47582.
125. Maurya, N.K. and A. Mandal, *Studies on behavior of suspension of silica nanoparticle in aqueous polyacrylamide solution for application in enhanced oil recovery.* Petroleum Science and Technology, 2016. **34**(5): p. 429-436.
126. Goodwin, D.J., et al., *Characterization of polymer adsorption onto drug nanoparticles using depletion measurements and small-angle neutron scattering.* Molecular pharmaceutics, 2013. **10**(11): p. 4146-4158.
127. Lu, Z., et al., *Effect of colloidal polymers with different surface properties on the rheological property of fresh cement pastes.* Colloids and Surfaces A: Physicochemical and Engineering Aspects, 2017. **520**: p. 154-165.
128. Yang, W., J. Qian, and Z. Shen, *A novel flocculant of Al (OH) 3–polyacrylamide ionic hybrid.* Journal of colloid and interface science, 2004. **273**(2): p. 400-405.
129. Ye, L., Y. Tang, and D. Qiu, *Enhance the mechanical performance of polyacrylamide hydrogel by aluminium-modified colloidal silica.* Colloids and Surfaces A: Physicochemical and Engineering Aspects, 2014. **447**: p. 103-110.
130. Silva, D., et al., *The effect of albumin and cholesterol on the biotribological behavior of hydrogels for contact lenses.* Acta biomaterialia, 2015. **26**: p. 184-194.
131. Wever, D.A., F. Picchioni, and A.A. Broekhuis, *Comblike polyacrylamides as flooding agent in enhanced oil recovery.* Industrial & Engineering Chemistry Research, 2013. **52**(46): p. 16352-16363.
132. Abidin, A., T. Puspasari, and W. Nugroho, *Polymers for enhanced oil recovery technology.* Procedia Chemistry, 2012. **4**: p. 11-16.
133. Ghriga, M.A., et al., *Review of recent advances in polyethylenimine crosslinked polymer gels used for conformance control applications.* Polymer Bulletin, 2019: p. 1-29.
134. Ghriga, M.A., et al., *Structure–property relationships of the thermal gelation of partially hydrolyzed polyacrylamide/polyethylenimine mixtures in a semidilute regime.* Polymer Bulletin, 2019: p. 1-24.
135. Cheng, G., W. Graessley, and Y. Melnichenko, *Polymer dimensions in good solvents: crossover from semidilute to concentrated solutions.* Physical review letters, 2009. **102**(15): p. 157801.
136. Maranzano, B.J. and N.J. Wagner, *The effects of interparticle interactions and particle size on reversible shear thickening: Hard-sphere colloidal dispersions.* Journal of Rheology, 2001. **45**(5): p. 1205-1222.

137. Maranzano, B.J. and N.J. Wagner, *The effects of particle size on reversible shear thickening of concentrated colloidal dispersions.* The Journal of chemical physics, 2001. **114**(23): p. 10514-10527.
138. Kalman, D.P., et al., *Effect of particle hardness on the penetration behavior of fabrics intercalated with dry particles and concentrated particle− fluid suspensions.* ACS applied materials & interfaces, 2009. **1**(11): p. 2602-2612.
139. Srivastava, A., A. Majumdar, and B. Butola, *Improving the impact resistance of textile structures by using shear thickening fluids: a review.* Critical Reviews in Solid State and Materials Sciences, 2012. **37**(2): p. 115-129.
140. Yan, F., L. Ye, and D. Qiu, *Effect of particle/polymer number ratio on the structure and dynamics of complex between large polymer and nanoparticle.* Colloids and Surfaces A: Physicochemical and Engineering Aspects, 2016. **507**: p. 67-75.
141. Yong, V. and H.T. Hahn, *Dispersant optimization using design of experiments for SiC/vinyl ester nanocomposites.* Nanotechnology, 2005. **16**(4): p. 354.
142. Amir, Z., I. Mohd Saaid, and B. Mohamed Jan, *An Optimization Study of Polyacrylamide-Polyethylenimine-Based Polymer Gel for High Temperature Reservoir Conformance Control.* International Journal of Polymer Science, 2018. **2018**.
143. Ghriga, M.A., et al., *Thermal gelation of partially hydrolysed polyacrylamide/polyethyleneimine mixtures using design of experiments approach.* Materials Today Communications, 2019: p. 100686.
144. Hasanzadeh, M., V. Mottaghitalab, and M. Rezaei, *Rheological and viscoelastic behavior of concentrated colloidal suspensions of silica nanoparticles: a response surface methodology approach.* Advanced Powder Technology, 2015. **26**(6): p. 1570-1577.
145. Ahmed, J., H. Ramaswamy, and M. Ngadi, *Rheological characteristics of Arabic gum in combination with guar and xanthan gum using response surface methodology: effect of temperature and concentration.* International Journal of Food Properties, 2005. **8**(2): p. 179-192.
146. Ahmed, J., et al., *Effect of particle size and temperature on rheological, thermal, and structural properties of pumpkin flour dispersion.* Journal of Food Engineering, 2014. **124**: p. 43-53.
147. Kennedy, J.R., K.E. Kent, and J.R. Brown, *Rheology of dispersions of xanthan gum, locust bean gum and mixed biopolymer gel with silicon dioxide nanoparticles.* Materials Science and Engineering: C, 2015. **48**: p. 347-353.
148. Feng, Y., et al., *Hydrophobically associating polyacrylamides and their partially hydrolyzed derivatives prepared by post-modification. 2. Properties of non-hydrolyzed polymers in pure water and brine.* Polymer, 2005. **46**(22): p. 9283-9295.
149. Pierre, T.S. and M. Geckle, *13-NMR analysis of branched polyethyleneimine.* Journal of Macromolecular Science—Chemistry, 1985. **22**(5-7): p. 877-887.
150. Rodriguez, L., et al. *Monitoring Thermal and Mechanical Stability of Enhanced Oil Recovery (EOR) Acrylamide Based Polymers (PAM) Through Intrinsic Viscosity (IV) Determination Using a New Capillary Rheology Technique*. in *SPE EOR Conference at Oil and Gas West Asia*. 2016. Society of Petroleum Engineers.
151. Kokkinidou, S. and D.G. Peterson, *Response surface methodology as optimization strategy for reduction of reactive carbonyl species in foods by means of phenolic chemistry.* Food & function, 2013. **4**(7): p. 1093-1104.
152. Candela, A.M., J. Coello, and C. Palet, *Doehlert experimental design as a tool to study liquid–liquid systems for the recovery of Uranium (VI) traces.* Separation and Purification Technology, 2013. **118**: p. 399-405.
153. Karanam, S.K. and N.R. Medicherla, *Application of Doehlert experimental design for the optimization of medium constituents for the production of L-asparaginase from Palm Kernal cake (Elaeis guineensis).* J Microbial Biochem Technol, 2010. **2**: p. 007-012.
154. Imandi, S.B., et al., *Optimization of medium constituents for the production of citric acid from byproduct glycerol using Doehlert experimental design.* Enzyme and Microbial Technology, 2007. **40**(5): p. 1367-1372.
155. Doehlert, D.H., *Uniform shell designs.* Applied statistics, 1970: p. 231-239.

156. Hu, Y. and D. Massart, *Uniform shell designs for optimization in reversed-phase liquid chromatography.* Journal of Chromatography A, 1989. **485**: p. 311-323.
157. Cataldi, T.R., et al., *A three-factor Doehlert matrix design in optimising the determination of octadecyltrimethylammonium bromide by cation-exchange chromatography with suppressed conductivity detection.* Analytica chimica acta, 2007. **597**(1): p. 129-136.
158. Campaña, A.G., et al., *Sequential response surface methodology for multioptimization in analytical chemistry with three-variable Doehlert designs.* Analytica chimica acta, 1997. **348**(1-3): p. 237-246.
159. Rigolini, J., et al., *2D-infrared thermography monitoring of ultrasound-assisted polymerization of water-soluble monomer in a gel process.* Macromolecules, 2011. **44**(11): p. 4462-4469.
160. Aslam, M., et al., *Application of Box–Behnken design for preparation of glibenclamide loaded lipid based nanoparticles: Optimization, in vitro skin permeation, drug release and in vivo pharmacokinetic study.* Journal of Molecular Liquids, 2016. **219**: p. 897-908.
161. Aalaie, J. and M. Youssefi, *Study on the dynamic rheometry and swelling properties of the polyacrylamide/laponite nanocomposite hydrogels in electrolyte media.* Journal of Macromolecular Science, Part B, 2012. **51**(6): p. 1027-1040.
162. Oliyaei, N., et al., *Study on Steady Shear Rheological Behavior of Concentrated Suspensions of Sulfonated Polyacrylamide/Na-Montmorillonite Nanoparticles.* Journal of Macromolecular Science, Part B, 2015. **54**(7): p. 761-770.
163. Lin, R. and G. Yin, *Bayes factor and posterior probability: Complementary statistical evidence to p-value.* Contemporary clinical trials, 2015. **44**: p. 33-35.
164. Khataee, A., et al., *Chemometrics approach for determination and optimization of simultaneous photooxidative decolourization of a mixture of three textile dyes.* Environmental technology, 2012. **33**(20): p. 2305-2317.
165. Yao, F. and A. Ullah, *A nonparametric R2 test for the presence of relevant variables.* Journal of Statistical Planning and Inference, 2013. **143**(9): p. 1527-1547.
166. Jarrah, N.A., *Studying the influence of process parameters on the catalytic carbon nanofibers formation using factorial design.* Chemical Engineering Journal, 2009. **151**(1): p. 367-371.
167. Derringer, G., *Simultaneous optimization of several response variables.* Journal of quality technology, 1980. **12**(4): p. 214-219.
168. Candioti, L.V., et al., *Experimental design and multiple response optimization. Using the desirability function in analytical methods development.* Talanta, 2014. **124**: p. 123-138.
169. Babaye Khorasani, F., et al., *Mobility of nanoparticles in semidilute polyelectrolyte solutions.* Macromolecules, 2014. **47**(15): p. 5328-5333.
170. Lebouachera, S.E.I., et al., *Rheological behaviour and adsorption phenomenon of a polymer–particle composite based on hydrolysed polyacrylamide/functionalized poly(styrene-acrylic acid) microspheres.* Soft Matter, 2019.
171. Hore, M.J., *Polymers on nanoparticles: structure & dynamics.* Soft Matter, 2019. **15**(6): p. 1120-1134.
172. Loste, J., et al., *Transparent polymer nanocomposites: An overview on their synthesis and advanced properties.* Progress in Polymer Science, 2018.
173. Sorichetti, V., V. Hugouvieux, and W. Kob, *Structure and dynamics of a polymer–nanoparticle composite: Effect of nanoparticle size and volume fraction.* Macromolecules, 2018. **51**(14): p. 5375-5391.
174. Nath, P., et al., *Dynamics of nanoparticles in entangled polymer solutions.* Langmuir, 2017. **34**(1): p. 241-249.
175. Cai, L.-H., S. Panyukov, and M. Rubinstein, *Mobility of nonsticky nanoparticles in polymer liquids.* Macromolecules, 2011. **44**(19): p. 7853-7863.
176. Mutch, K.J., J.S. van Duijneveldt, and J. Eastoe, *Colloid–polymer mixtures in the protein limit.* Soft Matter, 2007. **3**(2): p. 155-167.
177. Gam, S., et al., *Polymer diffusion in a polymer nanocomposite: effect of nanoparticle size and polydispersity.* Soft Matter, 2012. **8**(24): p. 6512-6520.
178. Wang, C., et al., *Regulating polymer adsorption on colloid by surface morphology.* Soft Matter, 2018. **14**(46): p. 9336-9342.

179. Yekeen, N., et al., *Nanoparticles applications for hydraulic fracturing of unconventional reservoirs: A comprehensive review of recent advances and prospects.* Journal of Petroleum Science and Engineering, 2019.
180. Tamsilian, Y., et al., *Nanostructured Particles for Controlled Polymer Release in Enhanced Oil Recovery*. Energy Technology, 2016. **4**(9): p. 1035-1046.
181. Aliabadian, E., et al., *Rheology of fumed silica nanoparticles/partially hydrolyzed polyacrylamide aqueous solutions under small and large amplitude oscillatory shear deformations.* Journal of Rheology, 2018. **62**(5): p. 1197-1216.
182. Peng, F., et al., *Big effects of small nanoparticles on hydrophobically modified polyacrylamide in an aqueous solution.* Journal of Applied Polymer Science, 2019. **136**(16): p. 47269.
183. Guillot, P. and A. Colin, *Determination of the flow curve of complex fluids using the Rabinowitsch–Mooney equation in sensorless microrheometer.* Microfluidics and nanofluidics, 2014. **17**(3): p. 605-611.
184. Pessoni, L., et al., *Soap-and metal-free polystyrene latex particles as a nanoplastic model.* Environmental Science: Nano, 2019. **6**(7): p. 2253-2258.
185. Goodall, A., M. Wilkinson, and J. Hearn, *Mechanism of emulsion polymerization of styrene in soap-free systems.* Journal of polymer science: Polymer chemistry edition, 1977. **15**(9): p. 2193-2218.
186. Aalaie, J., *Rheological behavior of polyacrylamide/laponite nanoparticle suspensions in electrolyte media.* Journal of Macromolecular Science, Part B, 2012. **51**(6): p. 1139-1147.
187. Aalaie, J., et al., *Effect of montmorillonite on gelation and swelling behavior of sulfonated polyacrylamide nanocomposite hydrogels in electrolyte solutions.* European polymer journal, 2008. **44**(7): p. 2024-2031.
188. Samoshina, Y., et al., *Adsorption of cationic, anionic and hydrophobically modified polyacrylamides on silica surfaces.* Colloids and Surfaces A: Physicochemical and Engineering Aspects, 2003. **231**(1): p. 195-205.
189. Kawaguchi, M., *Rheological properties of silica suspensions in polymer solutions.* Advances in Colloid and Interface Science, 1994. **53**: p. 103-127.
190. Fakoya, M.F. and S.N. Shah, *Rheological Properties of Surfactant-Based and Polymeric Nano-Fluids*, in *SPE/ICoTA Coiled Tubing & Well Intervention Conference & Exhibition*2013, Society of Petroleum Engineers: The Woodlands, Texas, USA. p. 17.
191. Lin, C.-C., et al., *Do attractive polymer–nanoparticle interactions retard polymer diffusion in nanocomposites?* Macromolecules, 2013. **46**(11): p. 4502-4509.
192. Liufu, S., H. Xiao, and Y. Li, *Adsorption of poly (acrylic acid) onto the surface of titanium dioxide and the colloidal stability of aqueous suspension.* Journal of colloid and interface science, 2005. **281**(1): p. 155-163.
193. Mardles, E., *Viscosity of suspensions and the Einstein equation.* Nature, 1940. **145**(3686): p. 970.
194. M'pandou, A. and B. Siffert, *Polyethyleneglycol adsorption at the TiO2□ H2O interface: Distortion of ionic structure and shear plane position.* Colloids and Surfaces, 1987. **24**(2-3): p. 159-172.
195. Maerker, J., *Shear degradation of partially hydrolyzed polyacrylamide solutions.* Society of Petroleum Engineers Journal, 1975. **15**(04): p. 311-322.
196. Jouenne, S., H. Chakibi, and D. Levitt. *Polymer Stability Following Successive Mechanical Degradation Events*. in *IOR 2015-18th European Symposium on Improved Oil Recovery*. 2015.
197. Llanos, S.n., et al., *Effect of Sodium Oleate Surfactant Concentration Grafted onto SiO2 Nanoparticles in Polymer Flooding Processes.* ACS Omega, 2018. **3**(12): p. 18673-18684.
198. Corredor-Rojas, L.M., et al., *Rheological behavior of surface modified silica nanoparticles dispersed in partially hydrolyzed polyacrylamide and xanthan gum solutions: Experimental measurements, mechanistic understanding, and model development.* Energy & Fuels, 2018. **32**(10): p. 10628-10638.
199. Dupas, A., et al., *Mechanical degradation onset of polyethylene oxide used as a hydrosoluble model polymer for enhanced oil recovery.* Oil & Gas Science and Technology–Revue d'IFP Energies nouvelles, 2012. **67**(6): p. 931-940.

200. Lopes, L. and B. Silveira, *Rheological Evaluation of HPAM fluids for EOR Applications.* 2014.
201. Hunkeler, D., T. Nguyen, and H. Kausch, *Polymer solutions under elongational flow: 1. Birefringence characterization of transient and stagnation point elongational flows.* Polymer, 1996. **37**(19): p. 4257-4269.
202. Nguyen, T.Q. and H.-H. Kausch, *Chain extension and degradation in convergent flow.* Polymer, 1992. **33**(12): p. 2611-2621.